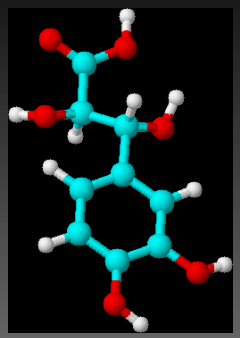
OMICS Group
Accelerating Scientific Discovery
9th American Biotechnology Congress
Aug 31-Sep2, 2015 Florida, USA

Biomacromolecule from Medicinal Plants, its Synthetic Basic Monomeric Moiety and their Anticancer Activity

Dr. Vakhtang Barbakadze
Head of the Laboratory of Plant Biopolymers

Tbilisi State Medical University
I.Kutateladze Institute of Pharmacochemistry
Tbilisi, Georgia, v_barbakadze@hotmail.com







PREFACE

"Actual isolation and purification of natural products must not be stereotyped; it requires critical spirit, creativity and originality.
In this sense, isolation is an "art" in natural product chemistry"

Y. Tsuda "Isolation of Natural Products", 2004, p. 1, Printed by Japan Analytical Industry Co., Ltd.

Symphytum asperum (prickly or rough comfrey)
Widely Distributed in the Caucasus and Anatolia Region of Turkey and Widespread all over the World





Symphytum caucasicum (Caucasian comfrey)
Caucasian Endemic





Symphytum officinale

Widely Distributed in Europe and Widespread all over the World





Symphytum grandiflorum DC (Creeping comfrey)
Georgian Endemic





Anchusa italica (Italian bugloss)

Widely Distributed in Europe and Widespread all over the World





Introduction

***Symphytum* L. (Comfrey) is a herb already mentioned in ancient literature for its wound-healing properties. Through the ages, *Symphytum* extracts have been used in folk medicine for treatment of different kinds of disorders and wounds due to analgesic, antimicrobial and anti-inflammatory effects.**

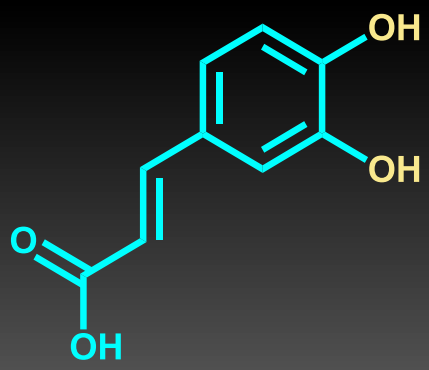
***Anchusa* (Bugloss) extracts also have been used in folk medicine due to anti-ulcer, wound healing and anticancer properties.**

The first representative of a new class of natural phenolic polyethers, namely regular caffeic acid-derived polymer - has been detected in the species of Comfrey - *Symphytum asperum* (SA) *S. caucasicum* (SC), *S. officinale* (SO) and Bugloss (*Anchusa)* – *Anchusa italica* (AI).

Caffeic acid and its derivatives of natural and synthetic origin have antioxidant, anti-inflammatory, hepatoprotective, antimutagenic, anticancer, immunomodulatory, pro-apoptotic activity and inhibitory effect on angiogenesis, tumor invasion, and metastasis. Their radical-scavenging and antioxidative activities are mainly due to the presence of two phenolic hydroxygroups at ortho positions.

It is suggested that antitumor activity of caffeic acid and its derivatives is related to the immunomodulatory properties of the compounds, particularly their capacity to induce apoptosis and necrosis.

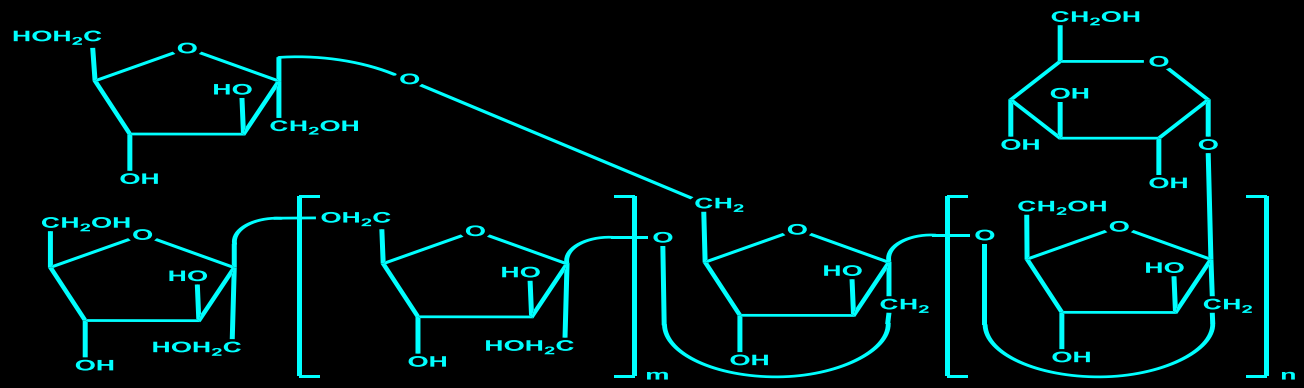
The results concerning the structure elucidation of this caffeic acid-derived polymer and its pharmacological efficacy are presented below.



Caffeic acid

Some known constituents of *Symphytum* and *Anchusa*

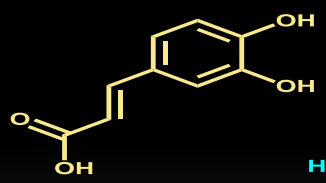
Acidic arabinogalactan



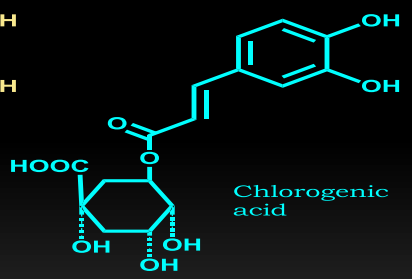
Glucofructan



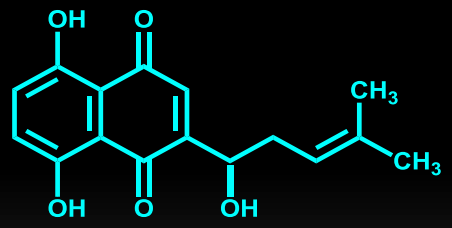
Allantoin



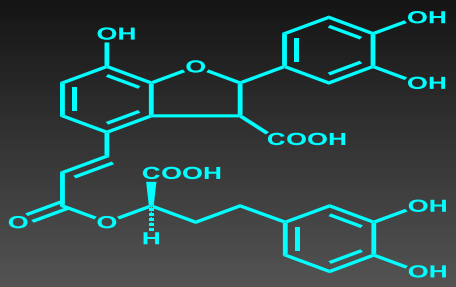
Caffeic acid



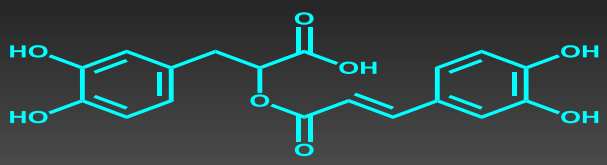
Chlorogenic acid



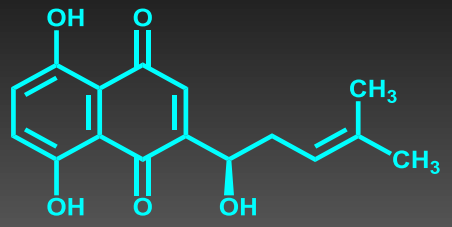
Alkanin



Lithospermic acid

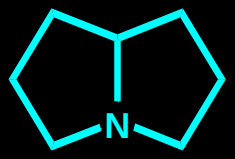


Rosmarinic acid

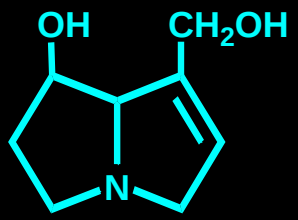


Shikonin

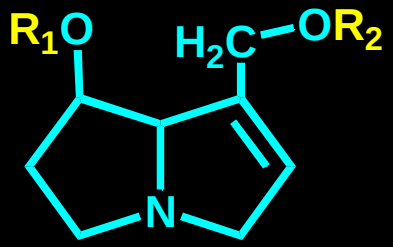
Overview of Pyrrolizidine alkaloids (PAs) found in *Symphytum* and *Anchusa*



A

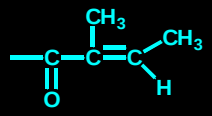
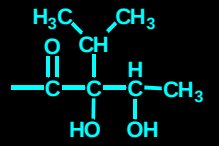
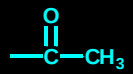
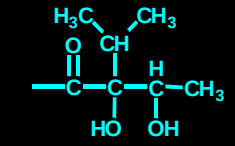
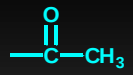
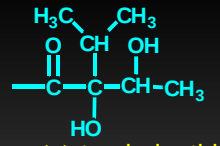
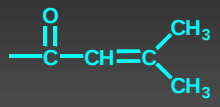
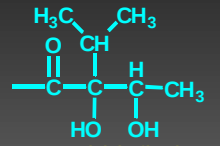


B

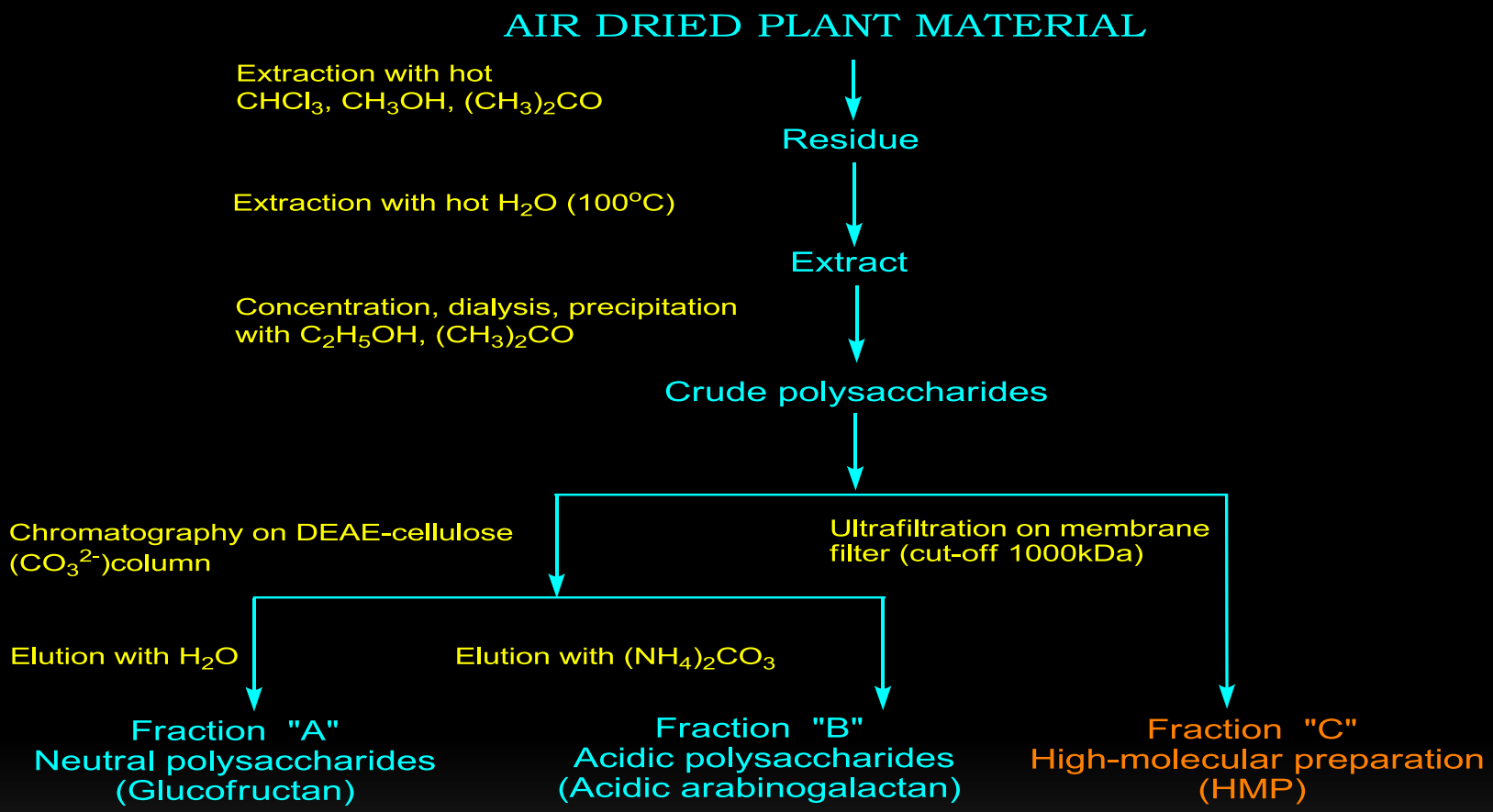


necic acid(s)

A – pyrrolizidine, the necine moiety of PAs
B – retronecine;
PAs of *Symphytum* are mono- or di-esters of retronecine

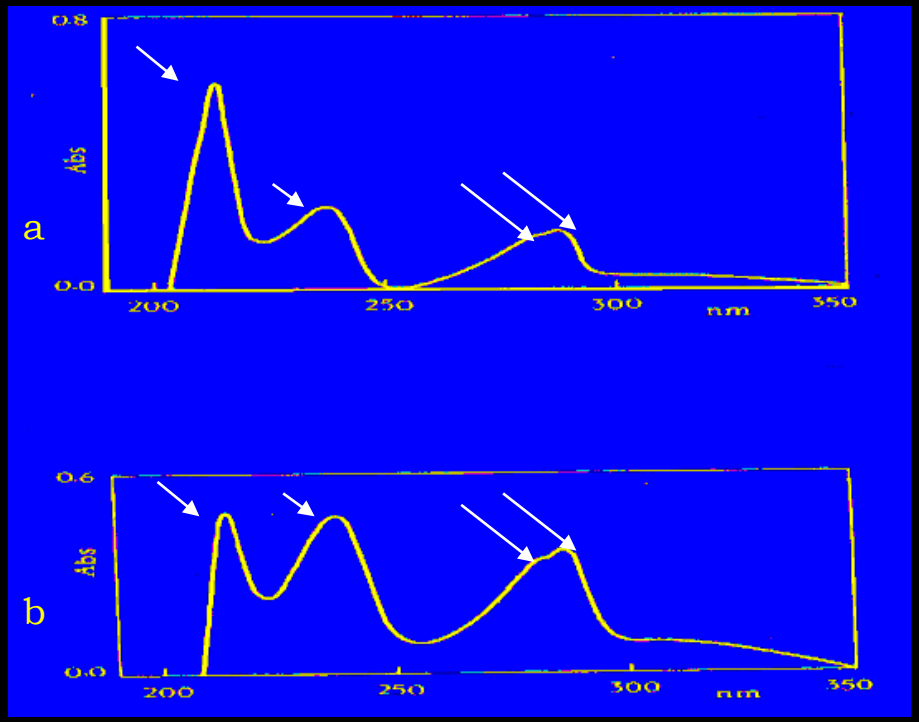
	R_1	R_2
symphytine	 tiglic	 (-)-viridofloric
lycopsamine	—H	 (-)-viridofloric
7-acetyllycopsamine	 acetic	 (-)-viridofloric
intermedine	—H	 (+)-trachelanthic
7-acetylintermedine	 acetic	 (+)-trachelanthic
symviridine	 cenecioic	 (-)-viridofloric

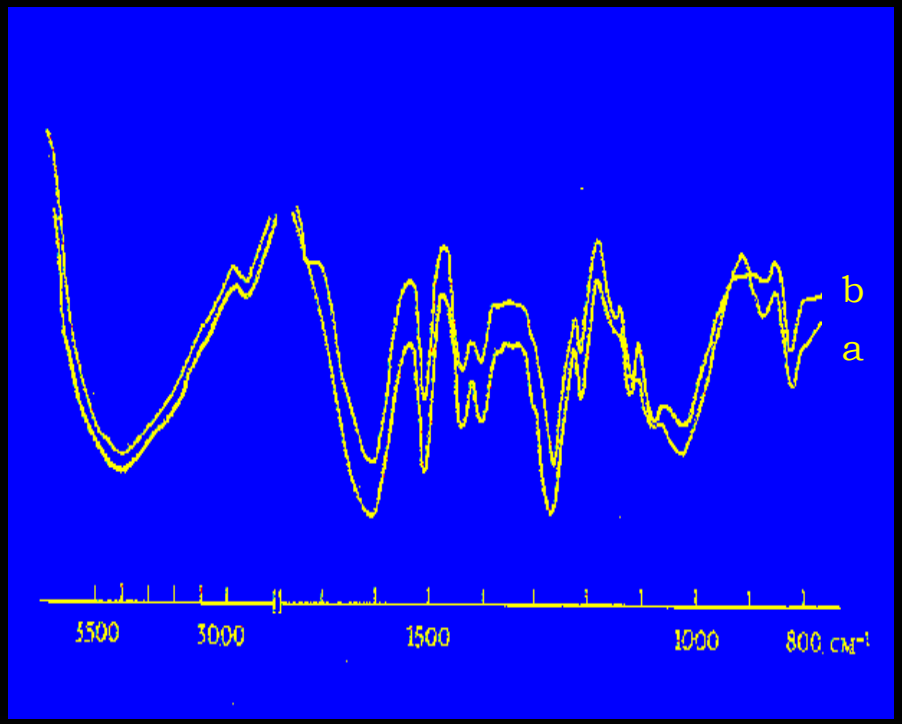
Isolation of SA, SC, SO and AI high-molecular preparation (HMP)



In order to determine the chemical nature of active components, crude polysaccharide preparations were fractionated by ultrafiltration on membrane filters with cut-off values of 10 kDa, 100 kDa and 1000 kDa, which resulted in the retaining of the main anti-complementary activity in the fractions with molecular masses exceeding 1 MDa. The water-soluble high-molecular fractions were additionally fractionated by gel chromatography on a Sepharose 2B column. These fractionation procedures allowed us to remove most ballast polysaccharides and to obtain water-soluble high-molecular (>1000 kDa) preparations (HMP).

UV (I) and IR (II) spectra of HMP from SA (a) and AI (b) (>1000 kDa)



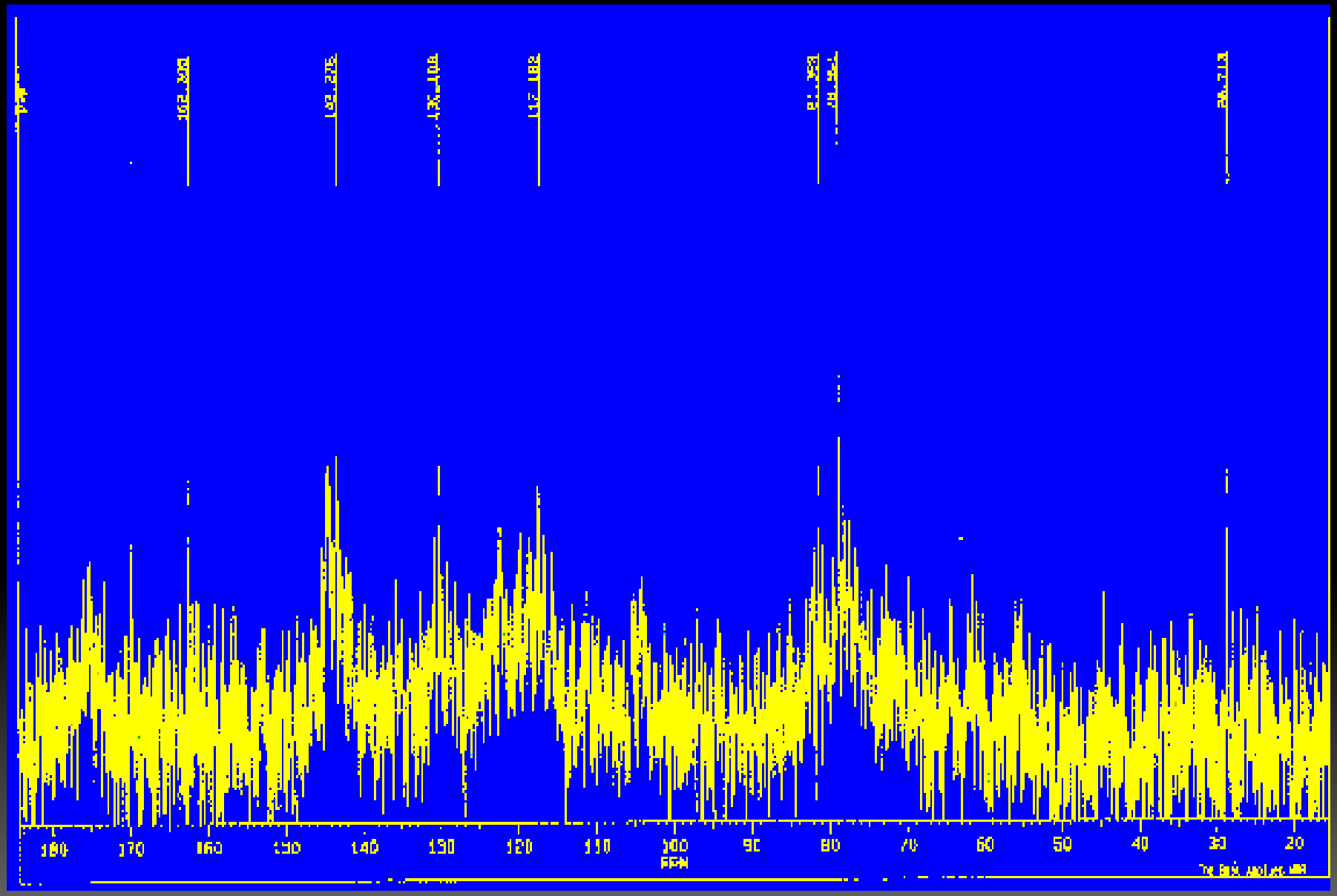


I. The absorption maxima at 213, 237, 282 (shoulder) and 286 nm were observed in the UV spectra of preparations (water) of S.A. (a) and A.I. (b), which could be attributable to substituted phenols.

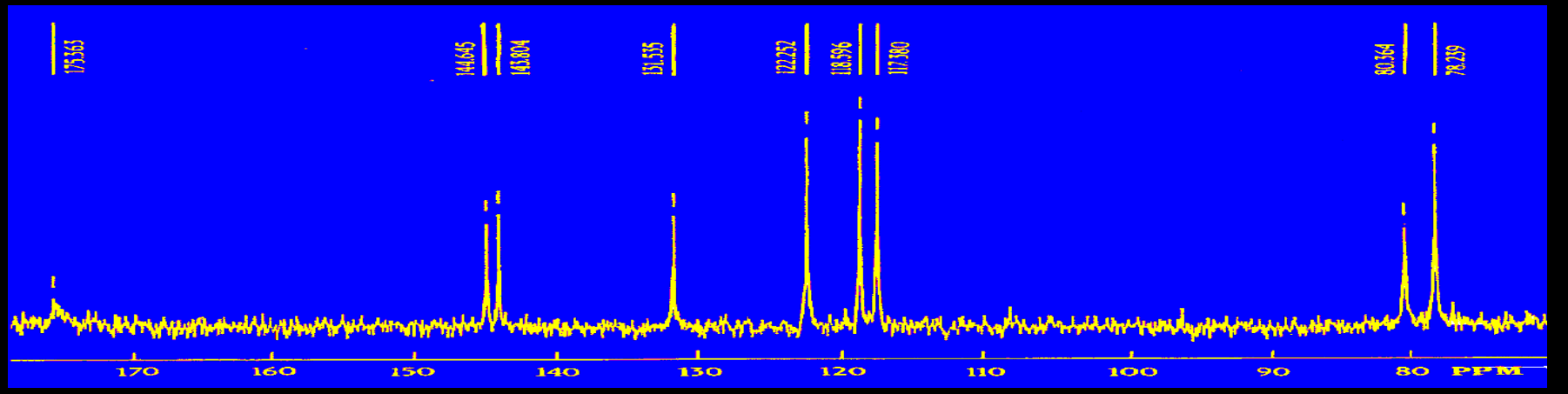
II. The IR spectra of preparations contain absorption bands characteristic of phenol-carboxylic acids: 3400 (OH); 2930 (CH); 1620 (ionized carboxyl) and 1736 cm^{-1} for its ester form (AI); **1600, 1510, and 1450 (aromatic C=C); 1410 and 1220 (phenols); 1270, 1130, 1075 and 1030 (R-O-R'); 880 (C-H in the aromatic ring with one isolated hydrogen atom); and 830 cm-1 (C-H in the aromatic ring with two neighboring hydrogen atoms).**

V.Barbakadze et al. Molecules, 2005, V. 10, N 9, P. 1135-1144; V.Barbakadze et al. Chem. Nat. Compds. 2009, V. 45, N 1, P. 6-10.

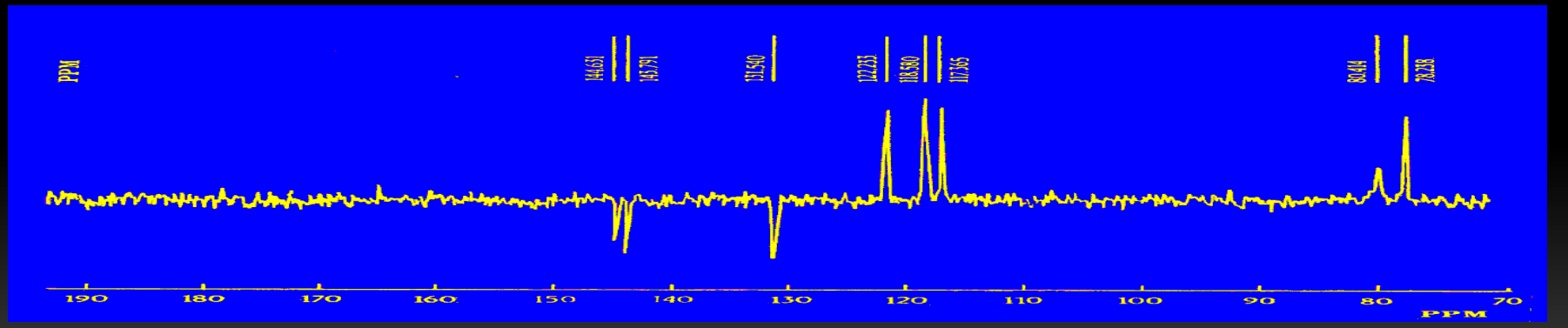
The ^{13}C NMR Initial Spectrum of HMP from SA (at room temperature)



The ^{13}C NMR (a) and APT (b) spectra of HMP from SA, SC, SO (at 80°C)



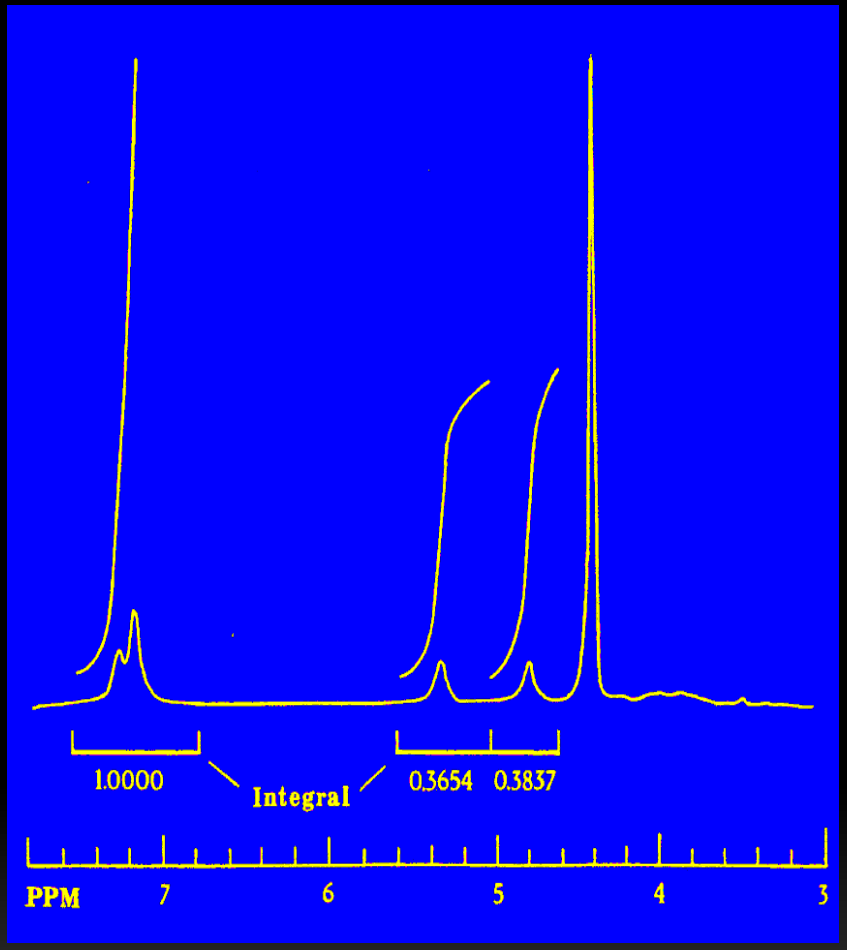
a) Nine distinct signals corresponding to the carbon atoms of the substituted phenylpropionic acid fragment are observed. A good resolution and the narrow shape of the ^{13}C NMR signals indicate that the compounds under study are regular polymers.

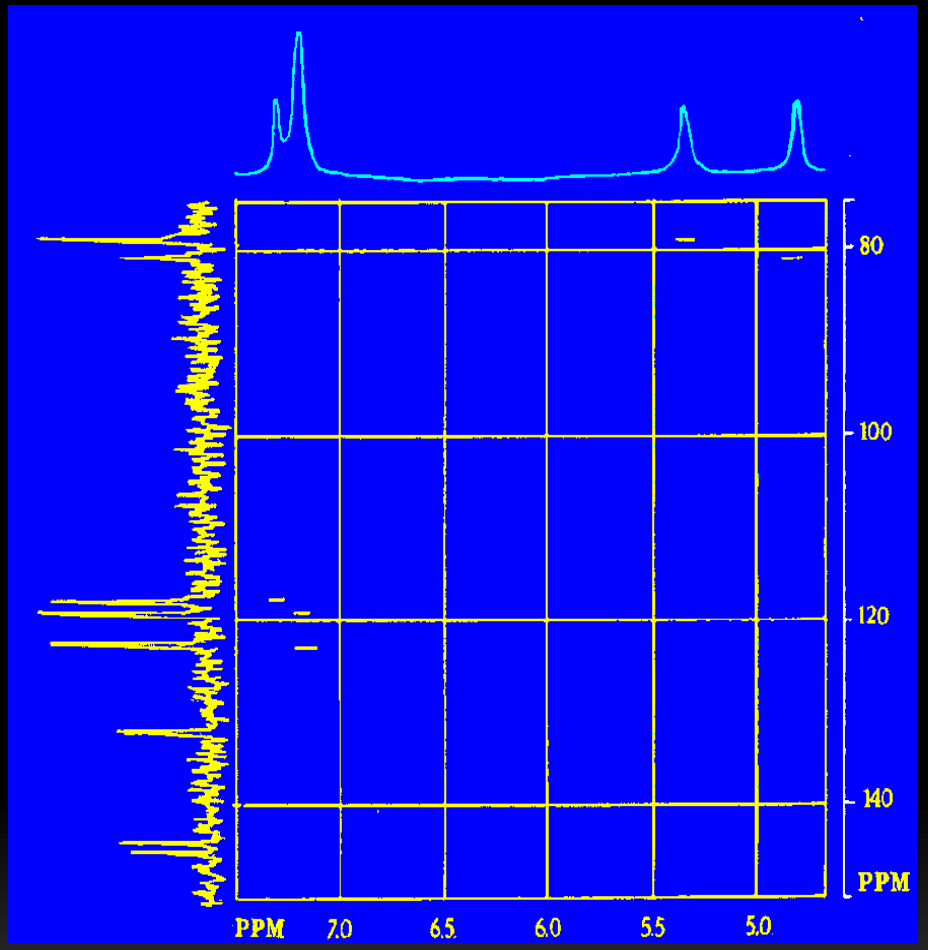


b) From signals observed five should be assigned to CH groups and four signals to the nonprotonated carbon atoms. The two signals with chemical shifts of 78.2 and 80.4 ppm obviously belong to oxygen-bound protonated aliphatic carbon atoms. Six signals were assigned to aromatic carbon atoms (protonated atoms at 117.4, 118.6, and 122.3 ppm and nonprotonated atoms at 131.5, 143.8, and 144.6 ppm). The broadened signal at 175.4 ppm was assigned to the carboxyl group in the compound.

V.Barbakadze et al. Molecules, 2005, V. 10, N 9, P. 1135-1144; V.Barbakadze et al. Chem. Nat. Compds. 2009, V. 45, N 1, P. 6-10.

The ^{1}H NMR (a) and HSQC (b) spectra of HMP from SA, SC, SO





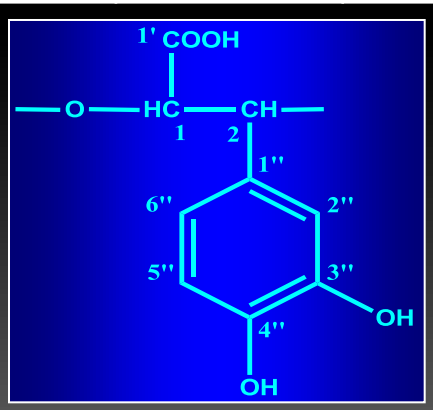
a) The ^{1}H NMR spectrum contains four signals at 4.88, 5.33, 7.13, and 7.24 ppm, one of them (7.13 ppm) with doubled intensity. These signals are broadened, and, therefore, the coupling constants cannot be determined.

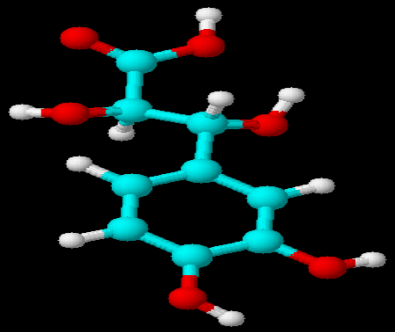
b) The 2D heteronuclear $^{1}H/^{13}C$ HSQC spectrum exhibits the following correlations between protons and carbon atoms: 4.88/80.4, 5.33/78.2, 7.13/118.6, 7.13/122.3, and 7.24/117.4 ppm.

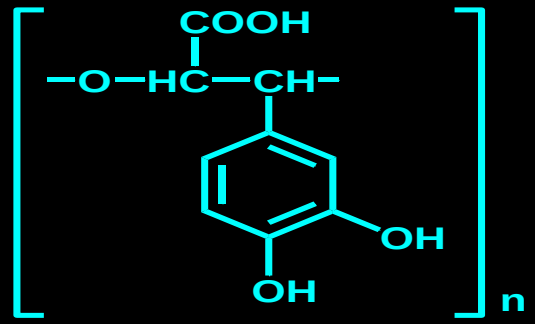
V.Barbakadze et al. Molecules, 2005, V. 10, N 9, P. 1135-1144; V.Barbakadze et al. Chem. Nat. Compds. 2009, V. 45, N 1, P. 6-10.

Assignments of signals in the ^{13}C and ^{1}H NMR spectra of HMP from SA, SC and SO

Atom No	Chemical shift ^{13}C, δ ppm	Chemical shift ^{1}H, δ ppm
1′	175.4	
1	78.2	5.33
2	80.4	4.88
1″	131.5	
2″	117.4	7.24
3″	144.7	
4″	143.8	
5″	118.6	7.13
6″	122.3	7.13







The hydroxyl groups in positions 3 and 4 of the phenyl ring were unambiguously established by a 1D-NOE experiment performed in the difference mode. Pre-irradiation of the proton 1 with a chemical shift of 5.33 ppm provided a NOE for two aromatic protons with chemical shifts of 7.13 (3%) and 7.24 (1%) ppm. Hence, these protons occupy positions 2 and 6 in phenyl ring. Thus, both of the *ortho*-positions in the dihydroxyphenyl ring were occupied by protons. Therefore, hydroxyl groups cannot occupy *o*-positions. The different values of NOE for these two protons, as well as their different chemical shifts in the ^{1}H NMR spectrum and different positions of resonances of the corresponding carbons in the ^{13}C NMR spectrum, excluded the possibility of symmetrical bis-*meta*-substitution of the aromatic ring by two hydroxy groups. Thus, according to different techniques of NMR spectroscopy t h e polyoxyethylene chain is the backbone of the polymer molecule. 3,4-Dihydroxyphenyl and carboxyl groups are regular substituents at two carbon atoms in the chain. The repeating unit of this regular polymer is 3-(3,4-dihydroxyphenyl)-glyceric acid residue. This compound is a representative of a new class of natural polyethers. Such biopolymer has not been known and has been identified for the first time.

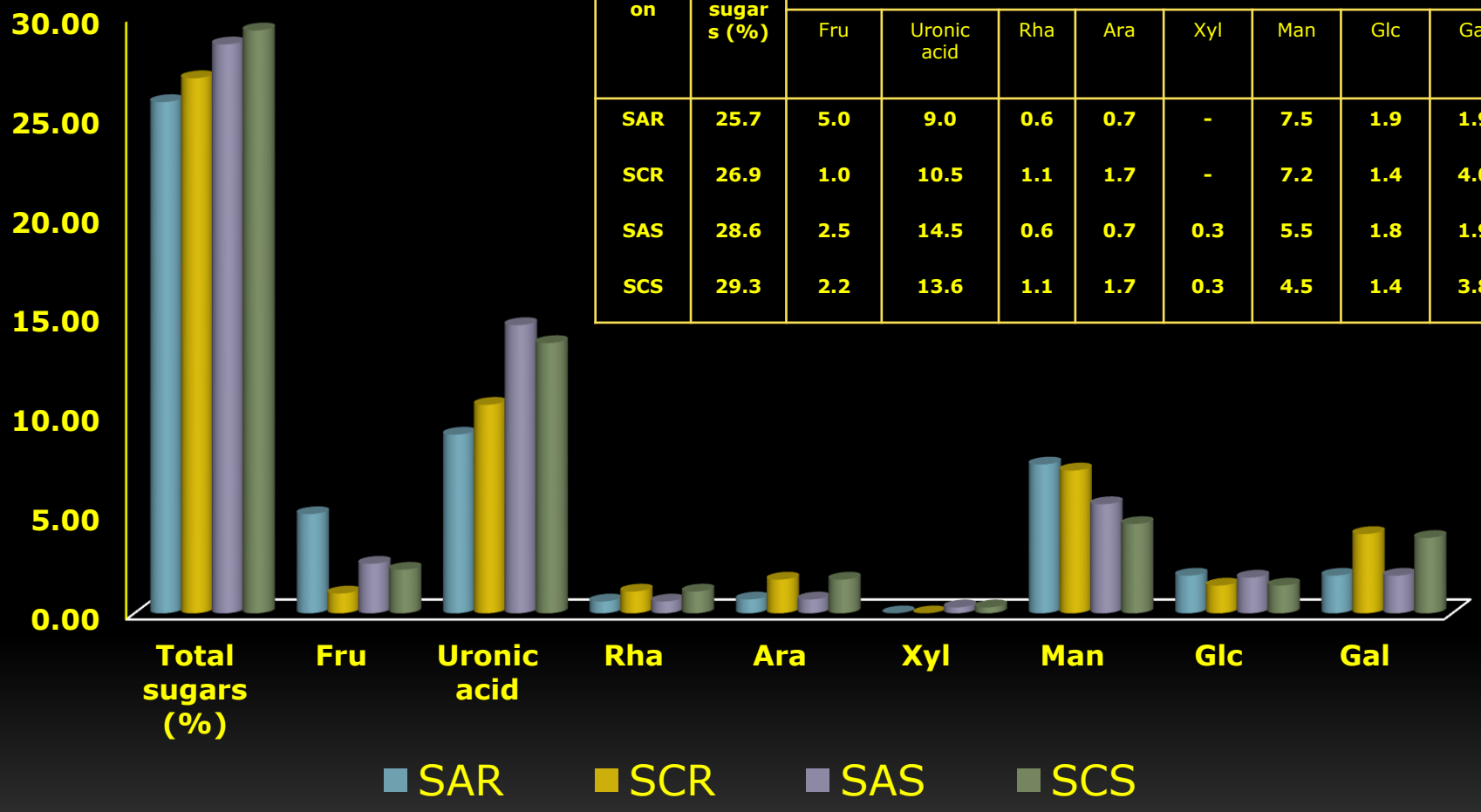
POLY [3-(3,4-DIHYDROXYPHENYL)-GLYCERIC ACID] (p-DGA);

POLY [OXY-1-CARBOXY-2-(3,4-DIHYDROXYPHENYL)ETHYLENE

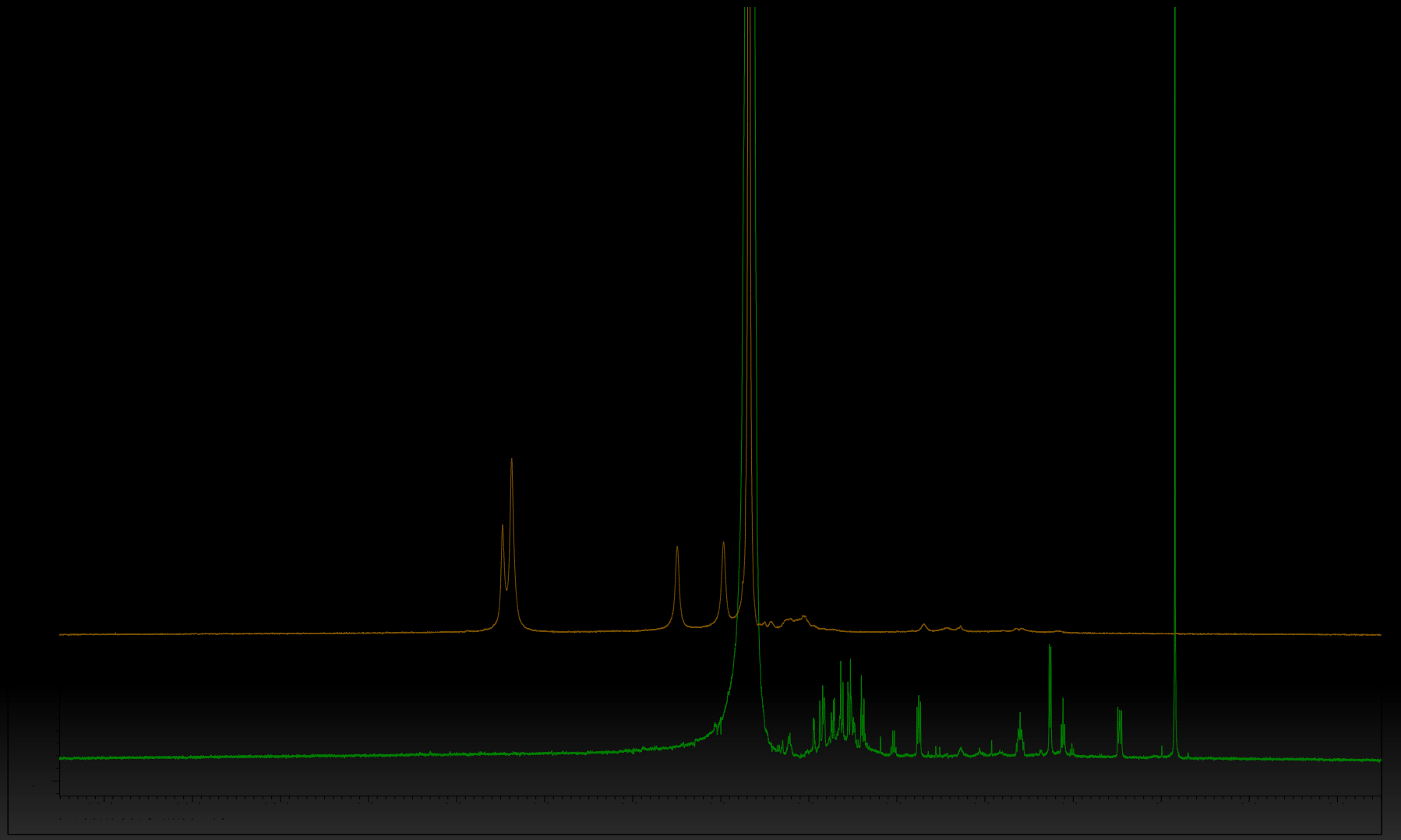
V.Barbakadze et al. Molecules, 2005, V. 10, N 9, P. 1135-1144; V.Barbakadze et al. Chem. Nat. Compds. 2009, V. 45, N 1, P. 6-10.

Sugar composition of HMP from SAR, SCR, SAS, SCS (%)

Fraction	Total sugars (%)	Monosaccharides (%)							
		Fru	Uronic acid	Rha	Ara	Xyl	Man	Glc	Gal
SAR	25.7	5.0	9.0	0.6	0.7	-	7.5	1.9	1.9
SCR	26.9	1.0	10.5	1.1	1.7	-	7.2	1.4	4.0
SAS	28.6	2.5	14.5	0.6	0.7	0.3	5.5	1.8	1.9
SCS	29.3	2.2	13.6	1.1	1.7	0.3	4.5	1.4	3.8

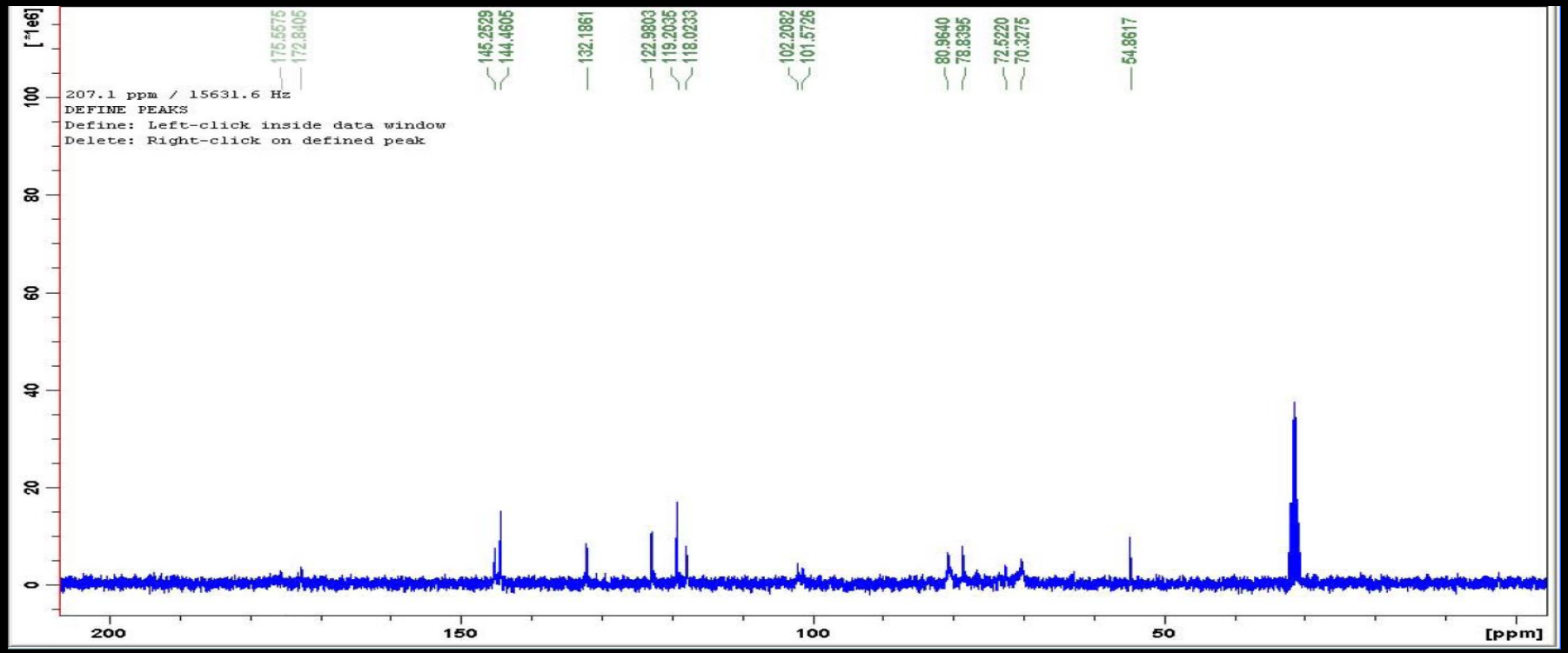


HMP from SAR, SCR, SAS, and SCS contained some amounts of carbohydrates. Interestingly, the signals of the carbohydrate components are practically unobservable in the NMR spectra of high molecular (>1000 kDa) preparations probably due to their variegated monosaccharide composition.



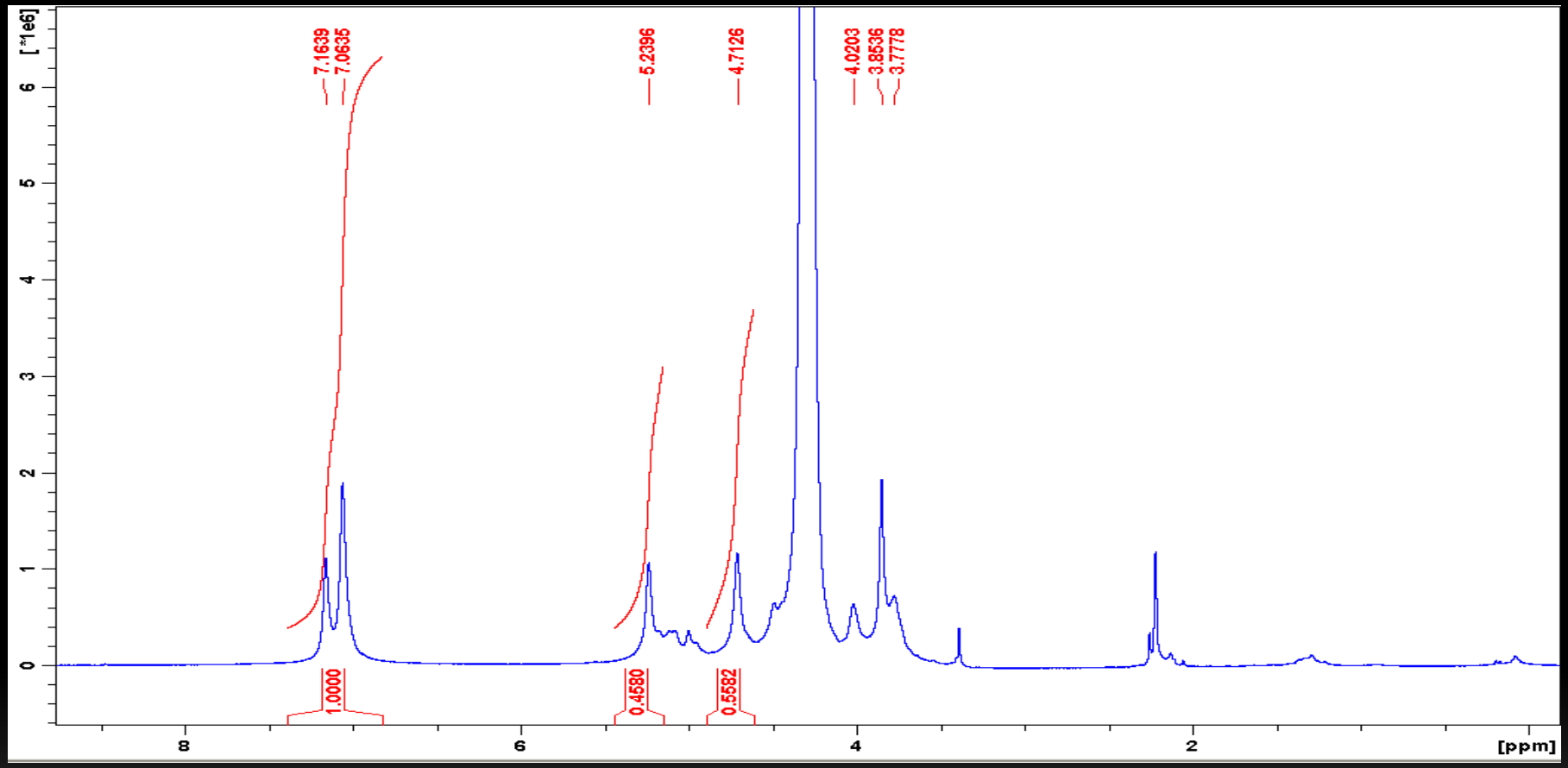
^{1}H NMR spectra of poly[3-(3,4-dihydroxyphenyl)glyceric acid] (p-DGA) preparation before (brown spectrum) and after (green spectrum) treatment by CF_3COOH. Such treatment caused sedimentation of p-DGA and disappearance of its signals in ^{1}H NMR spectrum and appearance of sugar signals in supernatant.

The ^{13}C NMR spectrum of HMP-AI



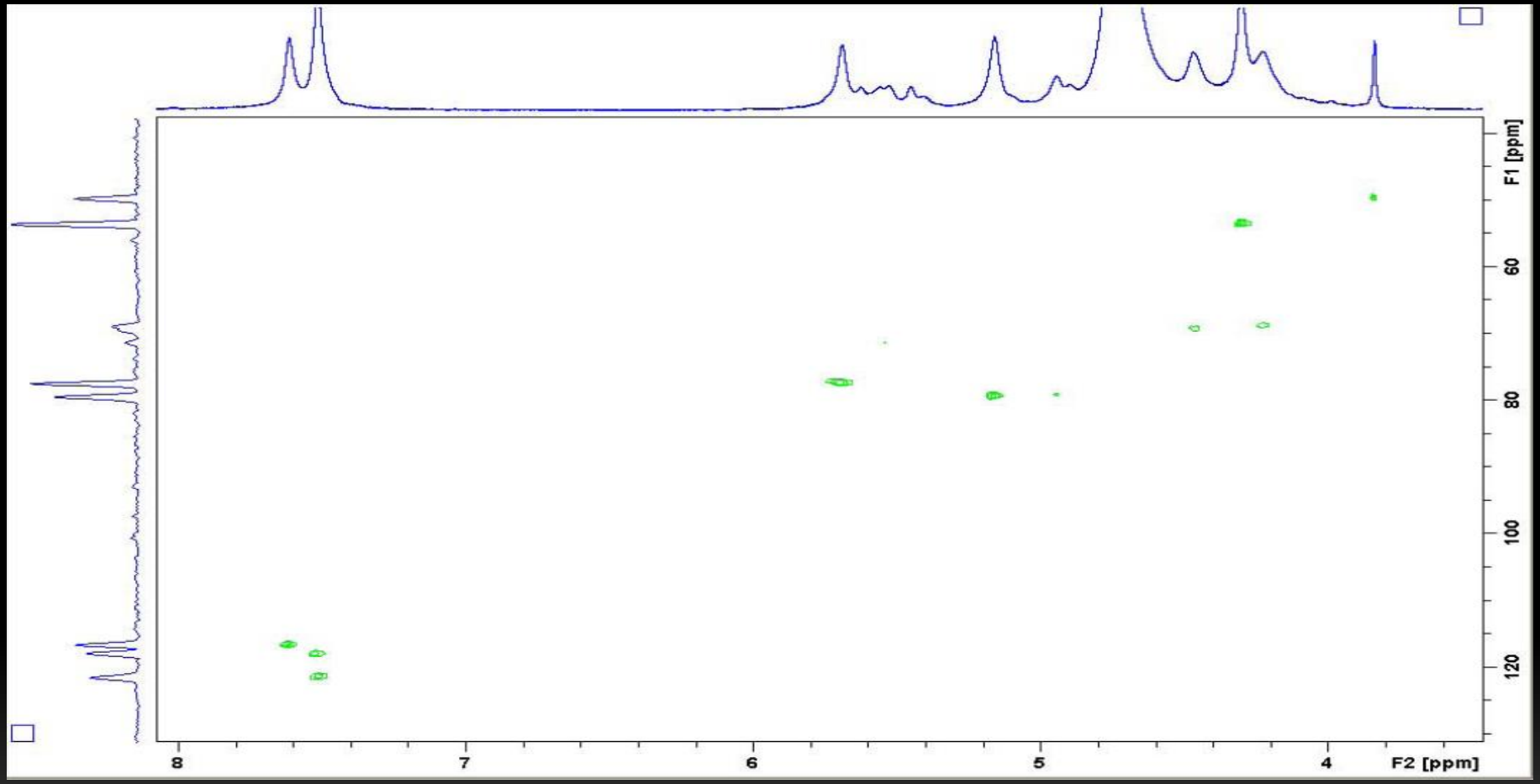
The two signals with chemical shifts of 78.84 and 80.96 ppm obviously belong to oxygen-bound protonated aliphatic carbon atoms. Six signals were assigned to aromatic carbon atoms (protonated atoms 118.02, 119.20 and 122.98 ppm and nonprotonated atoms at 132.19, 144.46, and 145.25 ppm). Then, two non-sharp signals (172.84 and 175.56 ppm) were thought to be due to two carboxyl groups. A resonance in the ^{13}C NMR spectrum at 54.86 ppm, which correlated with the ^{1}H resonance at 3.85 ppm, suggested the presence of methoxy groups in carboxylic acid methyl esters. With this, the signal at 175.56 ppm was attributed to a carboxylic acid group and the signal at 172.84 ppm was assigned to carboxyl groups in methyl ester-form (upfield shifted). About 70 % of the present carboxyl groups were methyl esterified (MeO: ^{13}C, 54.86 ppm; ^{1}H, 3.85 ppm).

The ^{1}H NMR spectrum of HMP-AI



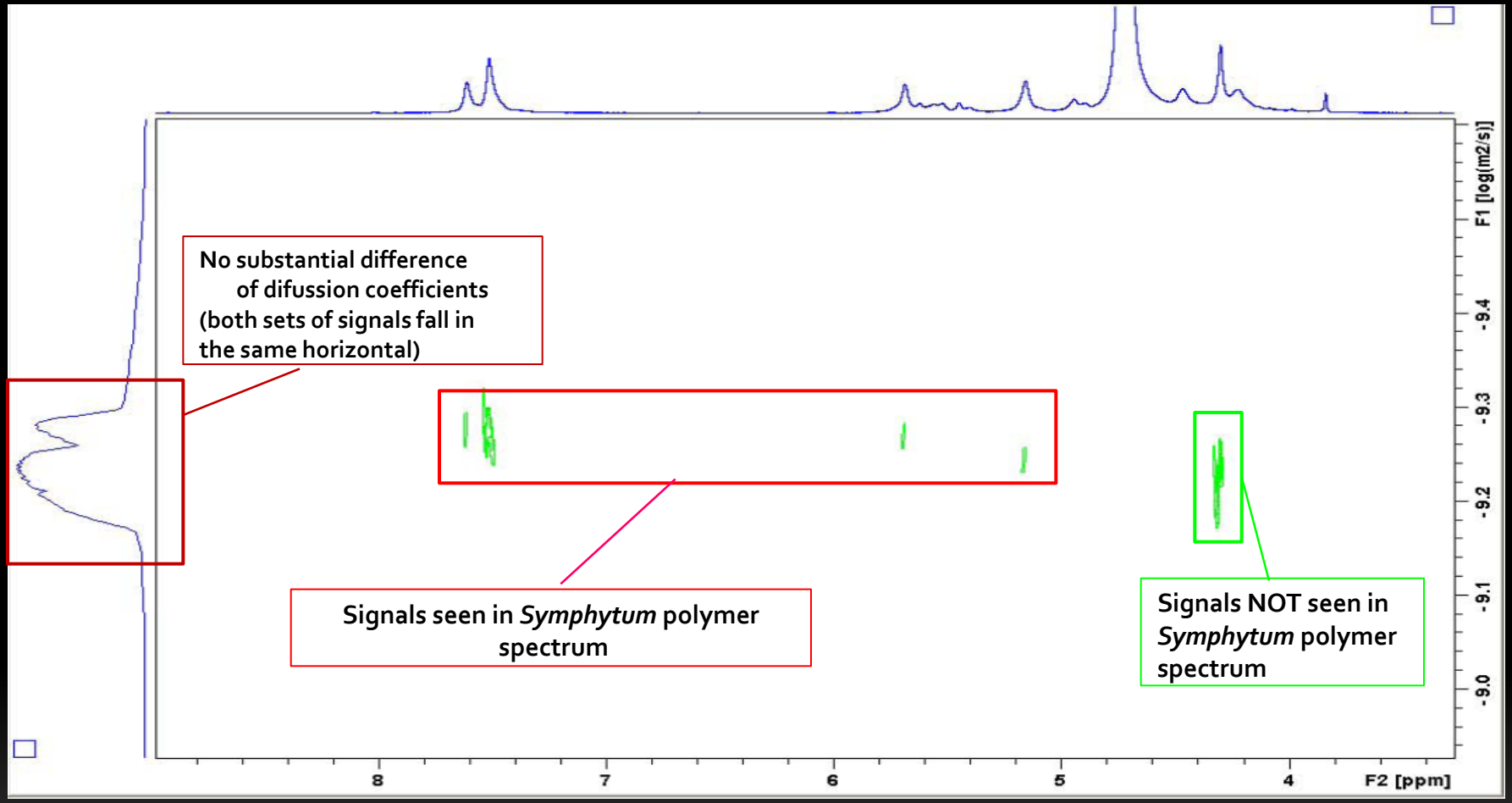
The ^{1}H NMR spectrum of HMP-AI contains five signals at 3.85, 4.71, 5.24, 7.06, and 7.16 ppm, one of them (7.06 ppm) with doubled intensity. These signals are broadened, and, therefore, the coupling constants cannot be determined. The ^{1}H resonance at 3.85 ppm, suggested the presence of methoxy groups in carboxylic acid methyl esters.

The 2D heteronuclear $^{1}H/^{13}C$ HSQC spectrum of HMP-AI



The following correlations between protons and carbon atoms: 3.85/54.86, 4.71/80.4, 5.24/78.84, 7.06/119.2, 7.06/122.98, and 7.16/118.02 ppm are detected. A resonance in the ^{13}C NMR spectrum at 54.86 ppm, which correlated with the ^{1}H resonance at 3.85 ppm, suggested the presence of methoxy groups in carboxylic acid methyl esters.

The 2D DOSY experiment



The similar diffusion coefficient for the methylated and non-methylated signals of HMP-AI is observed. Both sets of signals fell in the same horizontal. This would imply a similar molecular weight for methylated and non-methylated polymers. Thus, the NMR signals of both methylated and non-methylated carboxylic groups originate from the same poly[3-(3,4-dihydroxyphenyl)glyceric acid] polymer.

V.Barbakadze et al. Nat. Prod. Commun., 2010, V. 5, N 7, P.1091-1095.

Assignments of signals in the ^{13}C and ^{1}H NMR spectra of HMP-AI (δ, ppm)

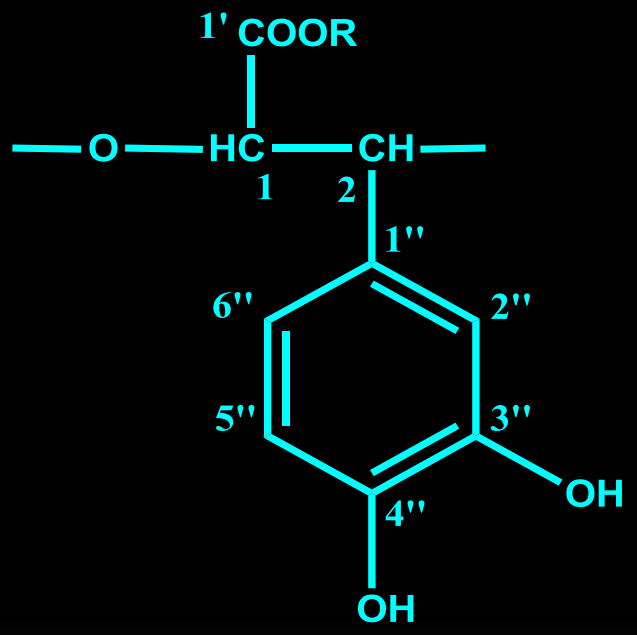
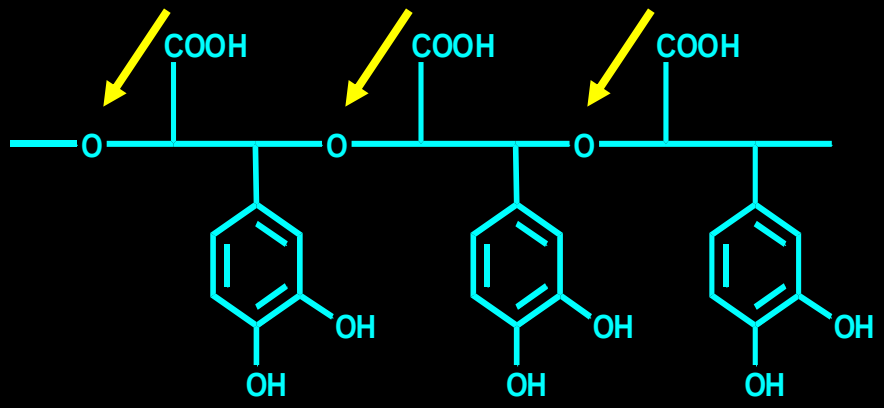


Fig. The repeating unit of HMP-AI; R=H, CH_3.

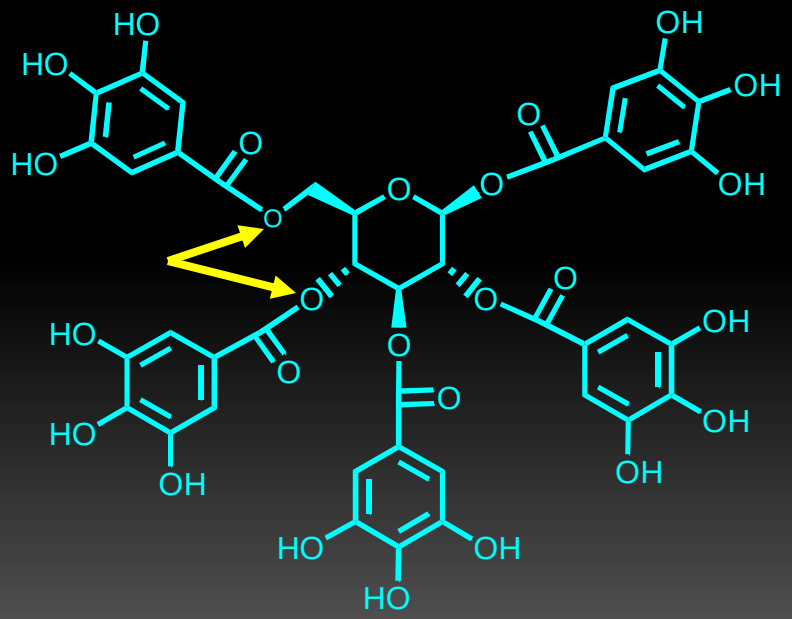
C atom no.	^{13}C chemical shift	^{1}H chemical shift
1'	175.56 (C̲OOH) 172.84 (C̲OOCH$_3$) 54.86 (OC̲H$_3$)	3.85 (OC̲H$_3$)
1	78.84	5.24
2	80.96	4.71
1''	132.19	
2''	118.02	7.16
3''	145.25	
4''	144.46	
5''	119.20	7.06
6''	122.98	7.06

Most of the carboxylic groups (70%) of HMP-AI unlike the HMP SA, SC, SO are methylated (MeO: ^{13}C, δ 54.86 ppm; ^{1}H, δ 3.85 ppm). The extent of methyl esterification was calculated by comparing the integral intensity of the methyl ester signal (3.85 ppm, 0.5 H) to that of the aliphatic proton signal at H1 (5.24 ppm, 0.7 H) in a ^{1}H NMR experiment.

V.Barbakadze et al. Nat. Prod. Commun., 2010, V. 5, N 7, P.1091-1095.



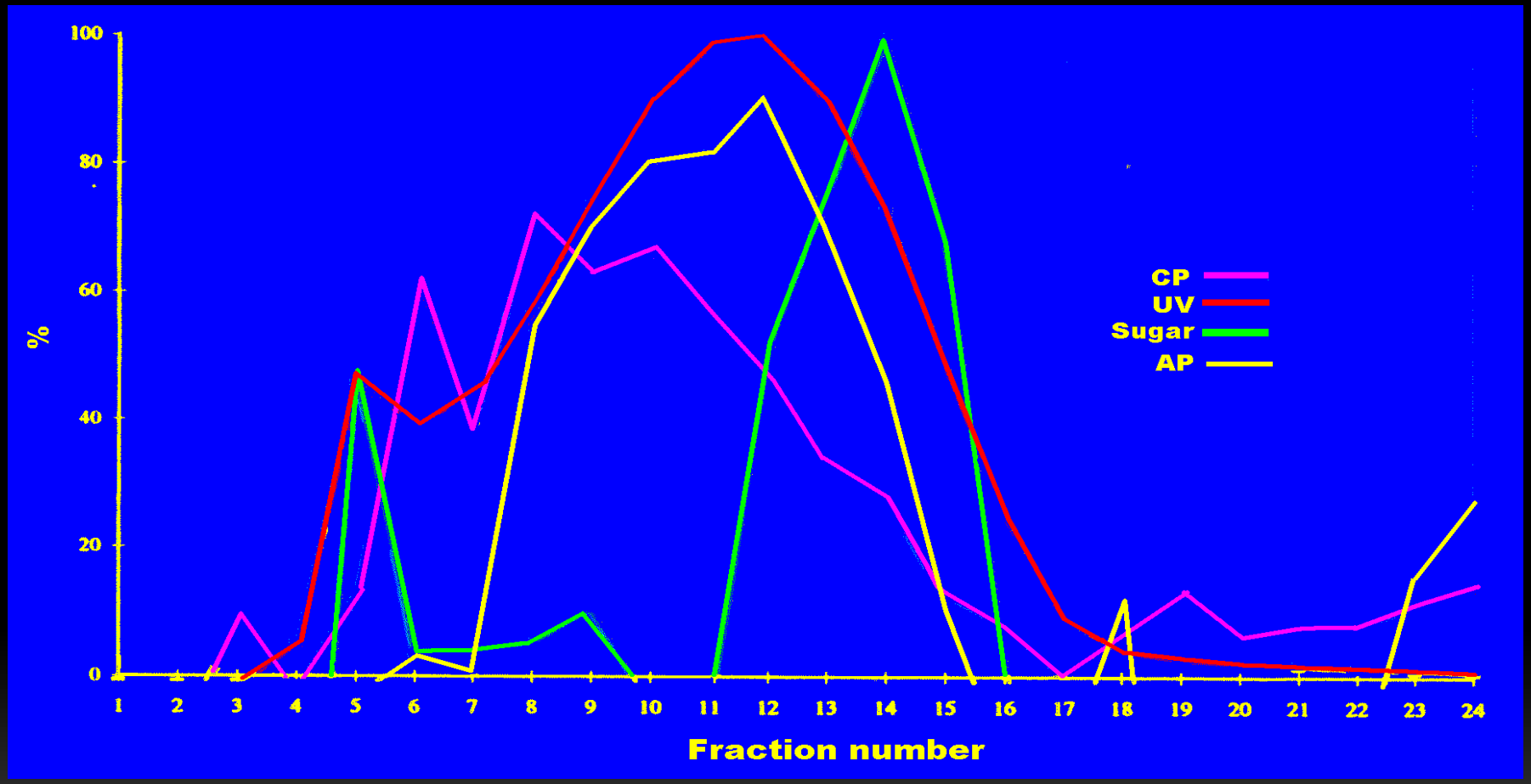
Caffeic acid-derived polyether



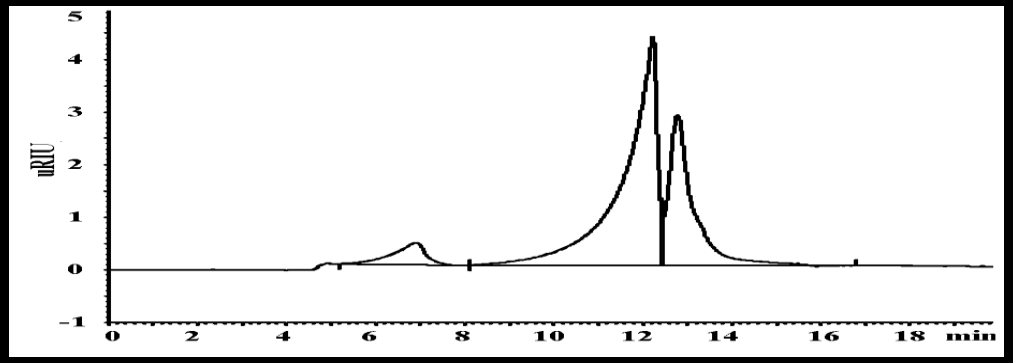
Pentagalloyl glucose (constituent of tannic acid)

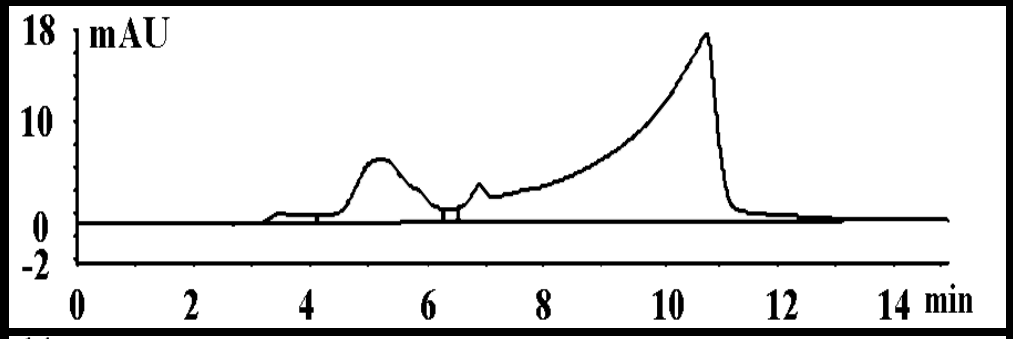
An advantage of this new polymer is the low susceptibility to hydrolysis and, hence, high stability, which is related to the presence of only ether bonds in the backbone structure thus being a much more stable compound than for example tannic acid that is composed of ester-linked glucose and gallic acid moieties.

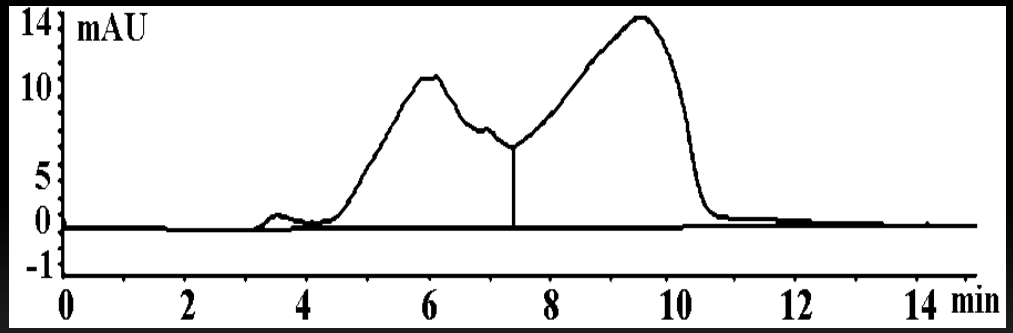
Gel Chromatography of Active Fraction of *Symphytum* on Sepharose 2B Column

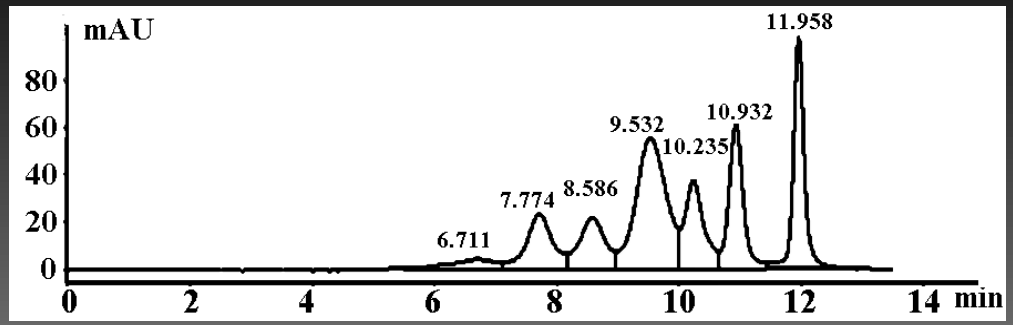


Percentage of inhibition of the classical pathway (CP) and the alternative pathway (AP) of complement activity, elution of polysaccharides (Sugar) and caffeic acid-derived polymer (UV-286 nm absorption pattern). The Figure shows that the anticomplementary activity was related to the dihydroxycinnamate-derived polymer (UV-286 nm absorption pattern), but did not coincide with carbohydrates elution. Two polysaccharides peaks are shifted from CP and AP anticomplementary activity peaks.





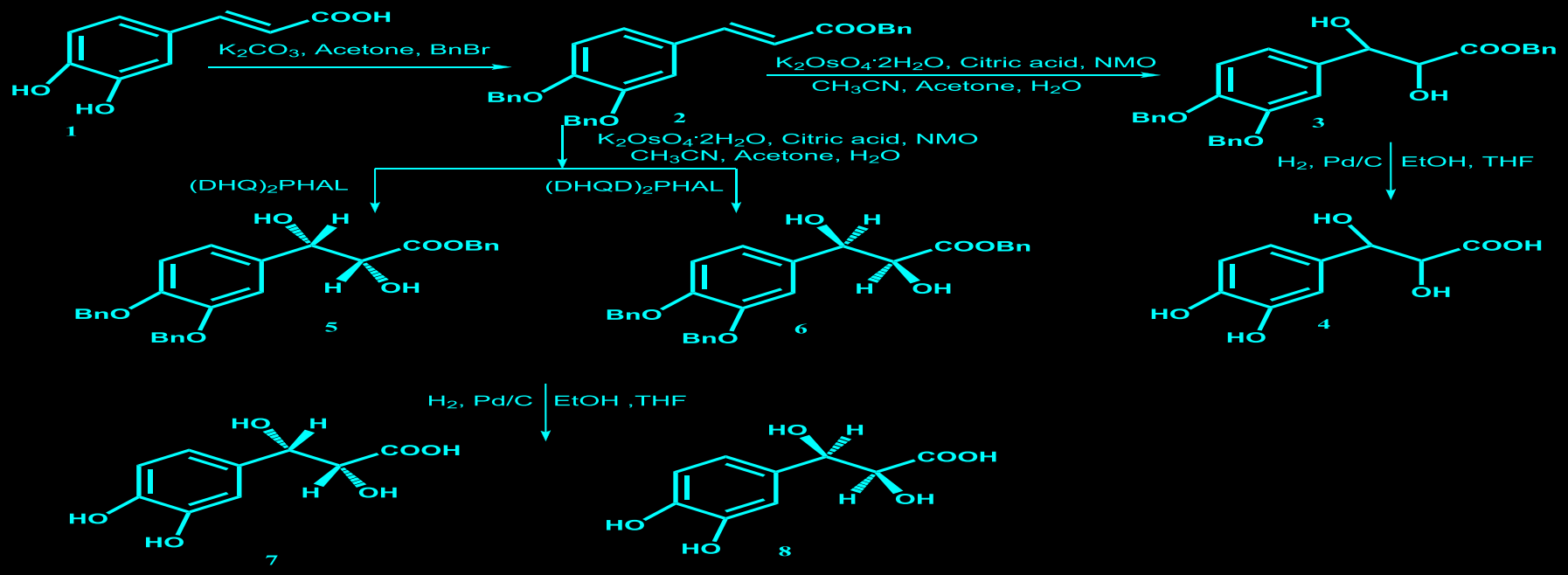




HPLC analysis of HMP-SA on column Polysep 6000; injection – 9 ul; detection – RI. Separation by HPLC on Polysep 6000 confirmed our previous supposition that polysaccharides contents are not covalently bounded with phenolic polymer. However it is very difficult to completely separate by GFC the polysaccharides from polymer. This phenomenon can be explained due to the presence of hydrogen bonds between phenolic polymer and residual polysaccharides which will hold the polysaccharides together with the phenolic polymer during fractionation by ultrafiltration and GFC. The polymer is chemically simple, but its molecules can form with each other and with the molecules of residual polysaccharides complex macromolecular associates up to their supramolecular organization due to hydrogen bonds.

HPLC analysis of HMP-SA (top) and HMP-AI (bottom) on column Biosep 4000; injection - 20 ul; detection – RI, shows that both polymers have high MW parts, which according to calibration of column by mixture of standard proteins are more than 669 KDa and supposedly might be phenolic polymer p-DGA. Relatively lower MW parts around 150 KDa that we could not see on UV detector presumably represent polysaccharides.

HPLC analysis of mixture of standard proteins on column Biosep 4000; injection - 5 ul; detection – UV. Samples - thyroglobulin (MW 669,000) – 7.774 min., IgA (MW 300,000) – 8.586 min., IgG (MW 150,000) – 9.532 min., ovalbumin (MW 44,000) – 10.235 min., myoglobin (MW 17,000) – 10.932 min and uridine (MW 244) – 11.958 min.

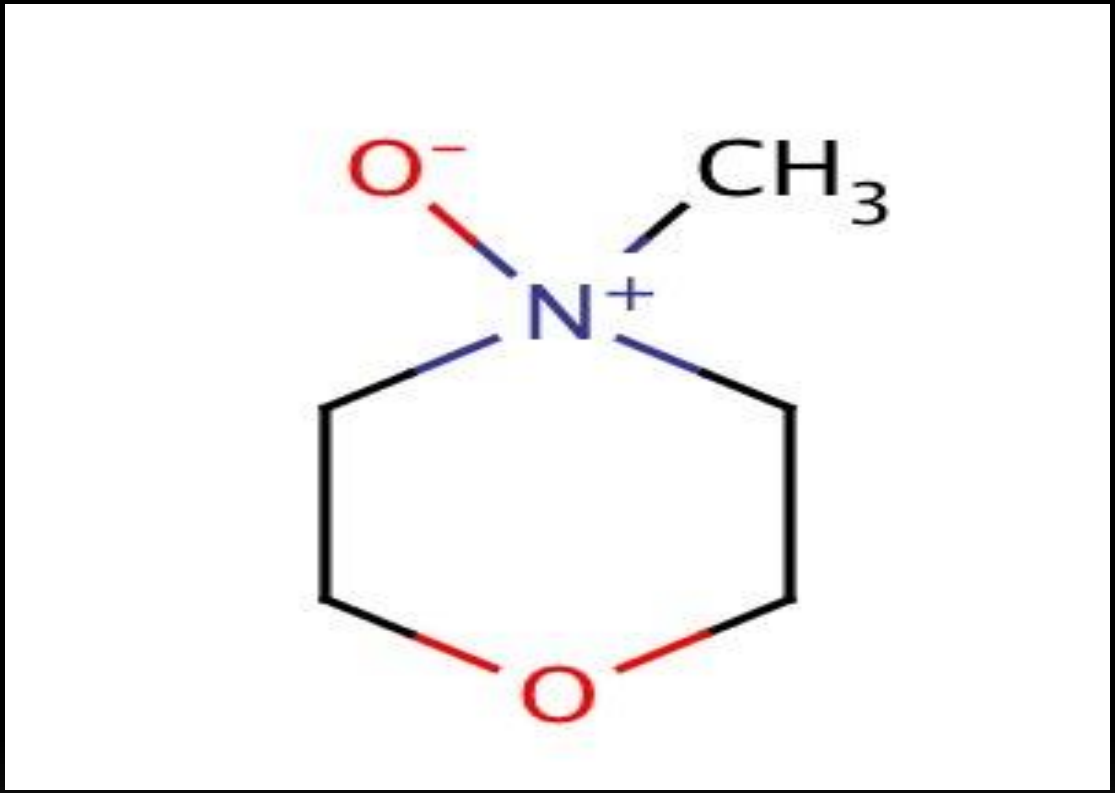


Then the racemic monomer (4) of novel caffeic acid-derived biopolymer as well as virtually pure its enantiomers (7) and (8) were synthesized for the first time via Sharpless asymmetric dihydroxylation (AD) of *trans*-caffeic acid derivatives using the enantiocomplementary catalysts, $(DHQ)_2$-PHAL and $(DHQD)_2$-PHAL. This procedure was performed with an osmium catalist and a stoichiometric oxidant *N*-methylmorpholine-*N*-oxide (NMO). Enantioselectivity was achieved through the addition of enantiomerically-enriched chiral ligands. Cinchona alkaloid derivatives $(DHQ)_2$-PHAL [1,4-bis(9-O-dihydroquinine)-phthalazine] and $(DHQD)_2$-PHAL [1,4-bis-(9-O-dihydroquinidine)-phthalazine] were used as chiral auxiliaries, respectively.

Synthesis of *rac* syn-2,3-dihydroxy-3-(3,4-dihydroxyphenyl)-propionic acid (4), $[\alpha]_D = 0^0$ (C = 1.0 H_2O); (+)-(*2R,3S*)-2,3-dihydroxy-3-(3,4-dihydroxyphenyl)-propionic acid (DDPPA) (7), $[\alpha]_D = +33.3^0$ (C = 0.48, H_2O); (–)-(*2S,3R*)-2,3-dihydroxy-3-(3,4-dihydroxyphenyl)-propionic acid (DDPPA) (8), $[\alpha]_D = -32.5^0$ (C = 0.40, H_2O).

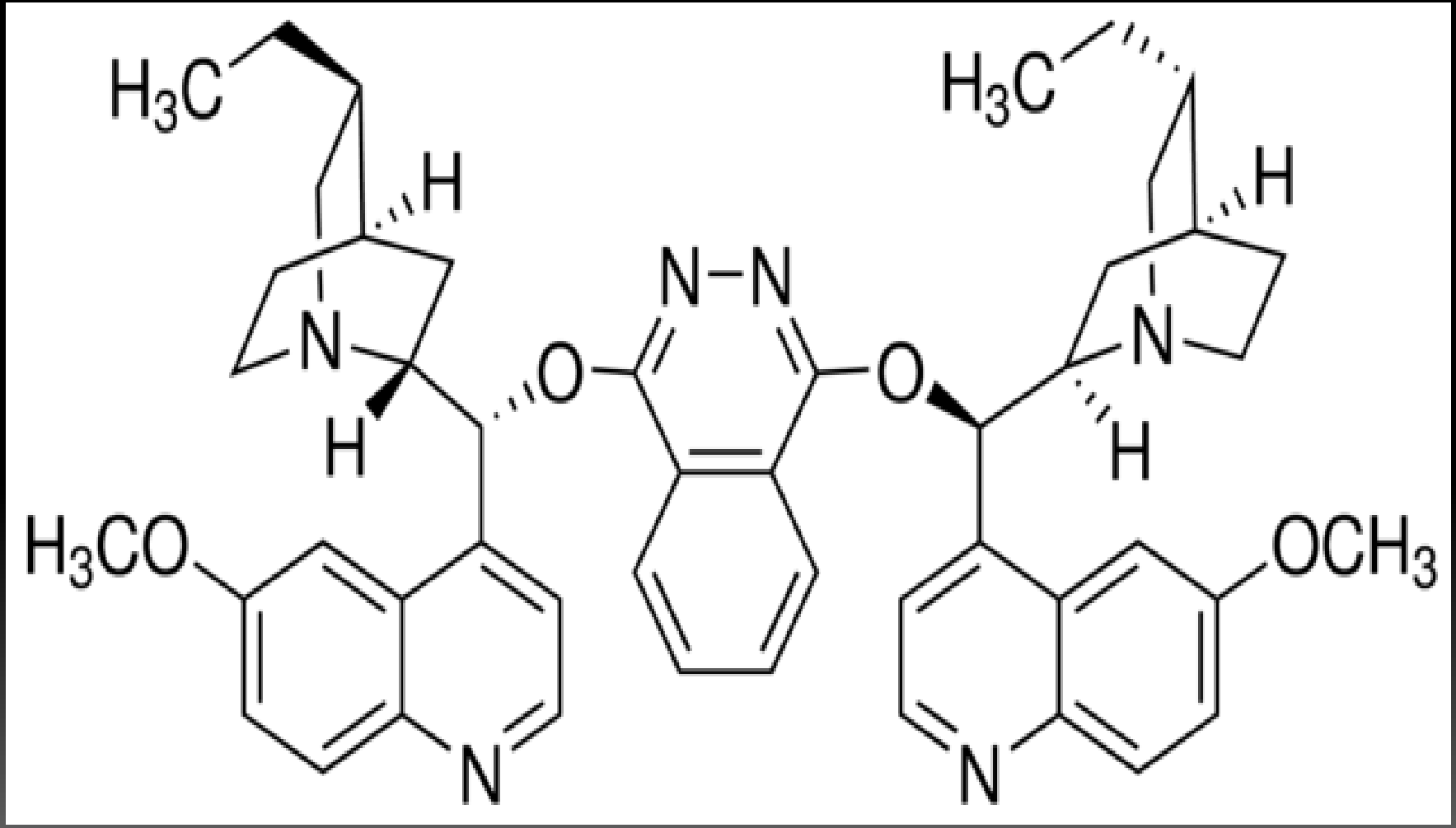
M.Merlani et al., Chirality, 2010, 22, 717-725.

N-Methylmorpholine-*N*-Oxide (NMO)

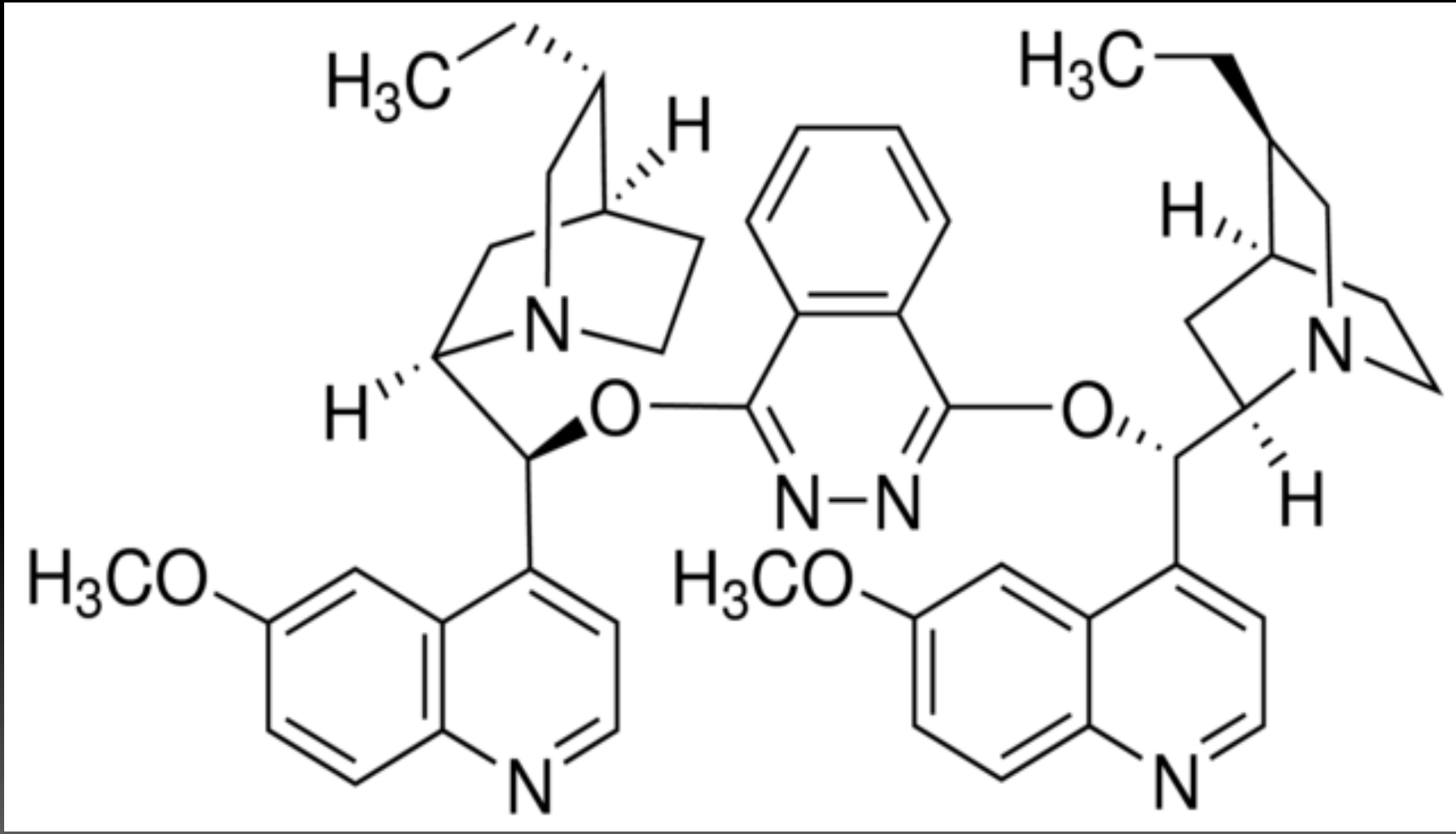


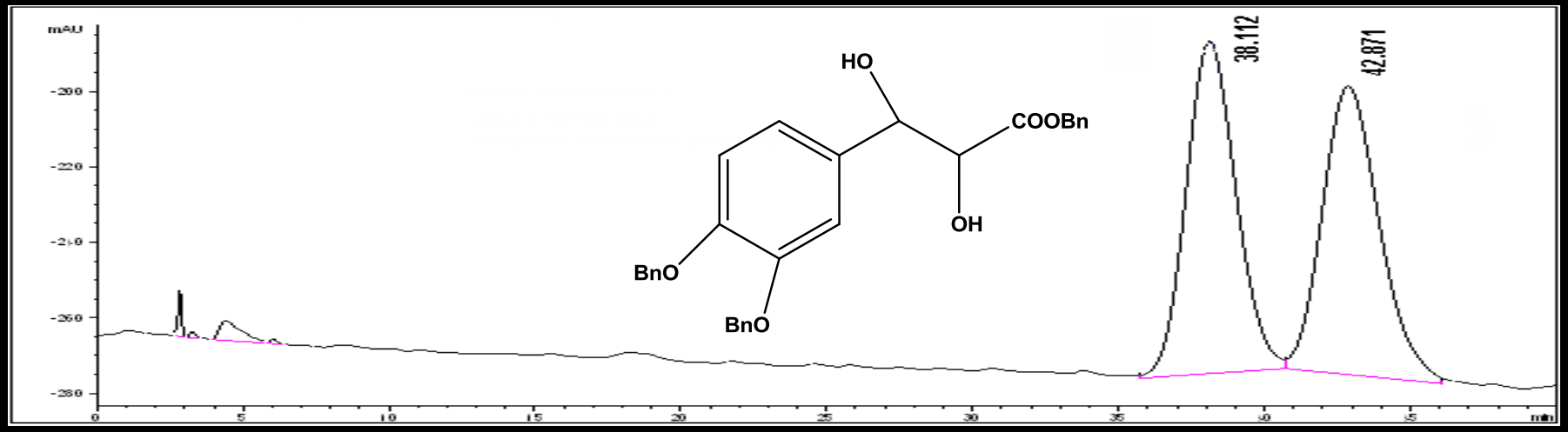
Highly toxic, very expensive and volatile osmium tetroxide can be prepared *in situ* by the oxidation of $K_2OsO_2(OH)_4$ with *N*-methylmorpholine-*N*-oxide (NMO). Besides, NMO is also the cooxidant that enables the use of a catalytic amount of osmium tetroxide, because NMO is able to reoxidize an Os(VI) species to an Os(VIII) species, and thus to regenerate catalytic amount of OsO_4.

A chiral quinine ligand: enantiocomplementary catalyst $(DHQ)_2PHAL$, the phthalazine adduct with dihydroquinine.

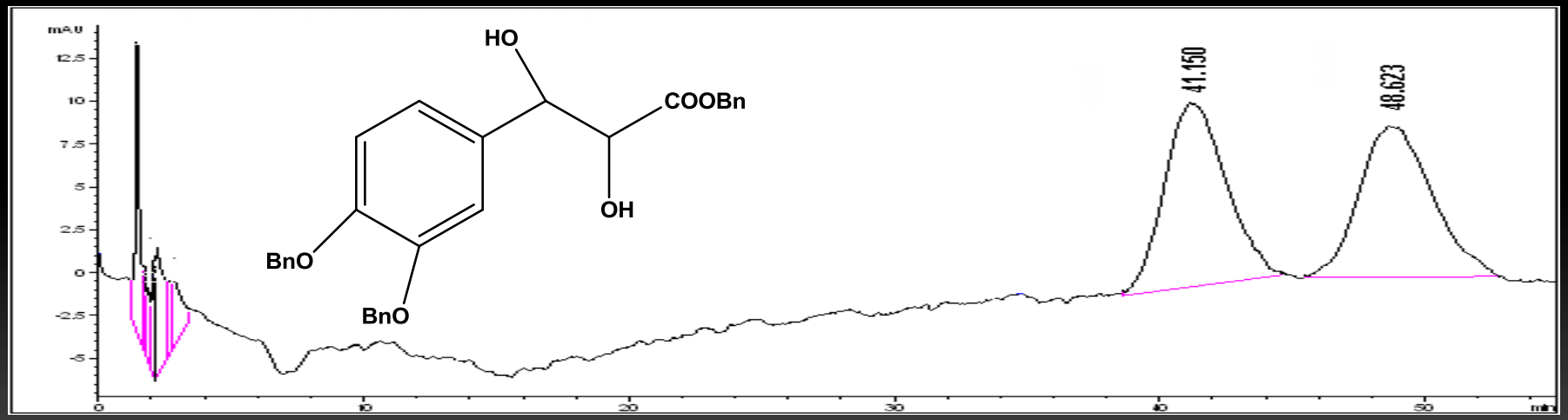


A chiral quinine ligand: enantiocomplementary catalyst $(DHQD)_2PHAL$, the phthalazine adduct with dihydroquinidine.

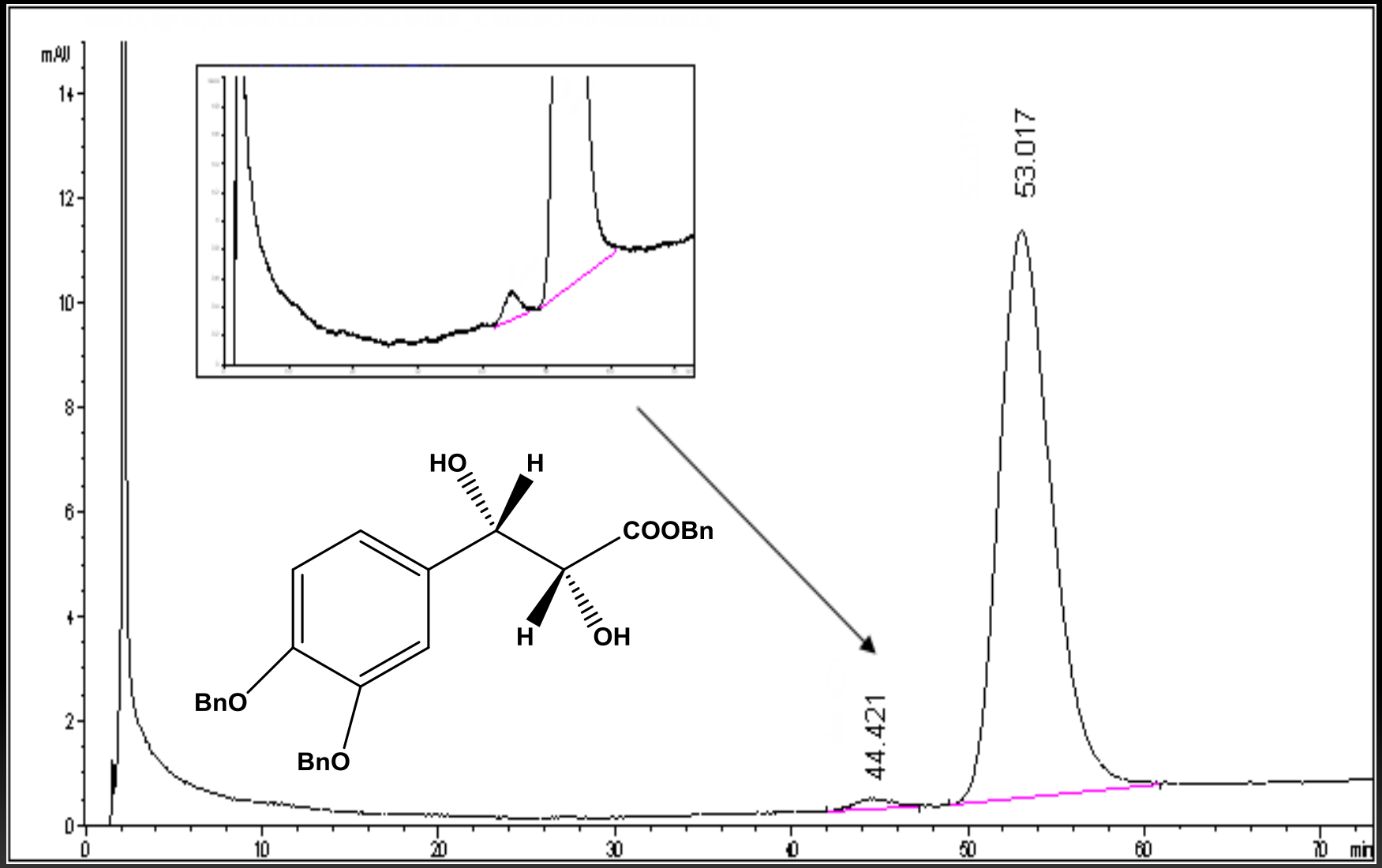




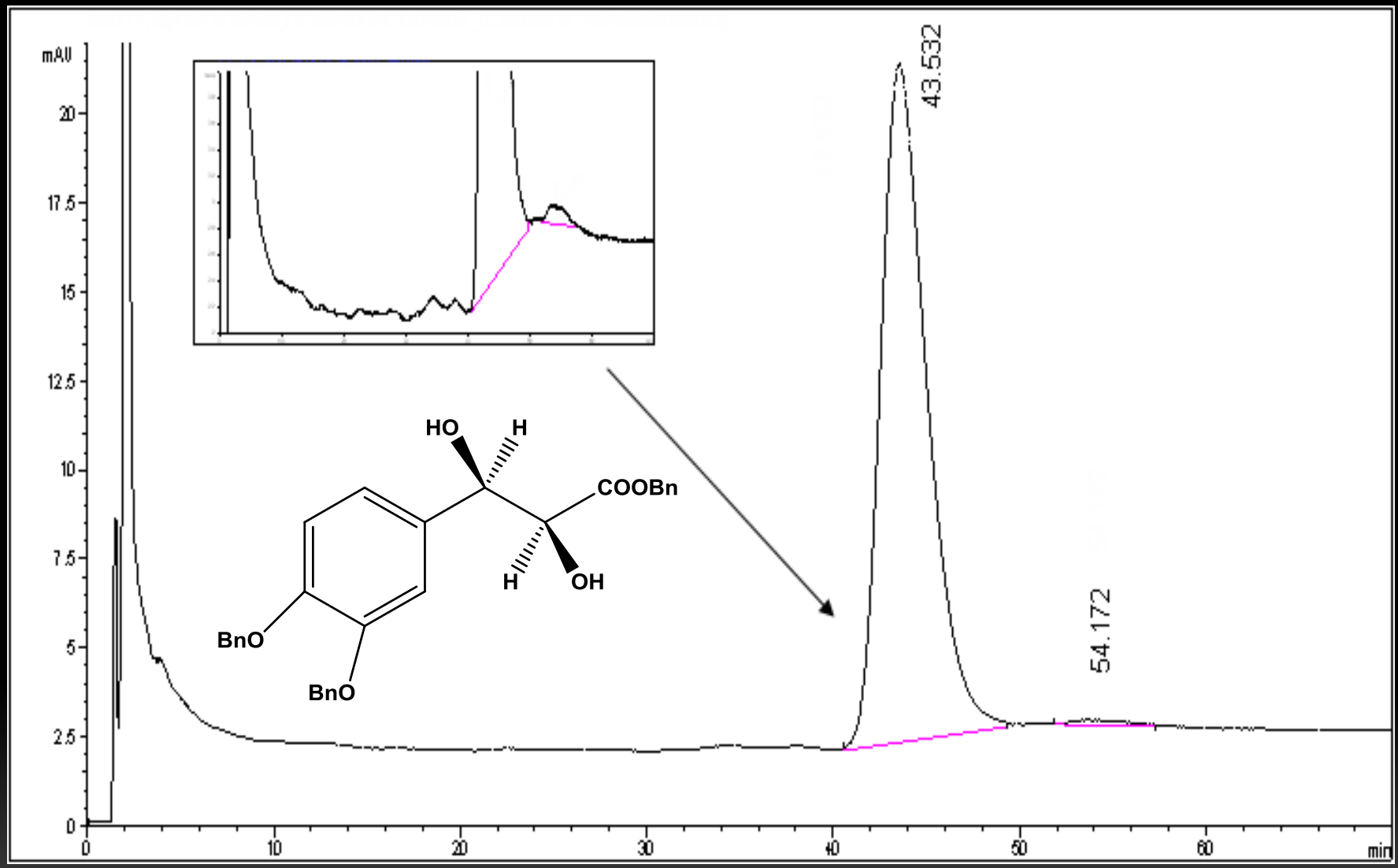
HPLC chromatogram of racemic benzyl-[2,3-dihydroxy-3-(3,4-dibenzyloxyphenyl)]-propionate. Chiral column: Sepapak-4 - [cellulose tris-(4-chloro-3-methylphenylcarbamate] column. Mobile phase: methanol/water, 80/20 (v/v). Flow rate 2.0 ml/min.



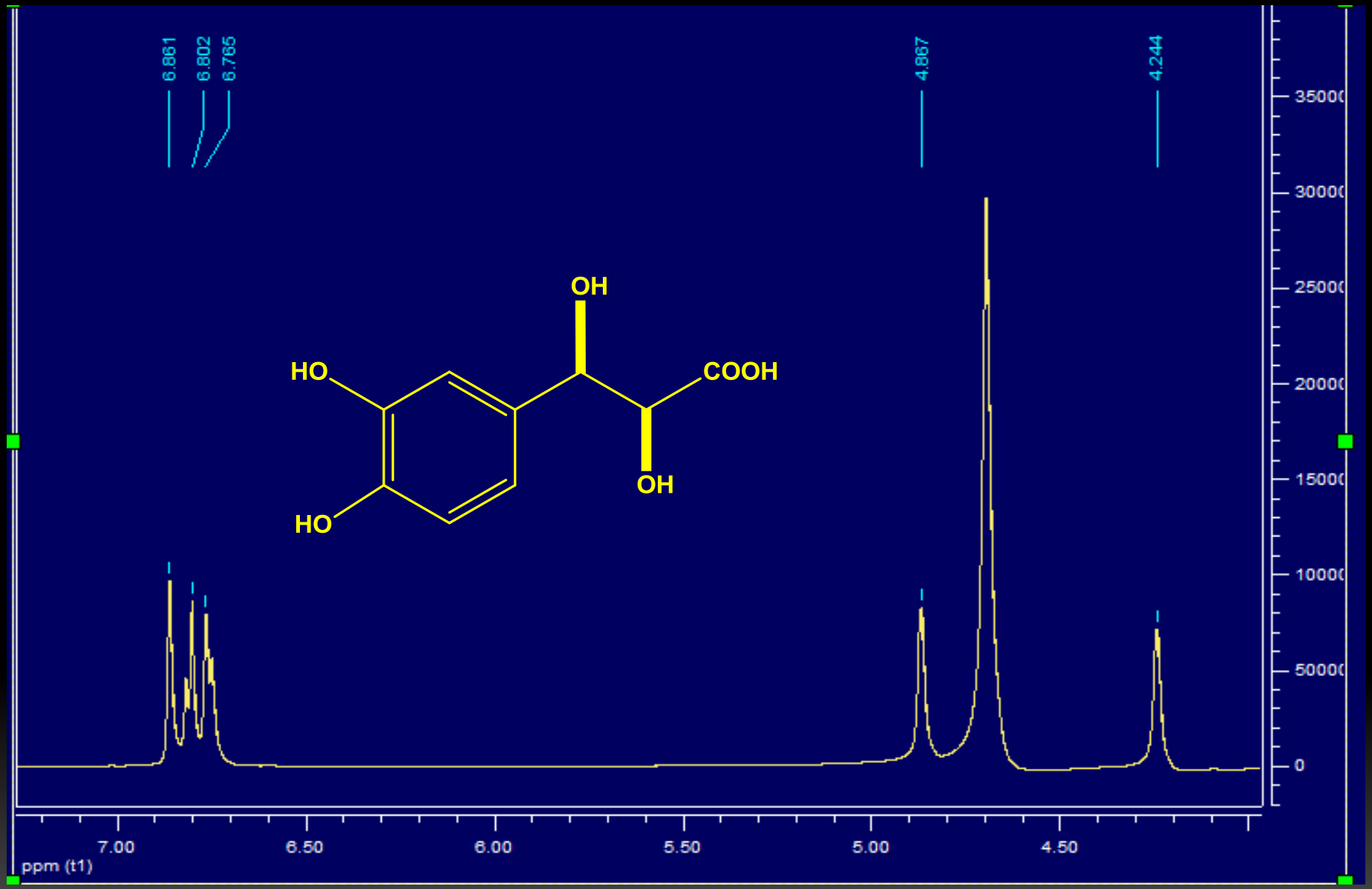
HPLC chromatogram of racemic benzyl-[-2,3-dihydroxy-3-(3,4-dibenzyloxyphenyl)]-propionate. Chiral column: Sepapak-4 - [cellulose tris-(4-chloro-3-methylphenylcarbamate] column. Mobile phase: n-hexane/2-propanol, 85/15 (v/v). Flow rate 2.0 ml/min.



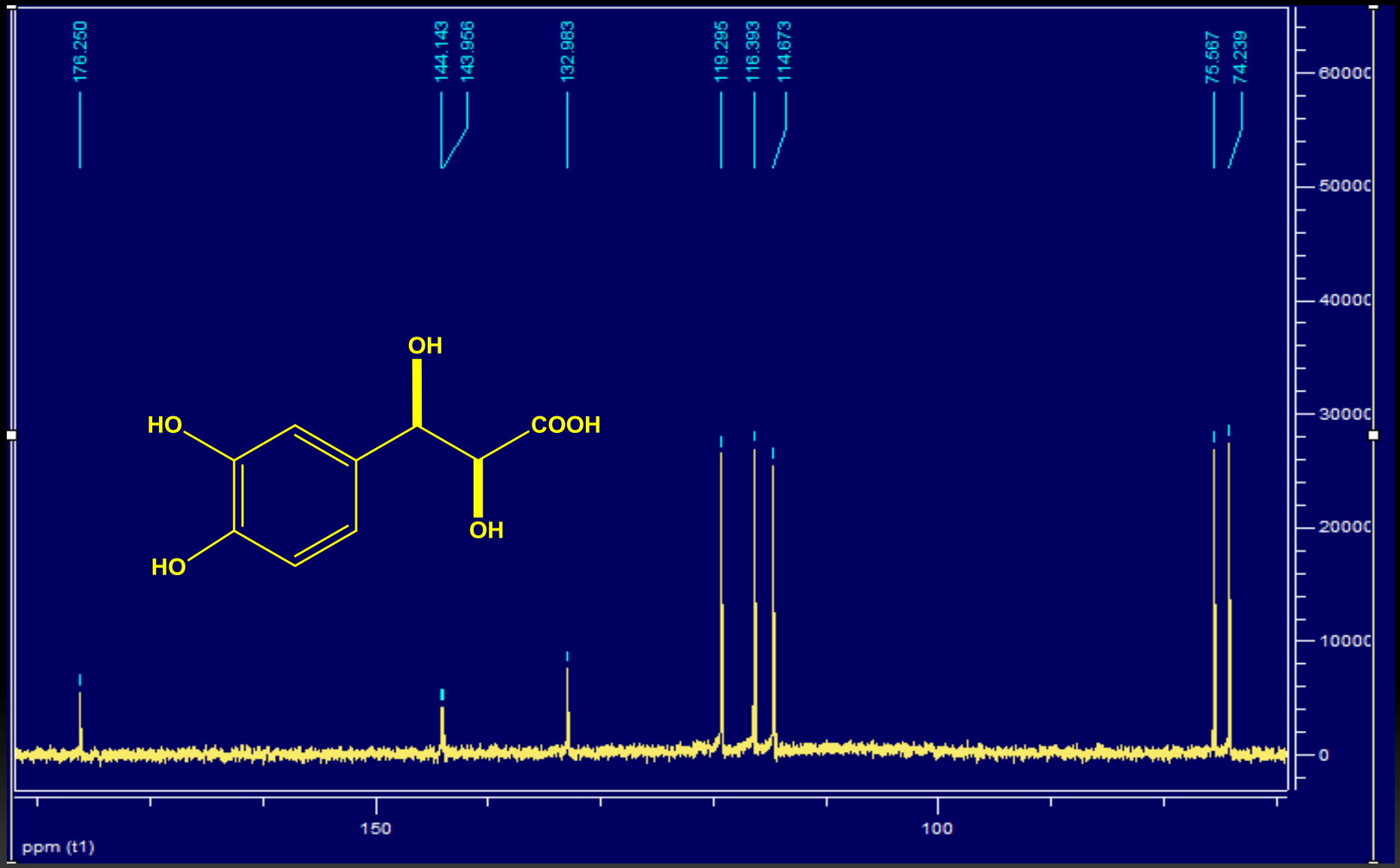
HPLC chromatogram of virtually enantiopure benzyl [(*2R,3S*)-2,3-dihydroxy-3-(3,4-dibenzyloxyphenyl)]-propionate. Chiral column: Sepapak-4 - [cellulose tris-(4-chloro-3-methylphenylcarbamate]; mobile phase: n-hexane/2-propanol, 85/15 (v/v); flow rate 2.0 ml/min. The major product is produced using the chiral auxiliary $(DHQ)_2$-PHAL . (ee = 97.18%).



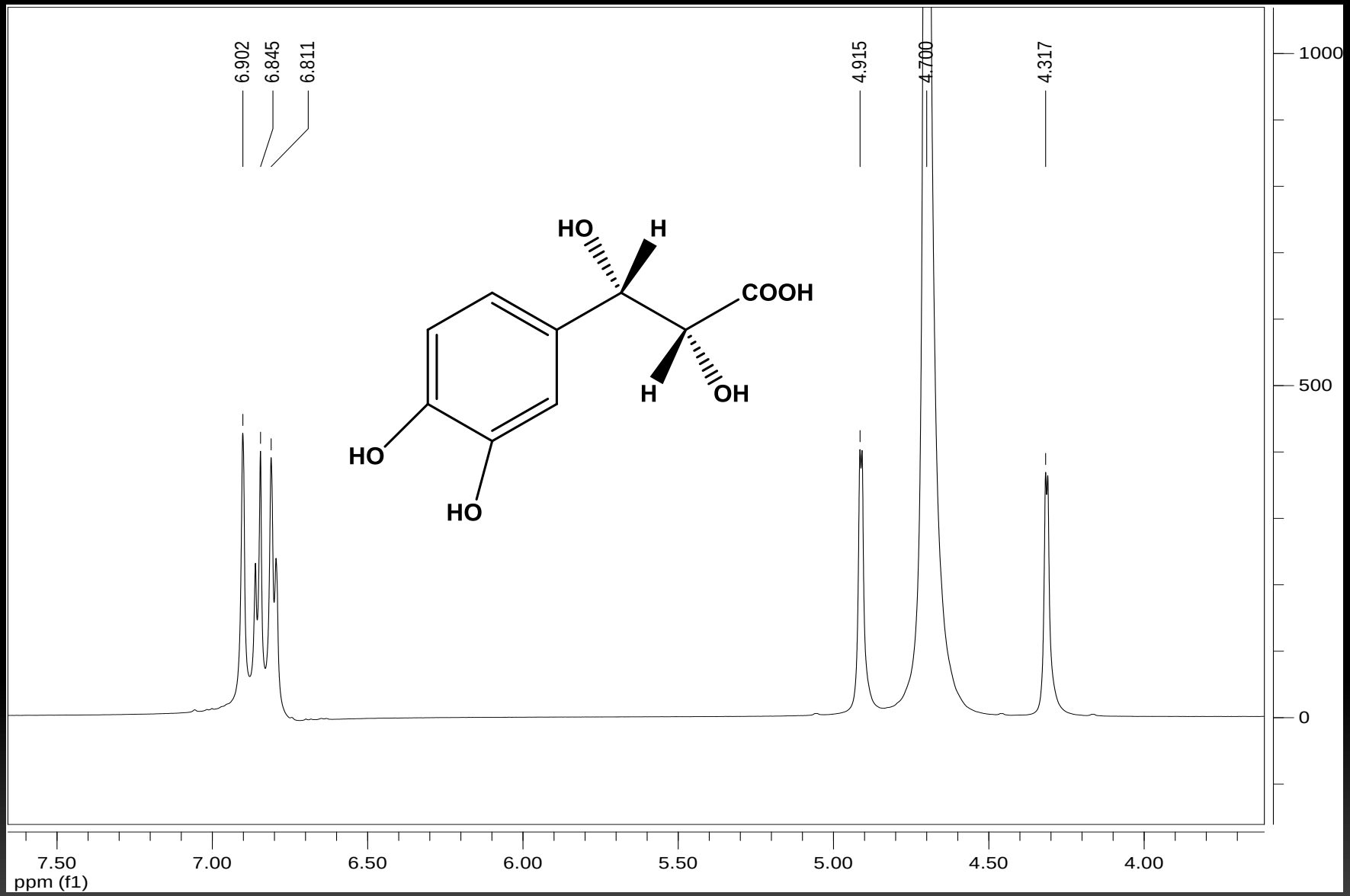
HPLC chromatogram of virtually enantiopure benzyl [(*2S,3R*)-2,3-dihydroxy-3-(3,4-dibenzyloxyphenyl)]-propionate. Chiral column: Sepapak-4 - [cellulose tris-(4-chloro-3-methylphenylcarbamate; mobile phase: n-hexane/2-propanol (85/15 v/v); flow rate 2.0 ml/min. The major product is produced using the chiral auxiliary $(DHQD)_2$-PHAL. (ee = 98.2%).



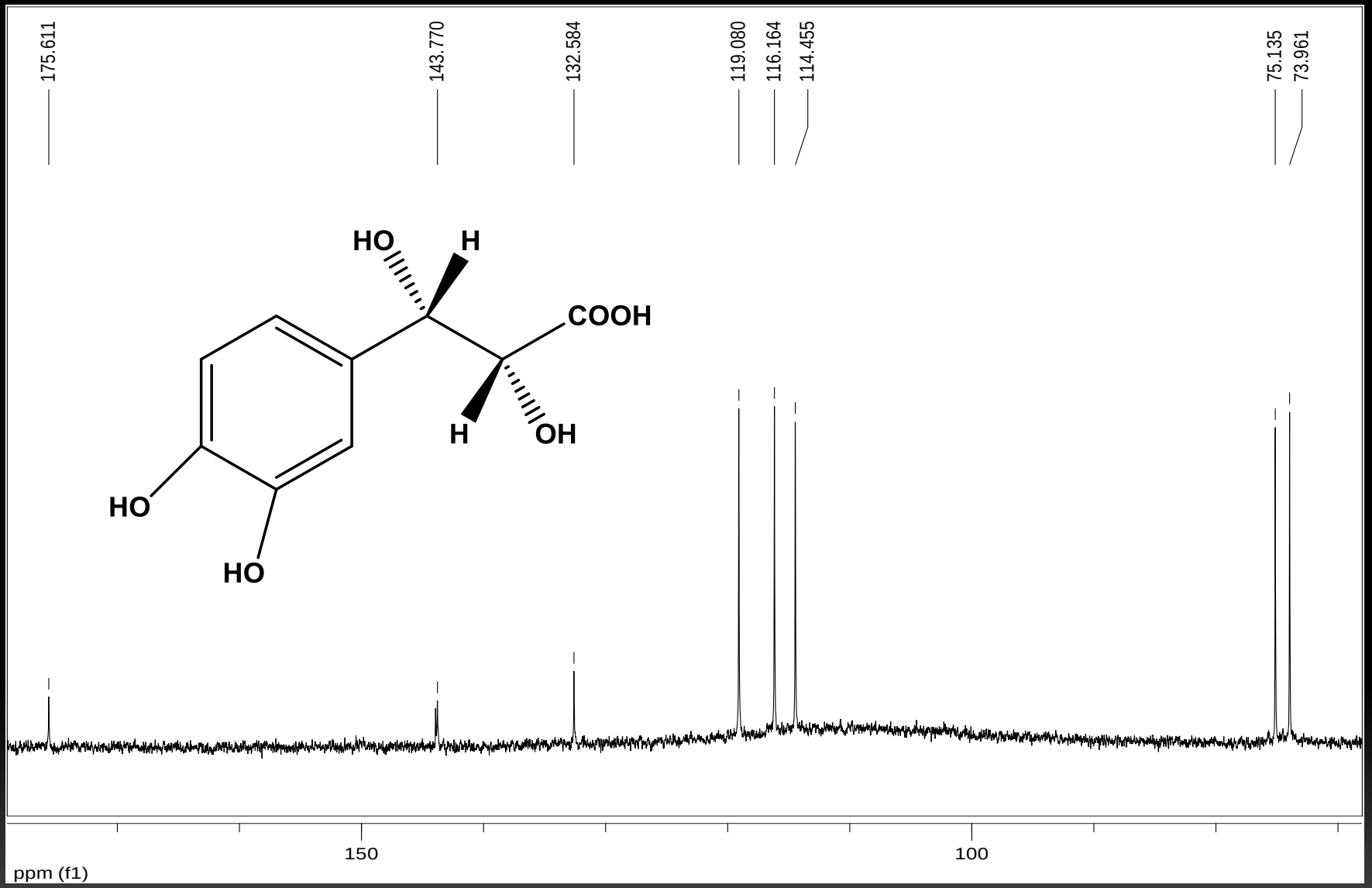
^{1}H NMR (500 MHz, D_2O) spectrum of synthetic racemate *rac syn*-2,3-dihydroxy-3-(3,4-dihydroxyphenyl)-propionic acid (4): δ=6.86 (1H, d, *J*=1.9 Hz), 6.80 (1H, dd, *J*=8.2, 1.9 Hz), 6.77 (1H, d, *J*=8.2 Hz), 4.87(1H, d, *J*=3.4 Hz, β-C<u>H</u>OH), 4.24(1H, d, *J*=3.4 Hz, α-C<u>H</u>OH) ppm.



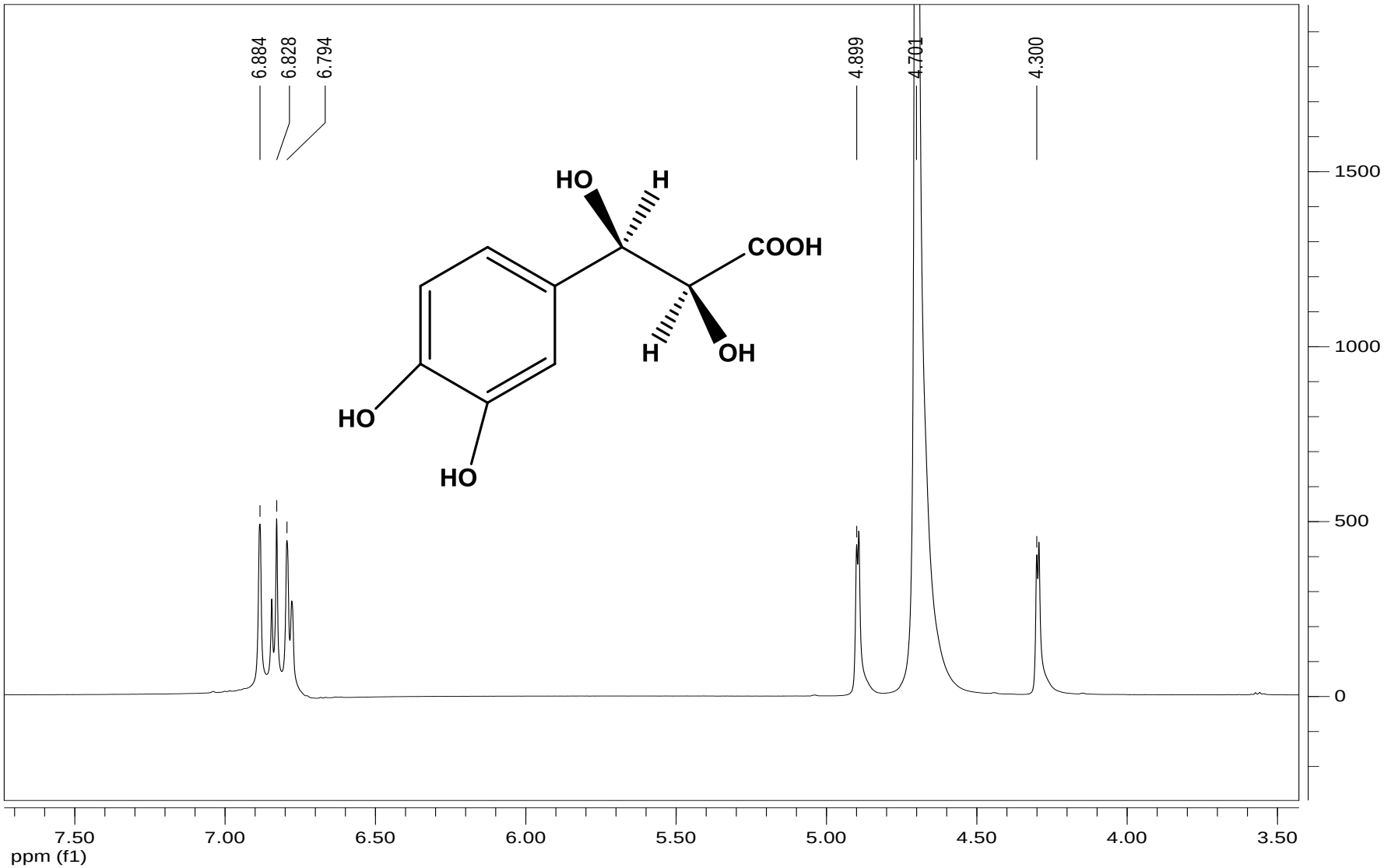
^{13}C NMR (125 MHz, D_2O) spectrum of synthetic racemate *rac syn*-2,3-dihydroxy-3-(3,4-dihydroxyphenyl)-propionic acid (4): δ=176.25 (C=O, carboxylic carbon), 144.14, 143.96, 132.96 ppm (non-protonated carbons), 119.3, 116.39, 114.07 ppm (protonated carbons), 75.57 (β-CHOH), 74.24 (α-CHOH) ppm.



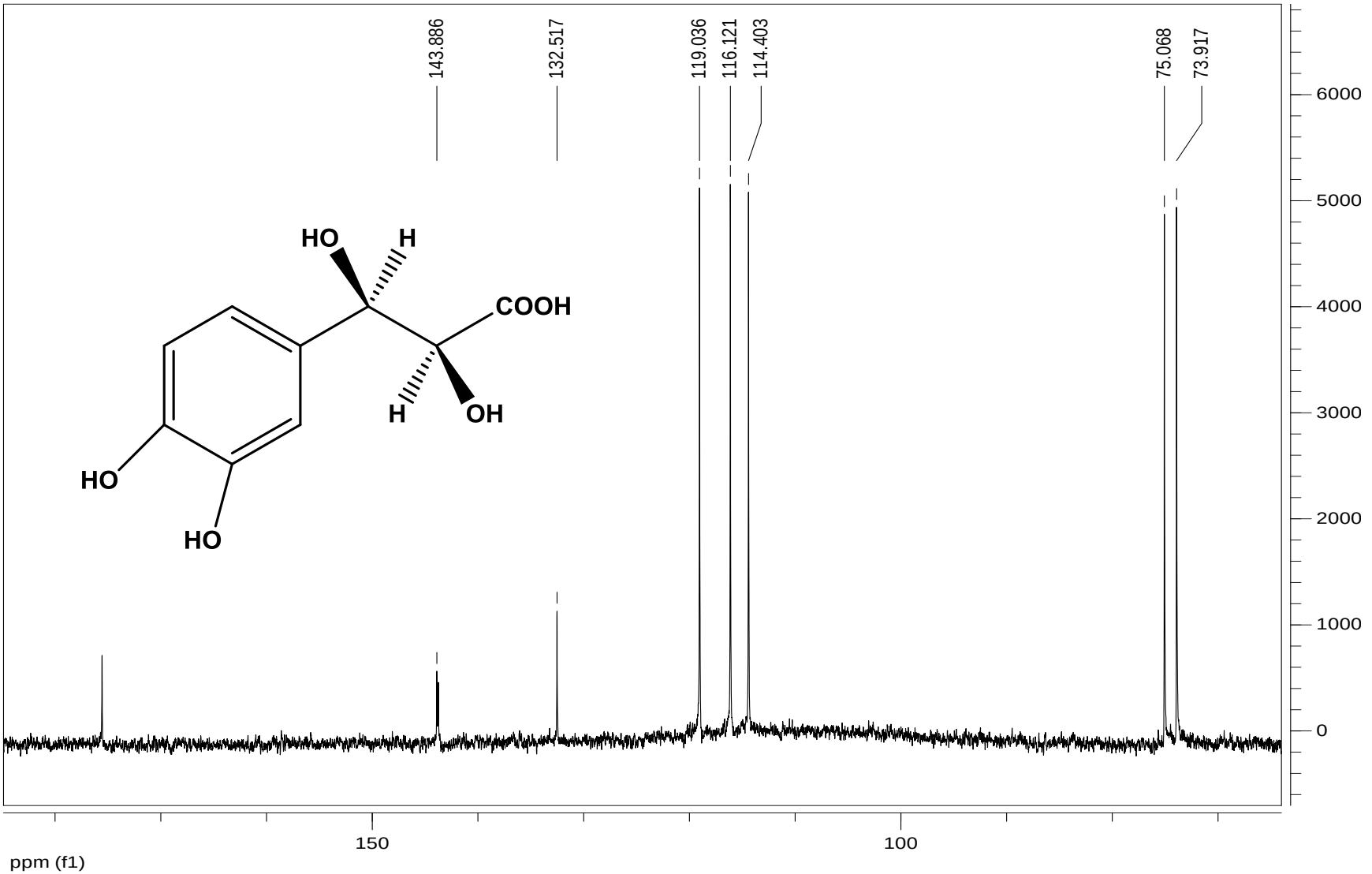
^{1}H NMR (500 MHz, D_2O) spectrum of synthetic enantiomer (+)-*(2R,3S)*-2,3-dihydroxy-3-(3,4-dihydroxyphenyl)-propionic acid (7) (DDPPA): δ=6.90 (1H, d, *J*=1.9 Hz), 6.85 (1H, dd, *J*=8.2, 1.9 Hz), 6.81 (1H, d, *J*=8.2 Hz), 4.92 (1H, d, *J*=3.4 Hz, β-C<u>H</u>OH), 4.32 (1H, d, *J*=3.4 Hz, α-C<u>H</u>OH) ppm.



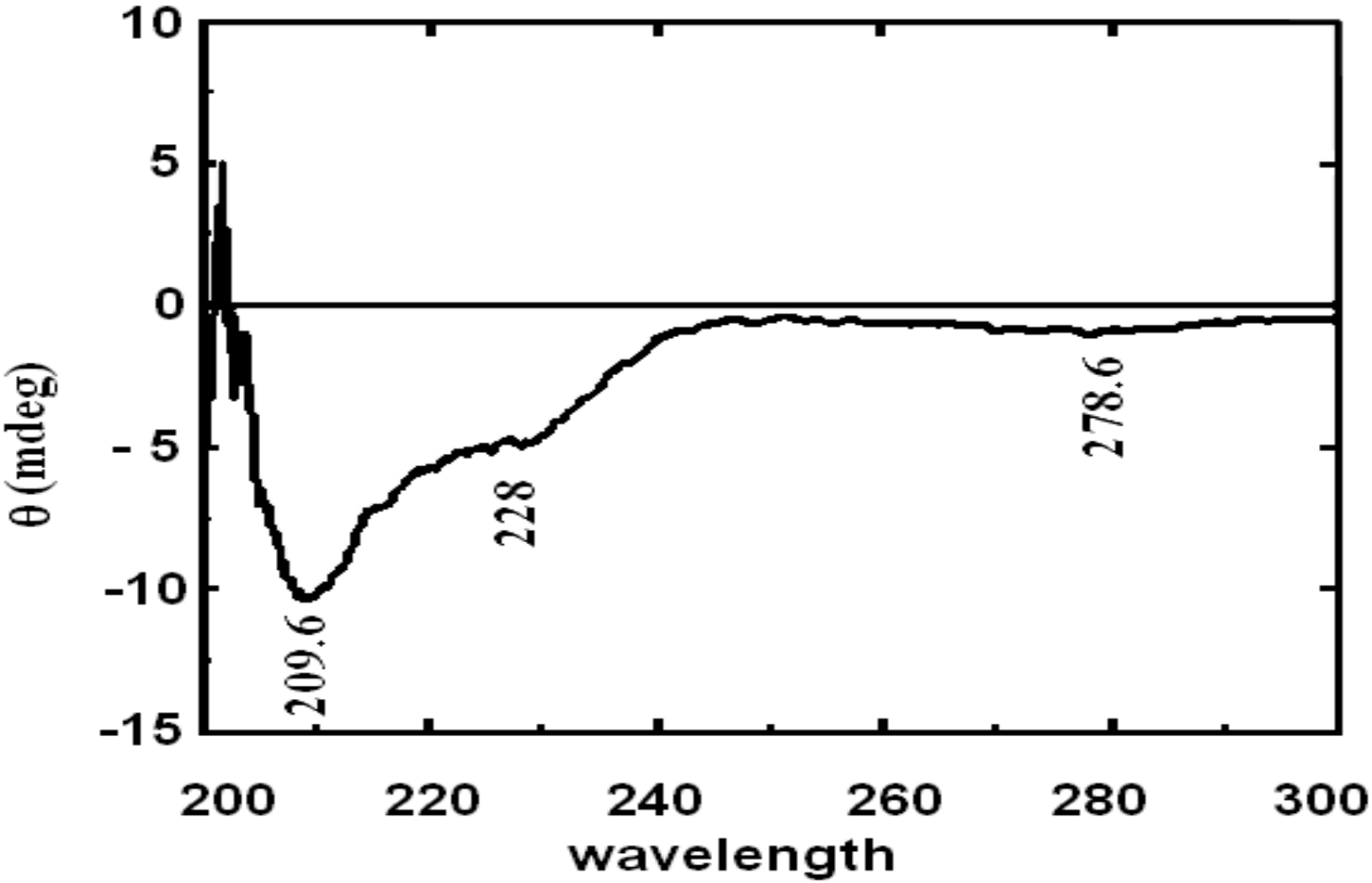
^{13}C NMR (125 MHz, D_2O) spectrum of synthetic enantiomer (+)-*(2R,3S)*-2,3-dihydroxy-3-(3,4-dihydroxyphenyl)-propionic acid (7) (DDPPA): δ=175.6 (C=O, carboxylic carbon), 144.0, 143.77, 132.58 ppm (non-protonated carbons), 119.08, 116.16, 114.46 ppm (protonated carbons), 75.14 (β-CHOH), 73.96 (α-CHOH) ppm.



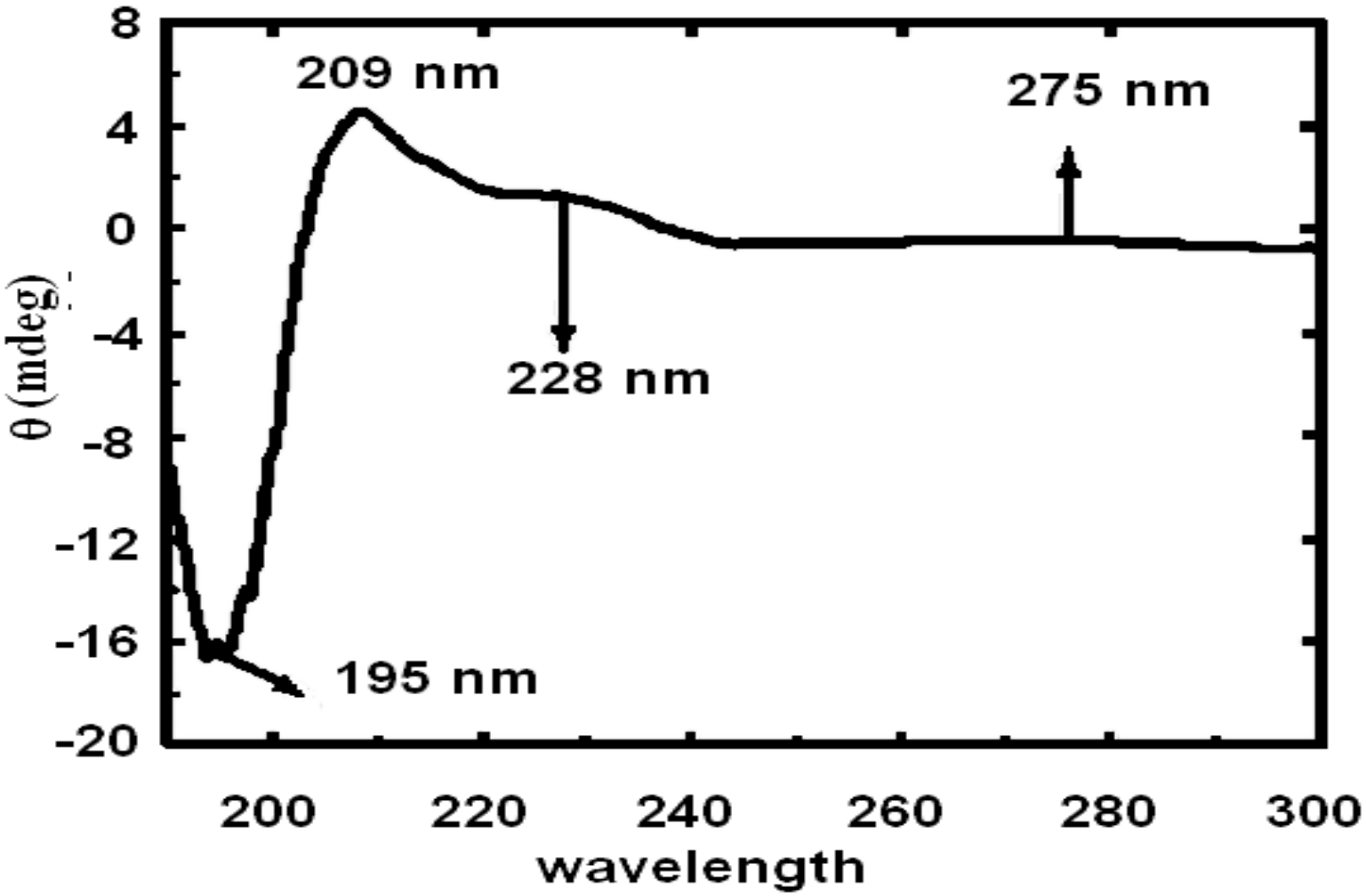
^{1}H NMR (500 MHz, D_2O) spectrum of synthetic enantiomer (–)-*(2S,3R)*-2,3-dihydroxy-3-(3,4-dihydroxyphenyl)-propionic acid (8) (DDPPA): δ=6.88 (1H, d, *J*=1.9 Hz), 6.82 (1H, dd, *J*=8.2, 1.9 Hz), 6.79 (1H, d, *J*=8.2 Hz), 4.90 (1H, d, *J*=3.4 Hz, β-C<u>H</u>OH), 4.30 (1H, d, *J*=3.4 Hz, α-C<u>H</u>OH) ppm.



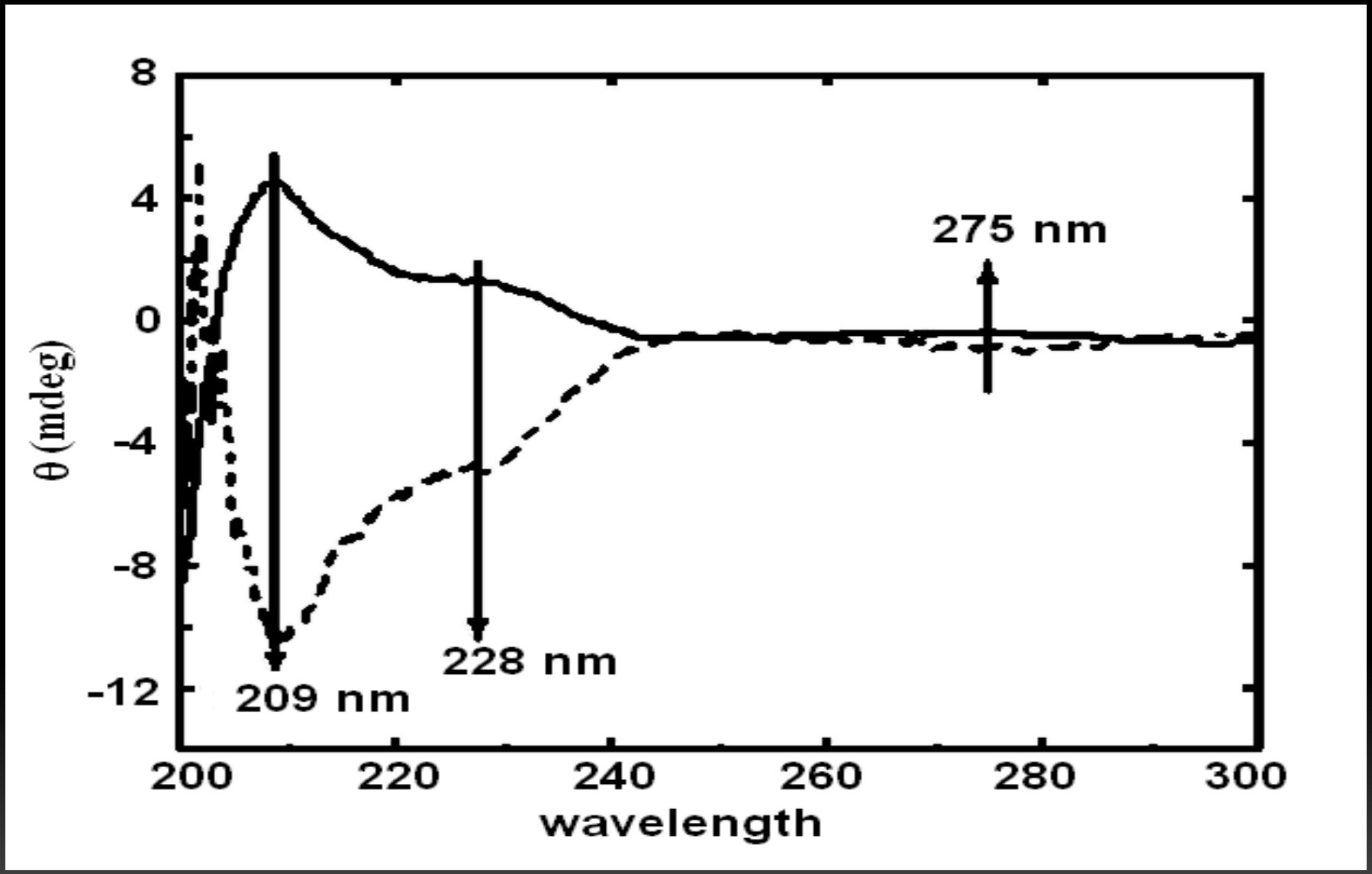
^{13}C NMR (125 MHz, D_2O) spectrum of synthetic enantiomer (–)-*(2S,3R)*-2,3-dihydroxy-3-(3,4-dihydroxyphenyl)-propionic acid (8) (DDPPA): δ=176.0 (C=O, carboxylic carbon), 144.1, 143.89, 132.52 ppm (non-protonated carbons), 119.04, 116.12, 114.40 ppm (protonated carbons), 75.07 (β-CHOH), 73.92 (α-CHOH) ppm.



Circular dichroism (CD) (C=0.5×10^{-3} M, H_2O): $\Delta\varepsilon_{275}$ −1, $\Delta\varepsilon_{228}$ −5, $\Delta\varepsilon_{209}$ −10.5 of (+)-(*2R,3S*)-2,3-dihydroxy-3-(3,4-dihydroxyphenyl)-propionic acid (DDPPA) (7).



CD (C=0.56×10^{-3} M, H_2O): $\Delta\varepsilon_{275}$ −0.4, $\Delta\varepsilon_{228}$ +2.5, $\Delta\varepsilon_{209}$ +4.8 of (−)-(*2S,3R*)-2,3-dihydroxy-3-(3,4-dihydroxyphenyl)-propionic acid (DDPPA) (8).



CD of (+)-(*2R,3S*)-2,3-dihydroxy-3-(3,4-dihydroxyphenyl)-propionic acid (DDPPA) (7) and (−)-(*2S,3R*)-2,3-dihydroxy-3-(3,4-dihydroxyphenyl)-propionic acid (DDPPA) (8).

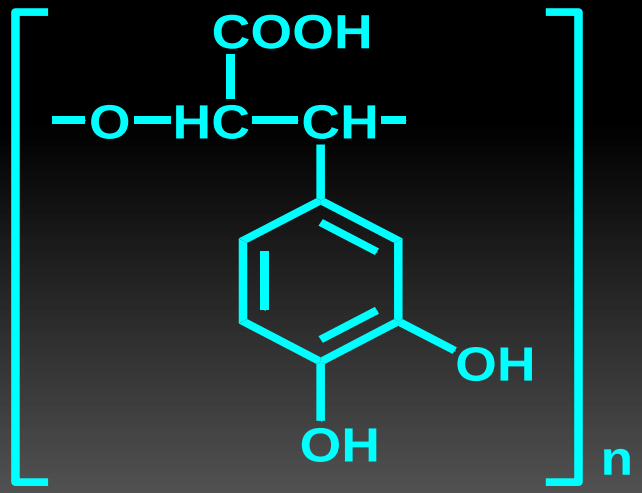
Measured antioxidant activities of racemic 4 and virtually enantiopure products 7 and 8 as well as those of natural polyether isolated from the roots of *S. asperum* and trans-caffeic acid against hypochlorite and DPPH-radicals.

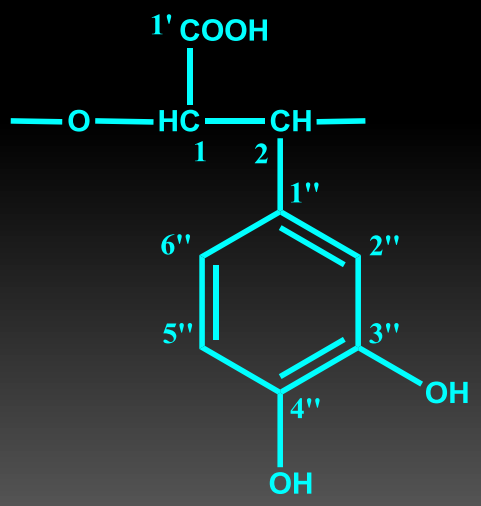
Compound	Antioxidant activity (IC50*, μg/ml)	
	DPPH-method	CL-method
rac 2,3-Dihydroxy-3-(3,4-dihydroxyphenyl)-propionic acid (4)	3,8±0,3	2,8±0,2
(+)-(2R,3S)-2,3-Dihydroxy-3-(3,4-dihydroxyphenyl)-propionic acid (7)	4,1±0,4	3,2±0,3
(-)-(2S,3R)-2,3-Dihydroxy-3-(3,4-dihydroxyphenyl)-propionic acid (8)	3,9±0,2	3,0±0,2
Poly-[oxy-1-carboxy-2-(3,4-dihydroxyphenyl)-ethylene]	146,5±7,6	120,4±9,8
trans-Caffeic acid	12,2±0,7	9,4±0,5

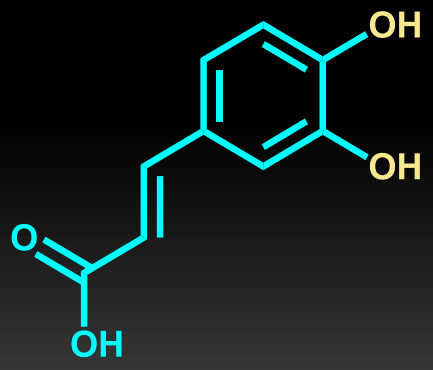
* IC_{50} ± standard deviation (n=4)

IN SUMMARY

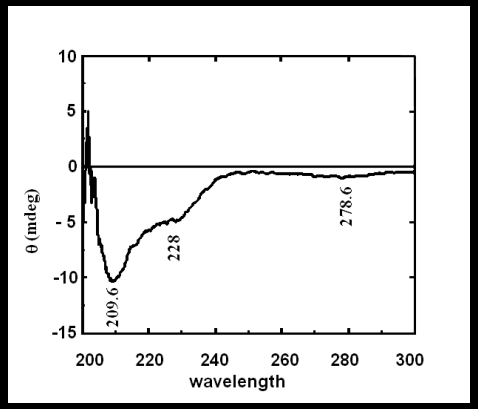
Thus, our results help conclude that one and the same poly[oxy-1-carboxy-2-(3,4-dihydroxyphenyl)ethylene] is the main structural element of high-molecular water-soluble preparations isolated from *Symphytum* and *Anchusa* species. This compound is a representative of a new class of natural polyethers with a residue of 3-(3,4-dihydroxyphenyl)glyceric acid as the repeating unit. We have no information on the biosynthesis of such a polymer in plants, but, from the chemical viewpoint, this process can be conceived as the epoxidation of the double bond in caffeic acid followed by the polymerization of the resulting epoxide. Further study should clarify the physiological function of these polyethers in plants and demonstrate whether their biosynthesis is the unique property of the genera *Symphytum* and *Anchusa* or whether such compounds are also generated in other plants. The determination of the structural importance of residual carbohydrates will be the subject of further work. The repeating unit of this polyether contains two asymmetric carbon atoms, but we do not yet have unambiguous data on the chirality of these centers. However, we have some information on that score.



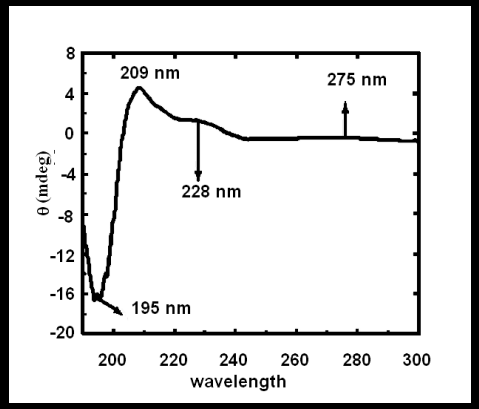




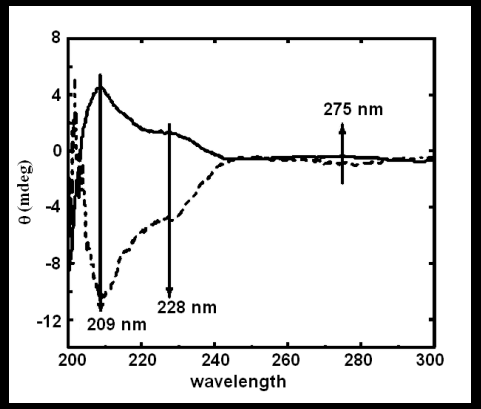
Caffeic acid



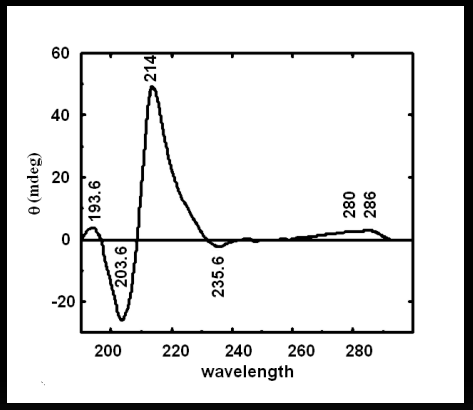
A



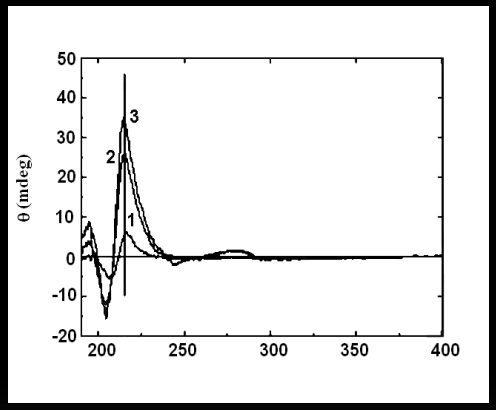
B



C



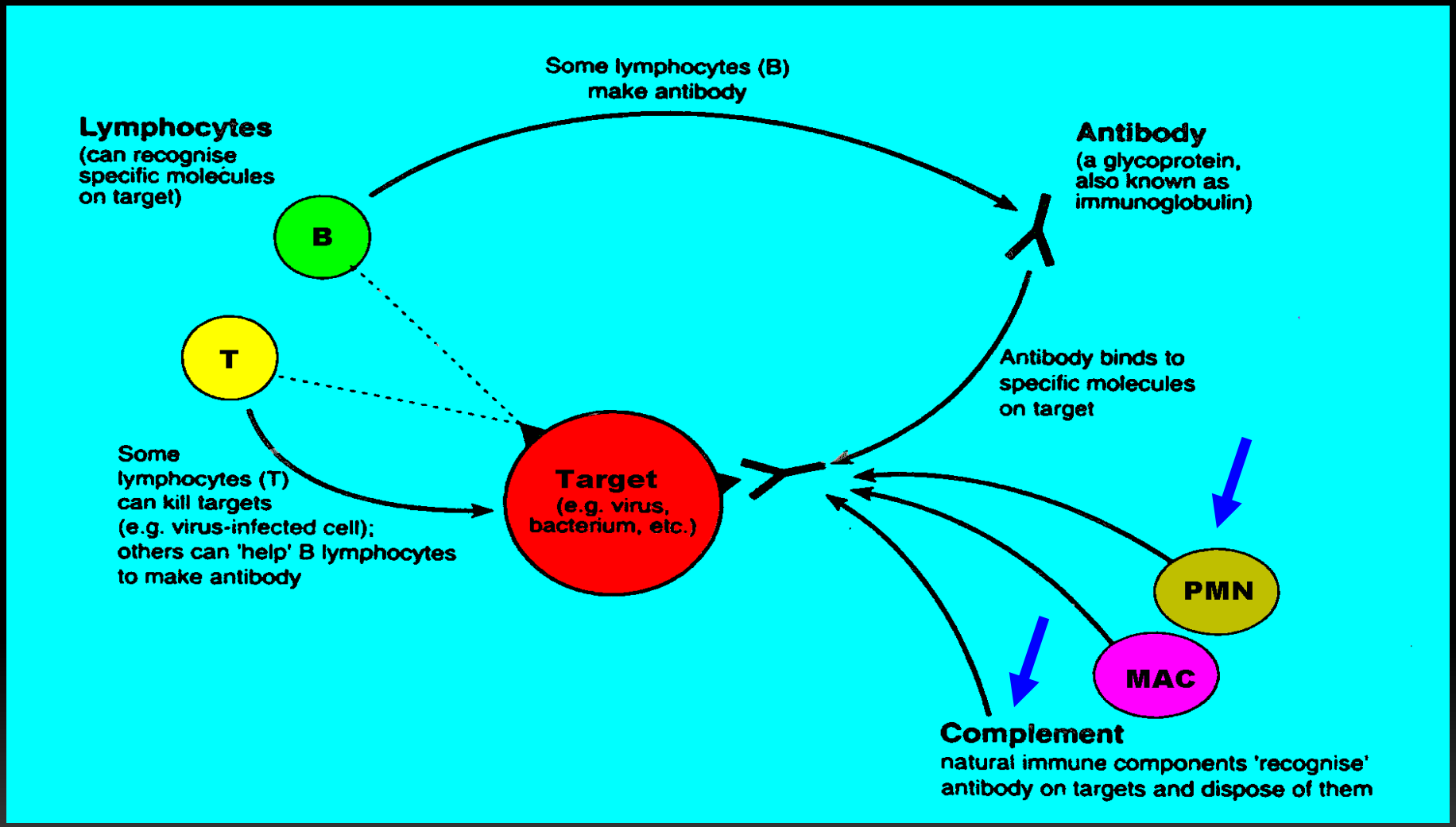
D



E

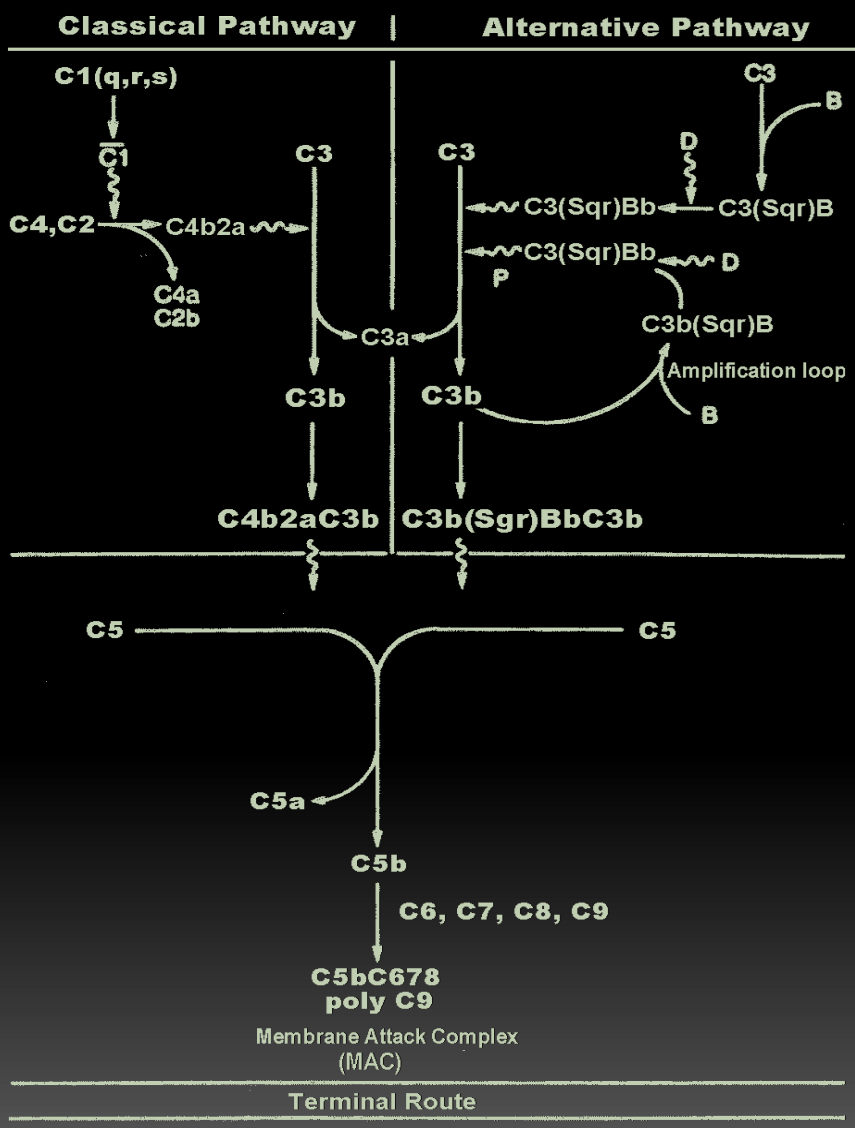
Cotton effects at 195, 209, 228 and 275 nm in CD spectra of (+)-(*2R,3S*)- and (–)-(*2S,3R*)-2,3-dihydroxy-3-(3,4-dihydroxyphenyl)-propionic acid (DDPPA) – (Figs. A, B) correspond to Cotton effects at the 204, 214, 236 and 286 nm in CD spectra of HMP-SA, SC, SO and AI. Besides, as the profiles of CD spectra of polymers [Figs. D (SA) and E - (SC-1), (SO-2), (AI-3)] do not coincide with CD spectra of (*2R,3S*)-DDPPA and (*2S,3R*)-DDPPA (Fig. C) we can exclude (*1R,2S*) and (*1S,2R*) configurations for chiral atoms C1 and C2 in the repeating units of HMP-SA, SC, SO and AI. Hence, we can suppose that C1 and C2 atoms have either (*1R,2R*) or (*1S,2S*) configurations and consequently denomination of polymer could be either poly[oxy-(*1R*)-1-carboxy-(*2R*)-2-(3,4-dihydroxyphenyl)ethylene] or poly[oxy-(*1S*)-1-carboxy-(*2S*)-2-(3,4-dihydroxyphenyl)ethylene].

Factors involved in immune response



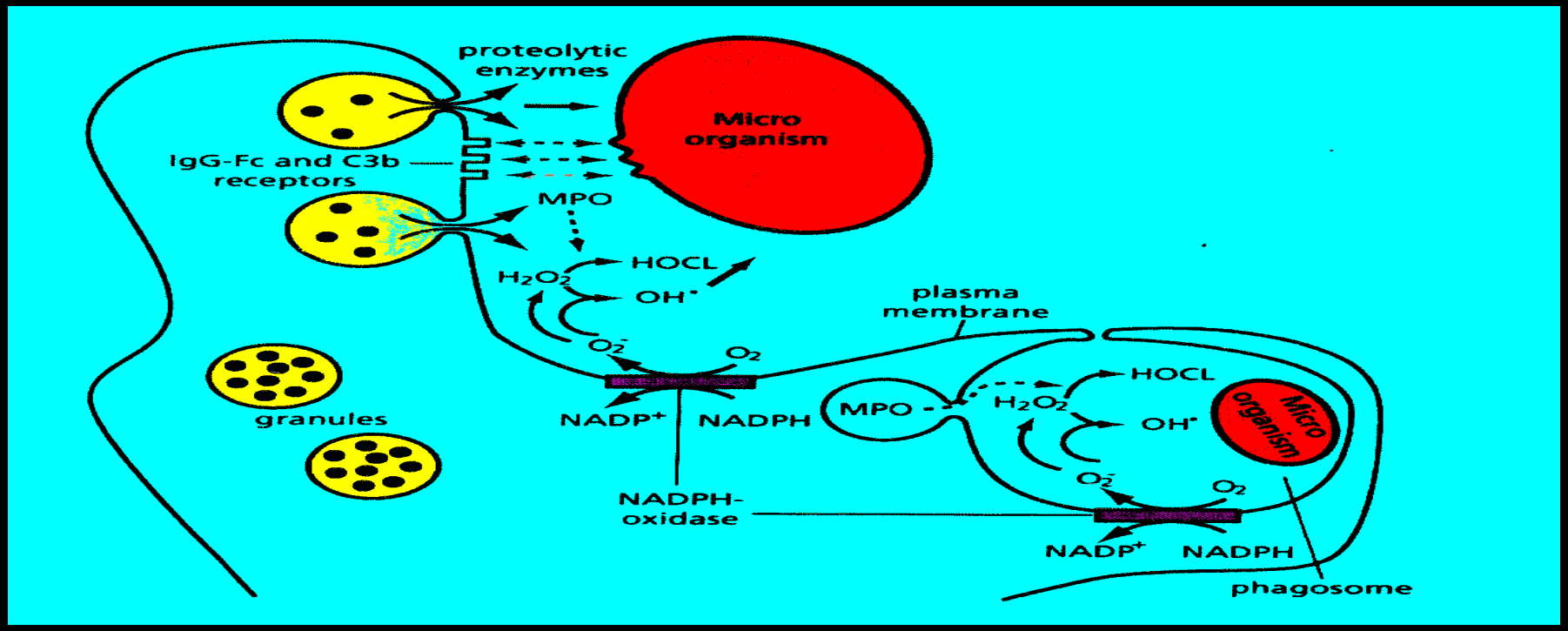
The immunomodulatory activities of caffeic acid-derived polymer were assessed by testing its effect on functional parameters of humoral and cellular branches of the innate immune system. For the humoral part human complement and for the cellular part human polymorphonuclear leukocytes (PMNs) were selected as relevant immune parameters.

Complement Cascade



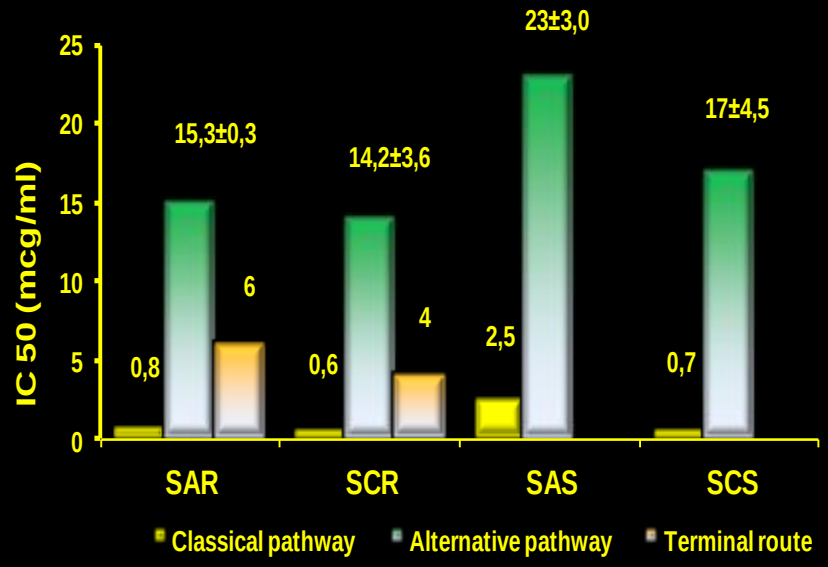
The complement system is one of the primary humoral mechanisms of host defence. Complement functions include promoting inflammation, opsonization of antigenic particles (including microorganisms), and membrane damage of pathogens. However, biological activities of complement are not always beneficial. In auto-immune disorders involving autoantigen-antibody complexes, complement activity can cause severe tissue damage. The man AP, CP, and TR activities can be estimated *in vitro* by using rabbit erythrocytes, antibody-coated sheep erythrocytes, and guinea-pig erythrocytes, respectively. The erythrocytes serve simultaneously as activating surface and as target cells. Activation of complement results in a (partiial) lysis of erythrocytes, and the amount of haemoglobin released is used as parameter of complement activity.

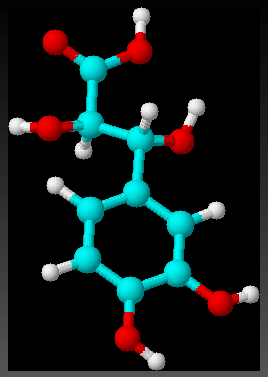
ROS Production in PMNs upon Phagocytosis

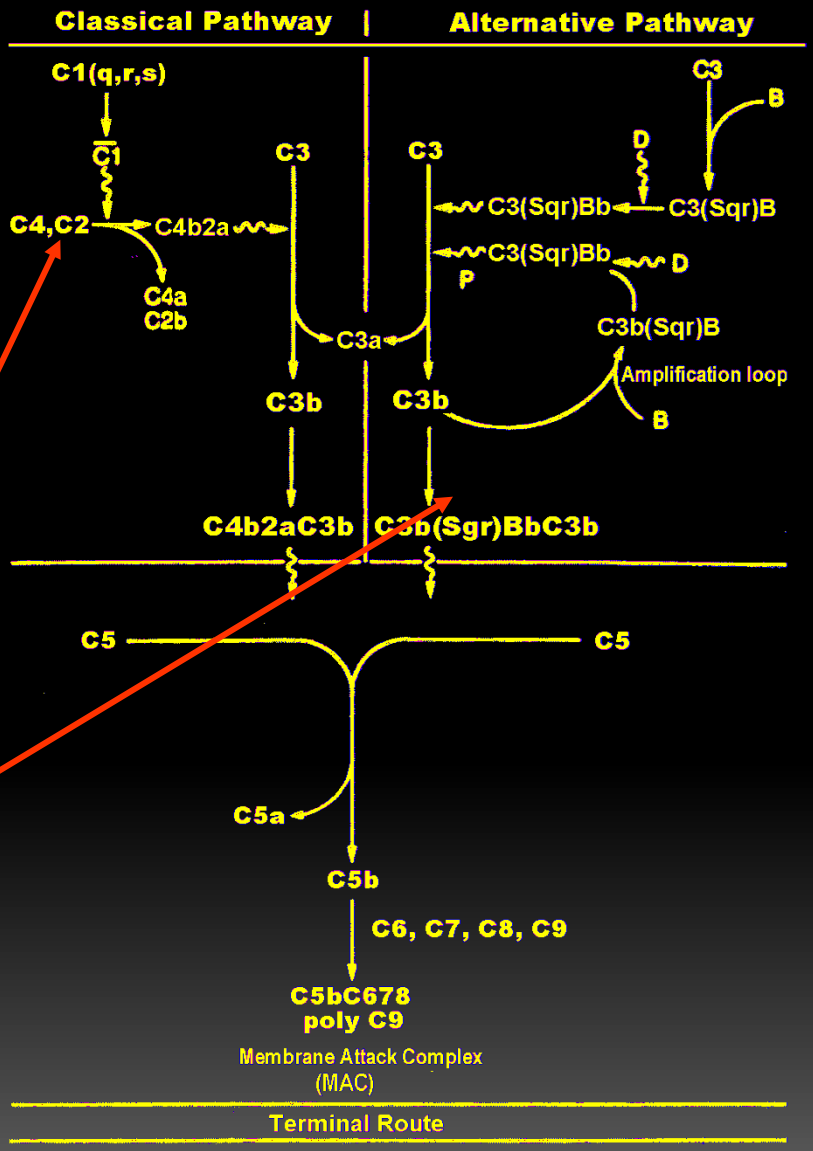


Upon phagocytosis, stimulated polymorphonuclear neutrophils (PMNs) produce reactive oxygen species (ROS): superoxide anions which formation is catalyzed enzimatically by NADPH-oxidase ($\cdot O^{2-}$) is regarded as a low toxic metabolite. Bacteriocidal and cytotoxic effects are particularly ascribed to other ROS formed by further conversion of superoxide anions, i.e. hydrogen peroxide (H_2O_2), hydroxyl radicals ($\cdot OH$), and hypochlorous acid (HOCI). ROS, produced by stimulated PMNs, play an important role in host defence against invading microorganisms. Upon triggering, PMNs start to consume a large amount of oxygen which is known as the respiratory or oxidative burst. Production of ROS occurs within the cell (phagosome), but also extracellularly, thus causing damage of surrounding tissue. In the assay used, the respiratory burst in human PMNs is initiated with opsonized (C3b complement fragment-coated) zymosan. The production of ROS is quantified as luminol-dependent chemiluminescence. Natural compounds which exhibit anticomplementary activity and/or interfere with ROS production may be useful tools to prevent tissue destruction.

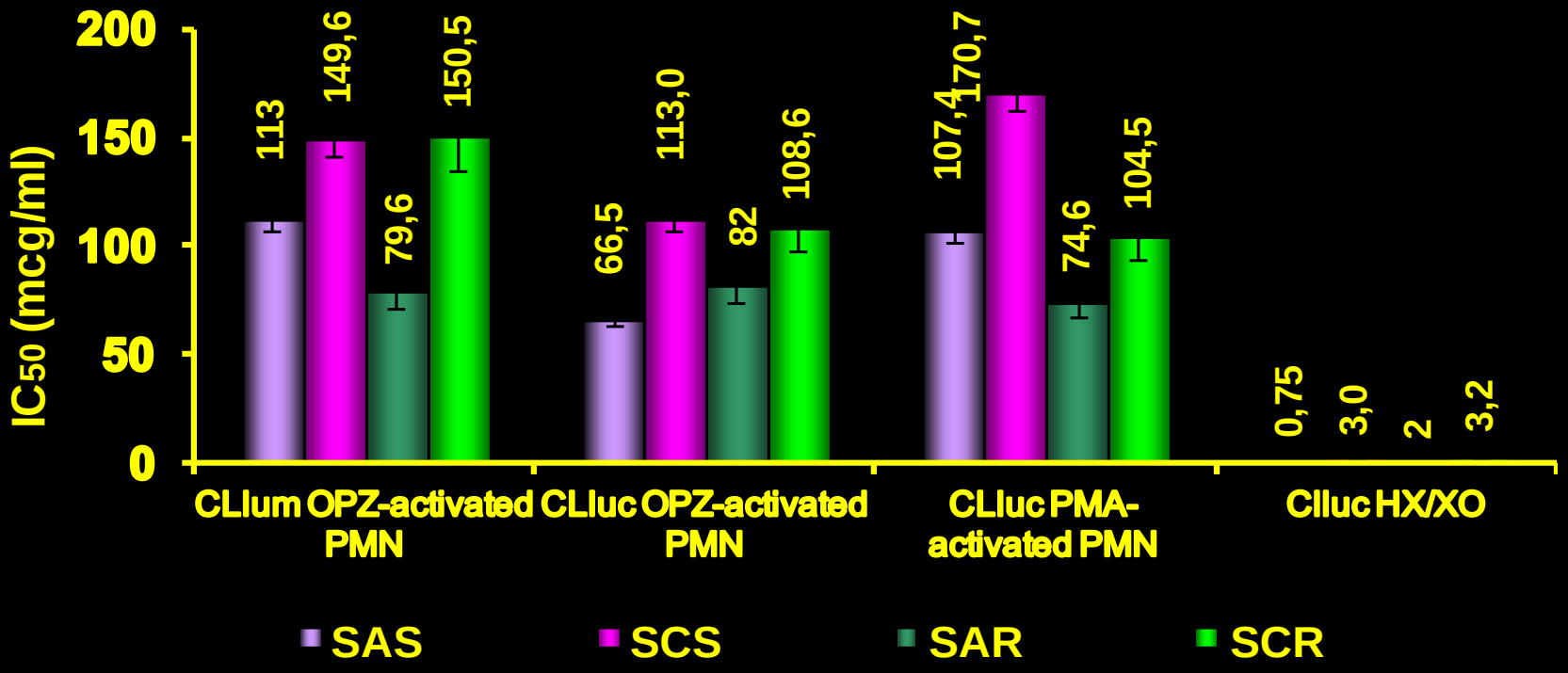
Anticomplementary activity of *Symphytum* polymer





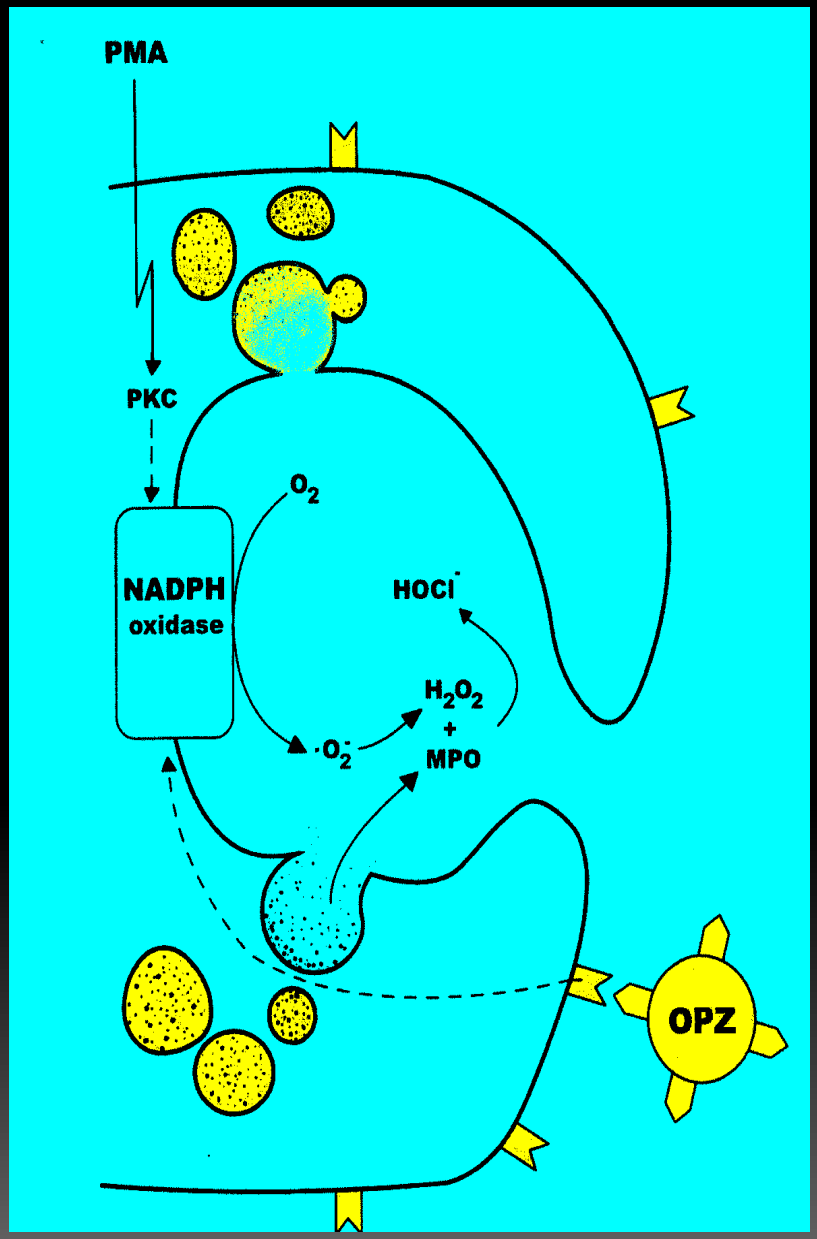


Antioxidant activities of *Symphytum* polymer



Receptor-dependent opsonized zymosan (OPZ) (C3b complement fragment is opsonizing agent), and receptor-independent phorbol myristate acetate (PMA), both stimulate the superoxide anions-generating NADPH-oxidase. The ability of caffeic acid-derived polymer from SAR, SCR, SAS and SCS to inhibit ROS production by human PMNs, mediated either by OPZ or PMA, was studied by monitoring the intensity of chemiluminescence enhanced by luminol (CLlum) or lucigenin(CLluc). The use of luminol reveals predominantly hypochlorous acid, while lucigenin is more selective with respect to superoxide anions. Luminol can detect both intra- and extracell ROS production, whereas lucigenin can not penetrate into PMNs and, hence, probes only the extracell space. In order to separate the ROS production and scavenging processes, we performed a control experiment, in which superoxide anions were generated in a cell-free HX/XO system, and measured the corresponding CLluc level.

Oxidative Burst of Neutrophils Caused by OPZ or PMA Stimulation



Specificity of the enhancers			
Luminol		Lucigenin	
$\cdot O_2^-$	+ +	$\cdot O_2^-$	+ + +
H_2O_2	+ +	H_2O_2	+ +
$HOCl^-$	+ + +		

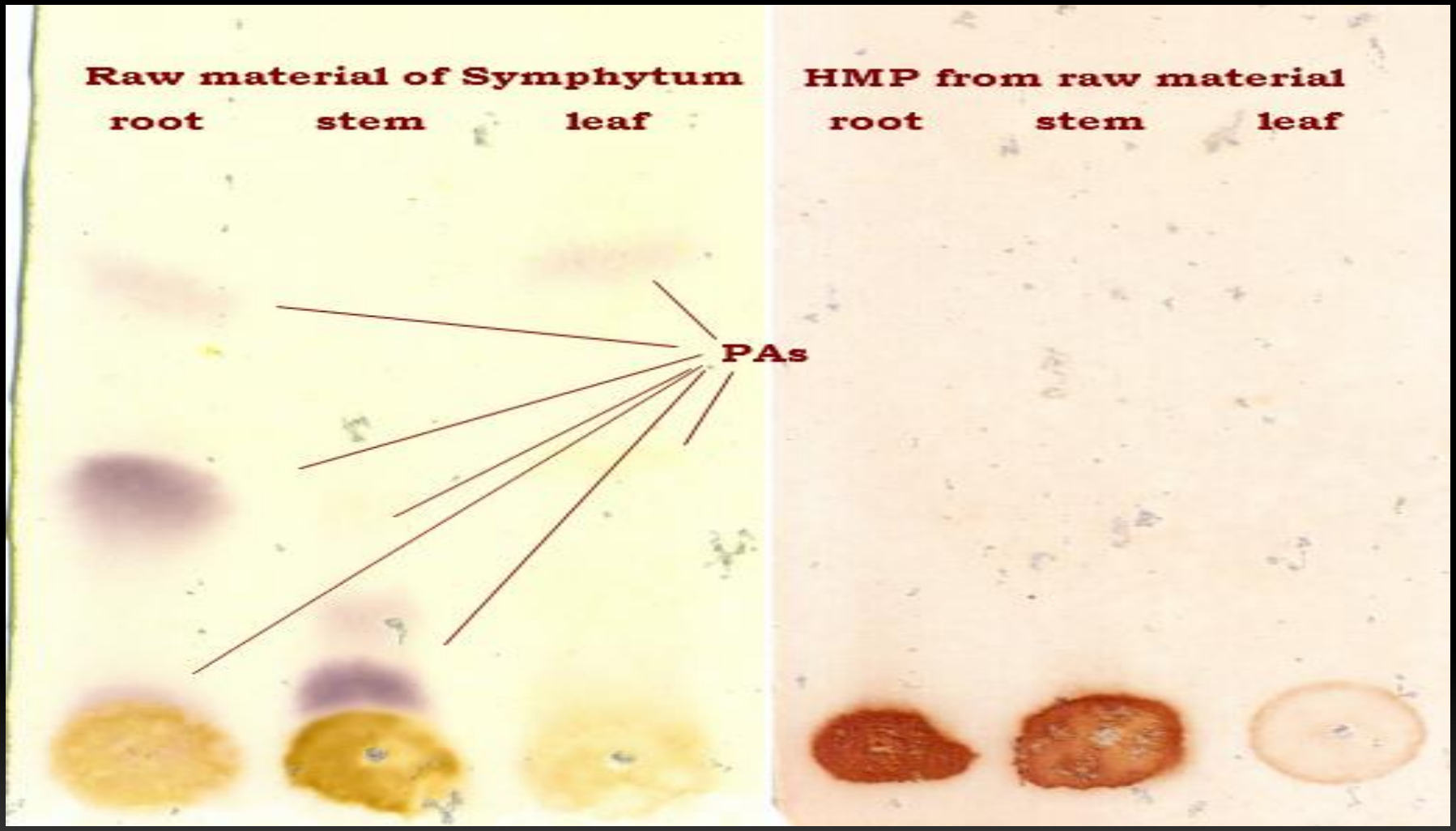
To quantitate the inhibitory effects of the compounds on the generation of ROS after stimulation of PMNs, we used two stimuli which represent different PMN-activation pathways. Opsonized zymosan (OPZ), was used as a model system for opsonized microorganisms. OPZ consists of cell walls of baker's yeast coated with IgG, mannose-binding lectin, and C3b complement fragments. C3b is opsonizing agent. Phagocytes have receptors for C3b. Therefore, covering of microorganisms with C3b will facilitate their recognition and uptake by phagocytes, the most pronounced function of complement activation. Phorbol myristate acetate (PMA) is a soluble agent activating PMNs directly at the level of protein kinase C (PKC) which also leads to the activation of the respiratory burst. Althoough OPZ and PMA both stimulate the superoxide anions-generating NADPH-oxidase, their transductional mechanisms within the neutrophil are quite different. The ability of SAR, SCR, SAS and SCS to inhibit ROS production by human PMNs (mediated either by receptor-dependent OPZ or by receptor-independent PMA) was studied by monitoring the intensity of chemiluminescence enhanced by luminol (CLlum) or lucigenin(CLluc). The use of luminol reveals predominantly hypochlorous acid, while lucigenin is more selective with respect to superoxide anions. Luminol can detect both intra- and extracell ROS production, whereas lucigenin can not penetrate into PMNs and, hence, probes only the extracell space. In order to separate the ROS production and scavenging processes, we performed a control experiment, in which superoxide anions were generated in a cell-free HX/XO system, and measured the corresponding CLluc level.

Traditionally *Symphytum* and *Anchusa* extracts have been used both internally and externally, but nowadays their internal usage are not recommended due to the presence of hepatotoxic and carcinogenic PAs. Obtaining of *Symphytum* extracts or preparations free of hazardous PAs is of great importance. PAs N-oxides, which are generally the predominant natural form of PAs, have been found to be not significantly toxic. Besides, medicinal use of comfrey aqueous extracts may be considered less hazardous since the PAs are particularly insoluble in water, and thus should contain only water-soluble N-oxides. Moreover the external use of comfrey preparations should not be hazardous since the alkaloids are converted to toxic pyrrolic metabolites (dehydroalkaloids) by mammalian liver oxidases only after being ingested.

The isolation scheme of water-soluble high-molecular (>1000 kDa) preparations from *Symphytum* and *Anchusa* permits to remove completely the toxic PAs. The isolation of high-molecular (> 1000 kDa) preparations was carried out using hot water extracts dialysis through the semipermeable cellophane membranes followed with ultrafiltration on membrane filters with cut-off value of 1000 kDa. These procedures suggested the removal of PAs with average molecular weight of 340 Da and their absence in the obtained high molecular fractions.

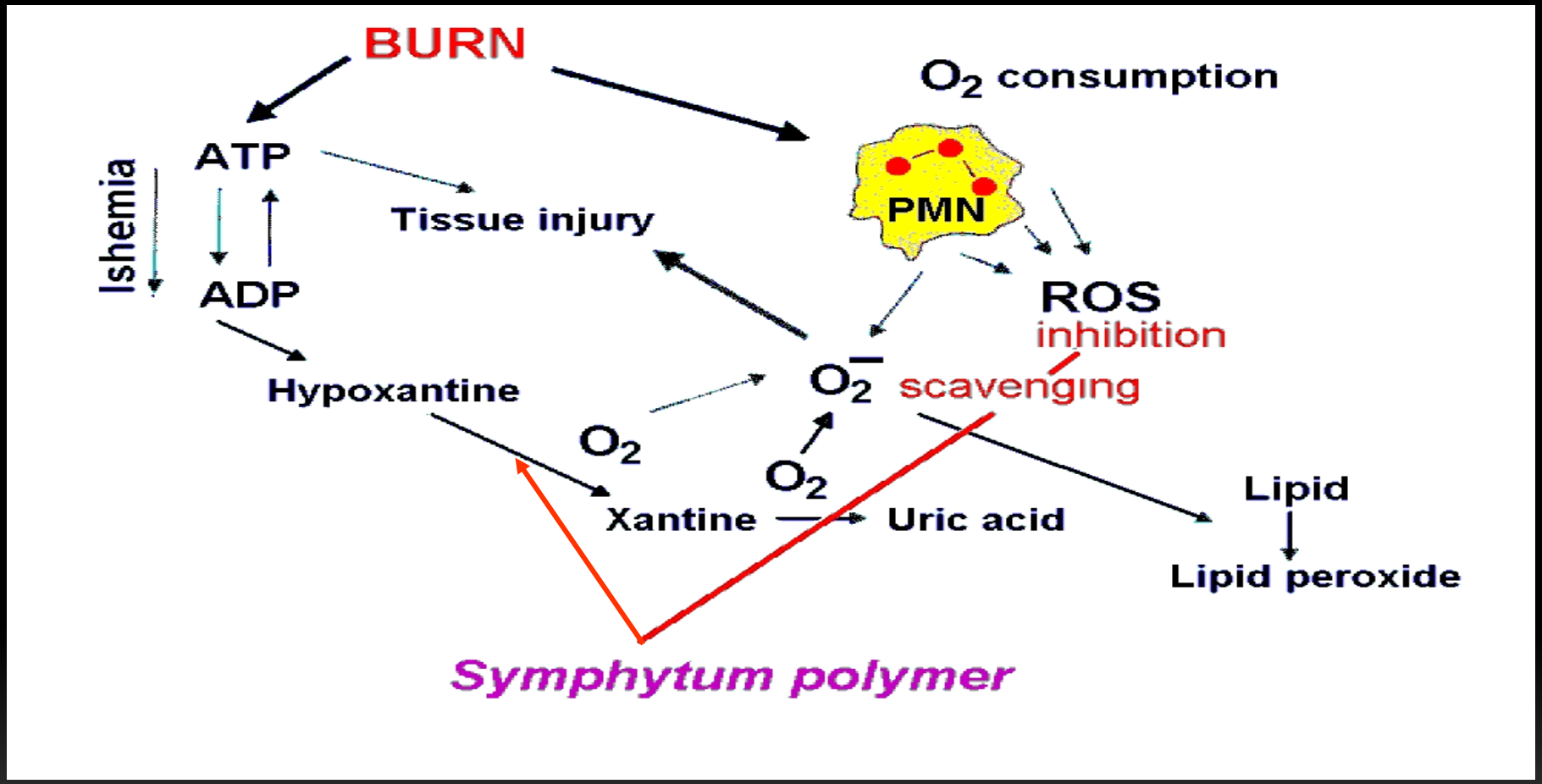
Thus, we can conclude, that due to immunomodulatory, antiinflammatory and antioxidative activity, these pyrrolizidine alkaloid-free preparations may have potential pharmaceutical importance and can be recommended for both external and internal medical application.

Absence of Pyrrolizidine alkaloids (PAs) in HMP



The TLC was chosen as cheap, rapid, simple and sensitive method for fast detection of PAs present in *Symphytum* and *Anchusa* extracts and subsequent fractions. After the TLC the alkaloids on the plate are converted to N-oxides by a hydrogen peroxide spray followed by heating. Treatment with acetic anhydride then converts the N-oxides to pyrroles, which give blue or mauve spots with Ehrlich regent (4-dimethylaminobenzaldehyde). The use of Ehrlich's reagent greatly improves the sensitivity of detection, bringing the limit down to 0.1 µg.

Generation of ROS in injured tissue and their scavenging by *Symphytum* polymer



Besides generation of superoxide anions by stimulated PMNs, these radicals may also arise in chronic wounds where ischemic conditions may convert the enzyme xanthine dehydrogenase into xanthine oxidase (XO) which catalyses the conversion of oxygen into superoxide anions causing tissue damage. During this process XO converts hypoxanthine (HX) to xanthine and subsequently to uric acid. So, scavenging of superoxide anions either produced by PMNs or through XO is regarded beneficial for wound healing and in inflammatory process.

Wound healing effect of *Symphytum* polymer



Day 4





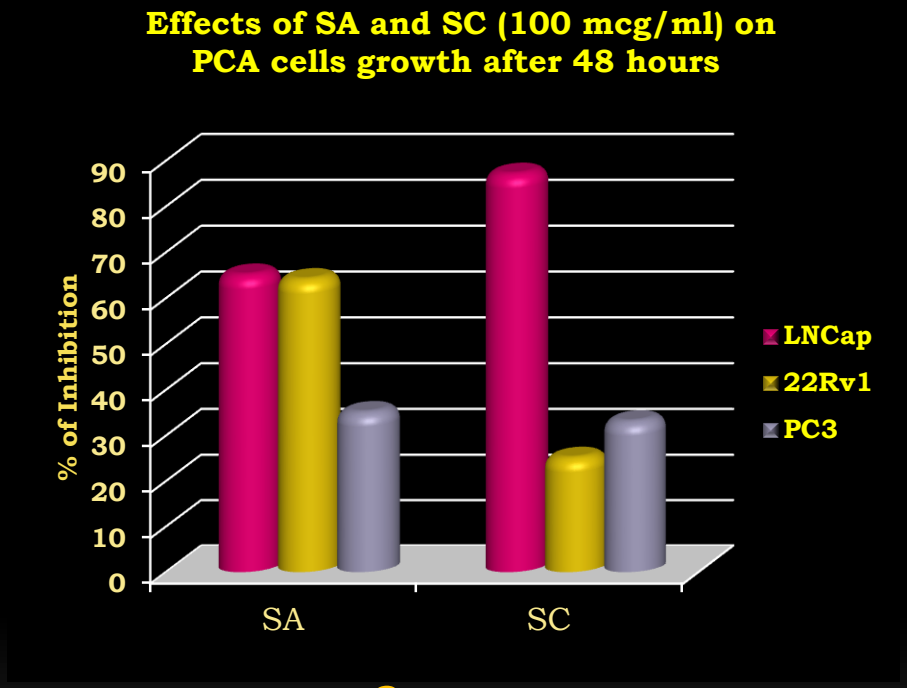
Day 10



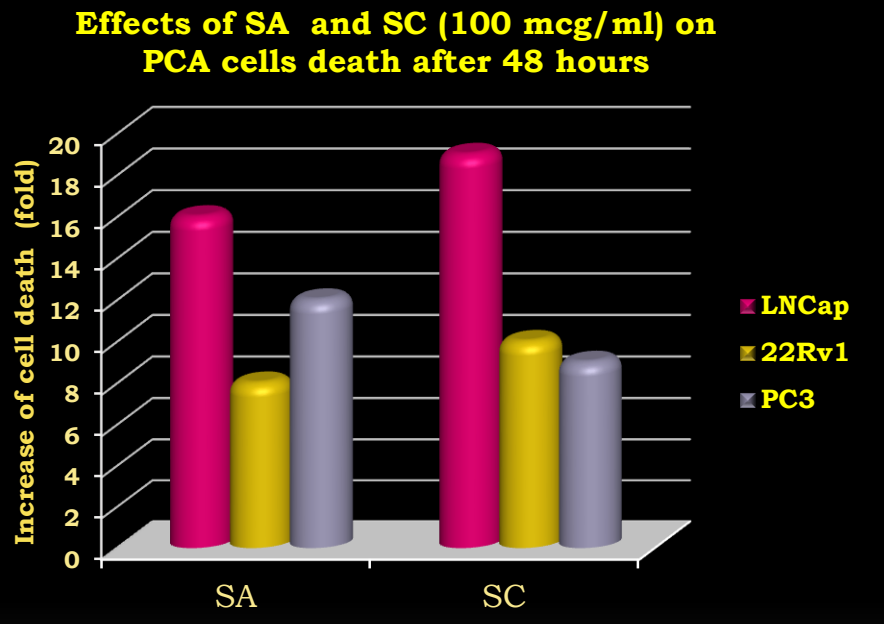
Symphytum Polymer's 1% ointment

Control (vehicle)

In vitro anti-cancer efficacy of novel phenolic polymers from *Symphytum asperum* (SA) and *S.caucasicum* (SC)



a

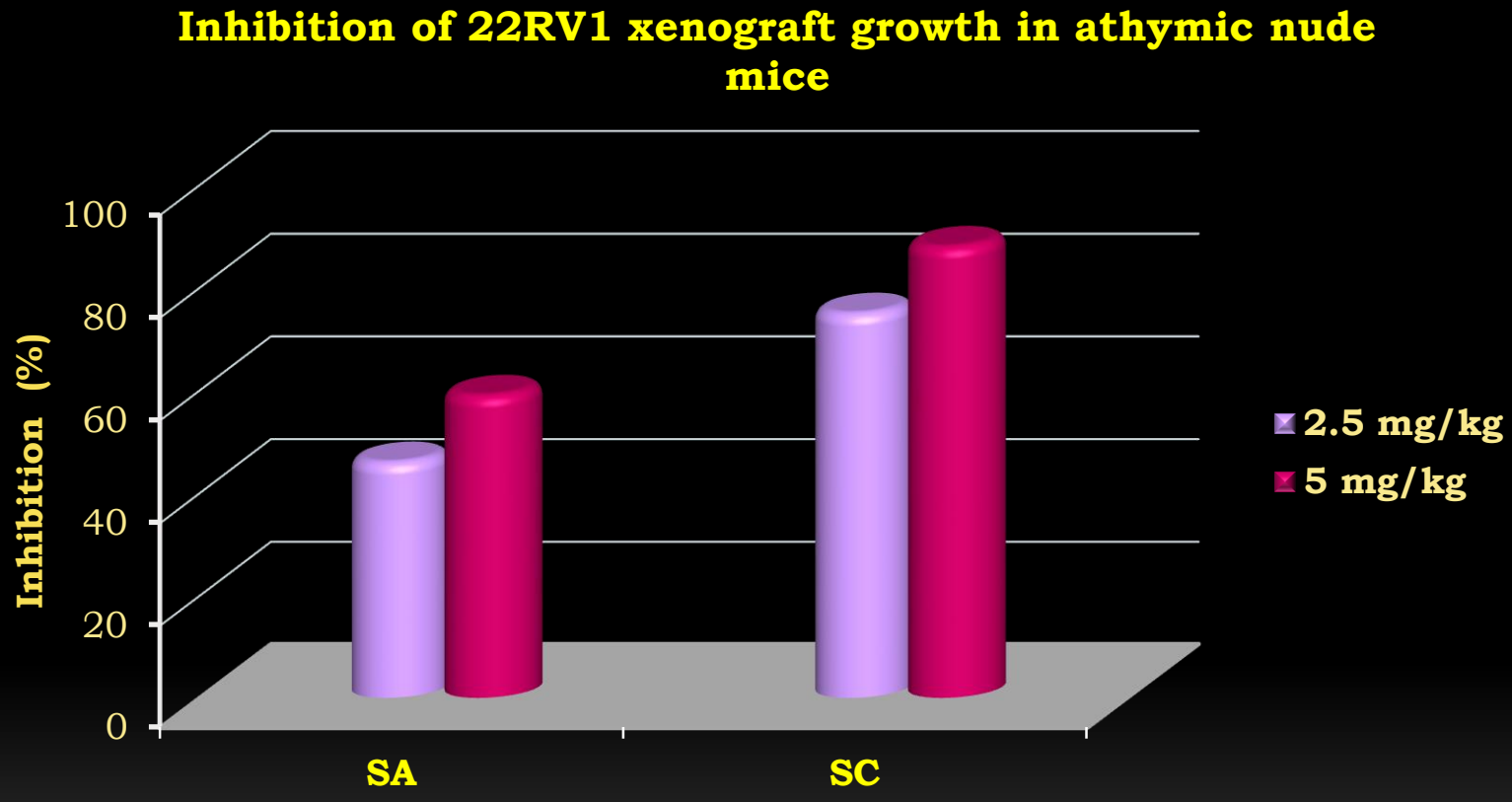


b

In androgen-dependent (LNCaP) and -independent (22Rv1 and PC3) human prostate cancer (PCA) cells SA polymer treatment (100 mcg/ml for 48h) decreases the live cell number by 65, 64 and 35% (a) and increases the cell death by 16, 8 and 12 folds (b) in LNCaP, 22Rv1 and PC3 cells, respectively. Similarly, SC polymer treatment (100 mcg/ml for 48h) decreased the live cell number by 87, 25 and 33% and increased the cell death by 19, 10 and 9 folds in LNCaP, 22Rv1 and PC3 cells, respectively.

S. Shrotriya et al. American Association for Cancer Research 100th Annual Meeting, Denver, Colorado, USA. Abstracts. 2009, N 921.

In vivo anti-cancer efficacy of novel phenolic polymers from *Symphytum asperum* (SA) and *S.caucasicum* (SC)

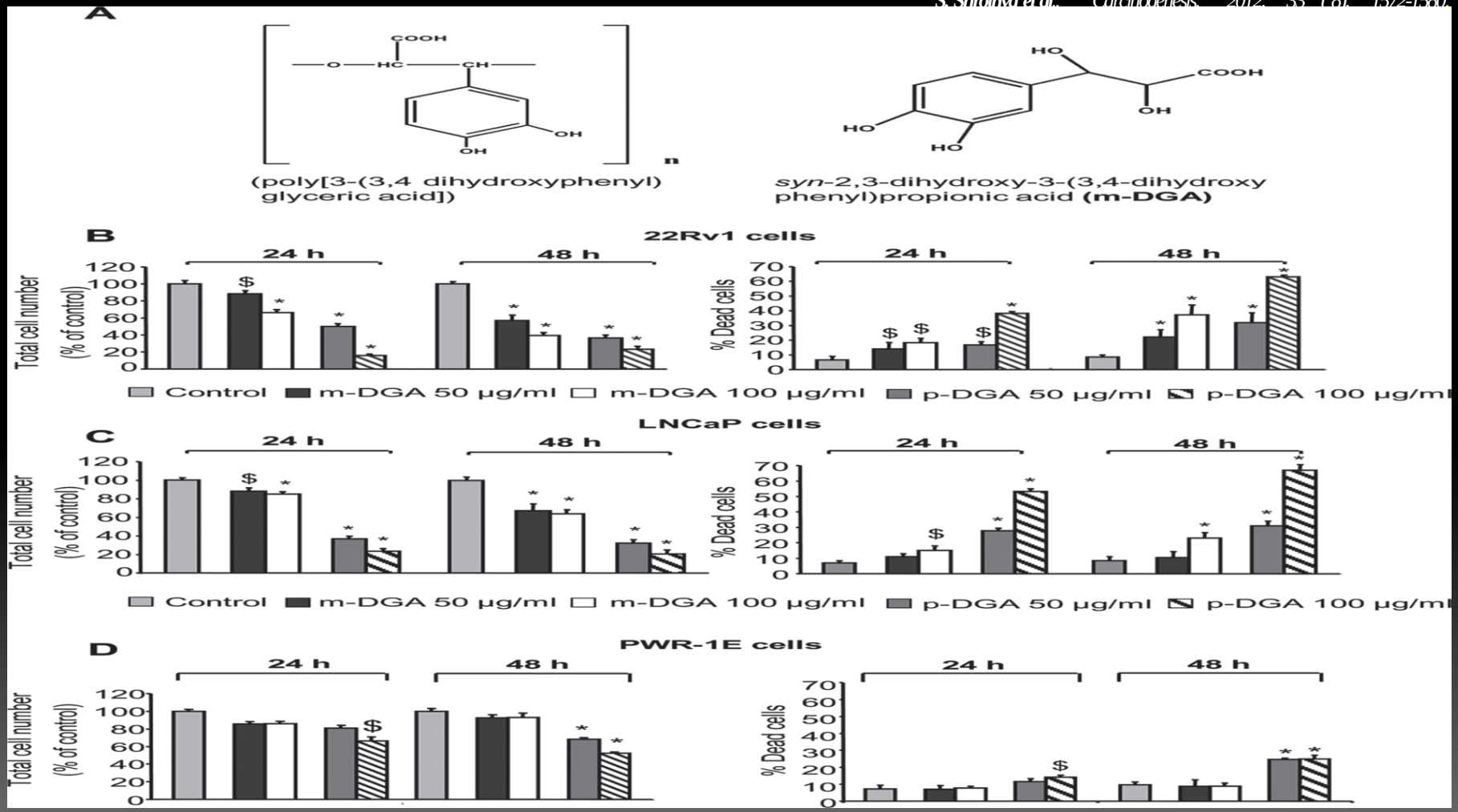


Oral gavage feeding of SA polymer (2.5 and 5.0 mg/kg body weight) and SC polymer (2.5 and 5.0 mg/kg body weight) 5 days/week for 5 weeks caused a marked time-dependent inhibition in 22RV1 tumor xenograft growth which accounts for 46% and 59% decrease in SA polymer treated animals and 75% and 88% decrease in SC polymer treated animals, respectively.

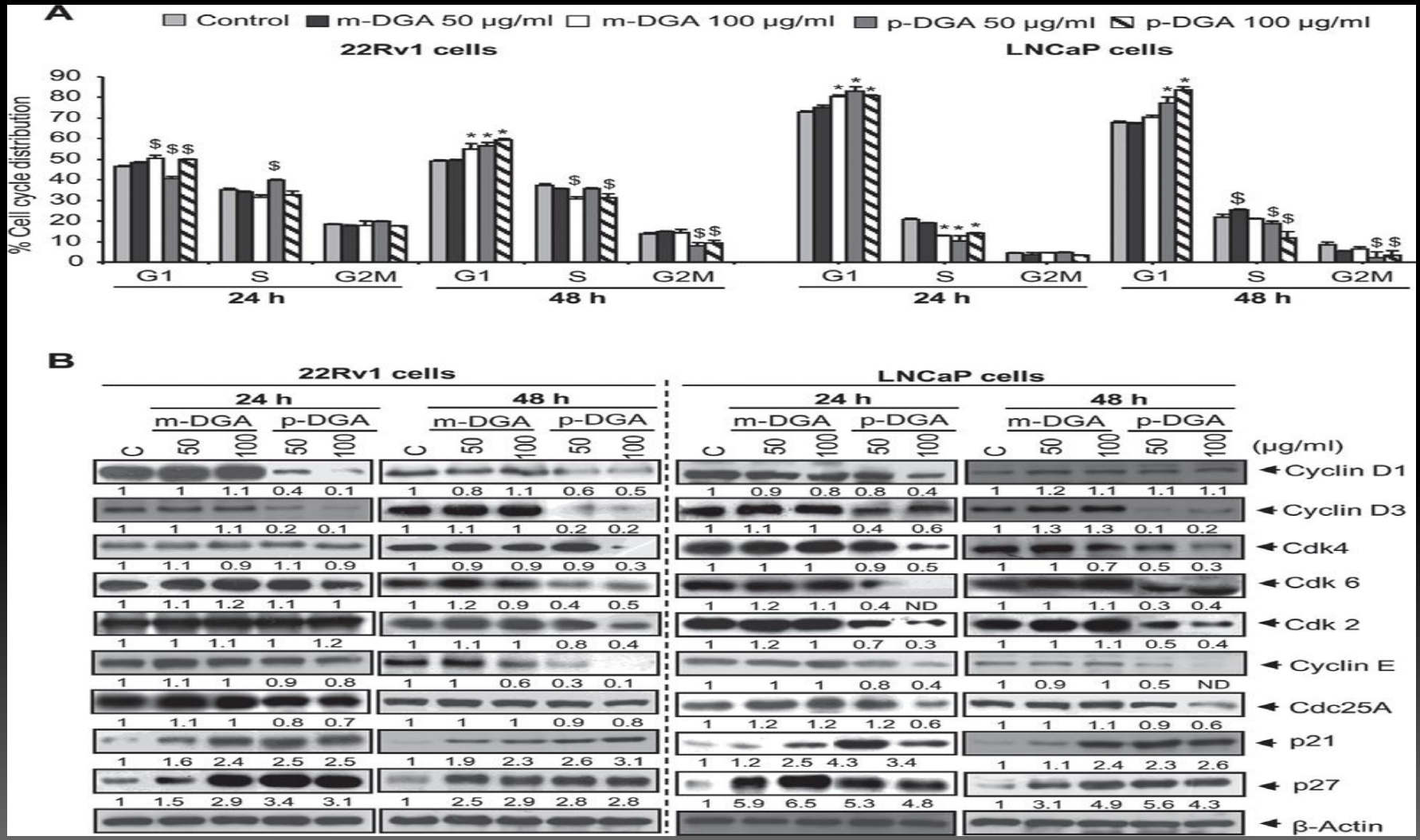
S. Shrotriya et al. Carcinogenesis, 2012, 33(8), 1572-1580.

Novel phytochemical poly[3-(3,4-dihydroxyphenyl)glyceric acid] (p-DGA) (Zebra columns) and its synthetic monomer (m-DGA) (White columns) suppressed the growth and induced death in prostate cancer (PCA) cells, LNCaP and 22Rv1, with comparatively lesser cytotoxicity (Zebra and White columns) towards non-neoplastic human prostate epithelial PWR-1E cells. Thus, p-DGA and m-DGA selectively inhibit growth and induce death in human prostate cancer (PCA) cells. (A) The chemical structure of p-DGA and m-DGA. (B-D) PCA androgen-independent 22Rv1, androgen-dependent LNCaP cells and immortalized non-neoplastic prostate epithelial PWR-1E cells were treated with vehicle (sterile DI water) or two different concentrations of m-DGA or p-DGA (50 and 100 µg/mL) for 24 and 48 h. Afterwards, cells were collected and total cell number (viable plus dead cells) as well as dead cell population were determined by trypan blue exclusion assay. The data are presented as mean (n=3) ± standard error of mean (SEM) and represent at least three independent experiments. *, P<0.001; $, P<0.05.

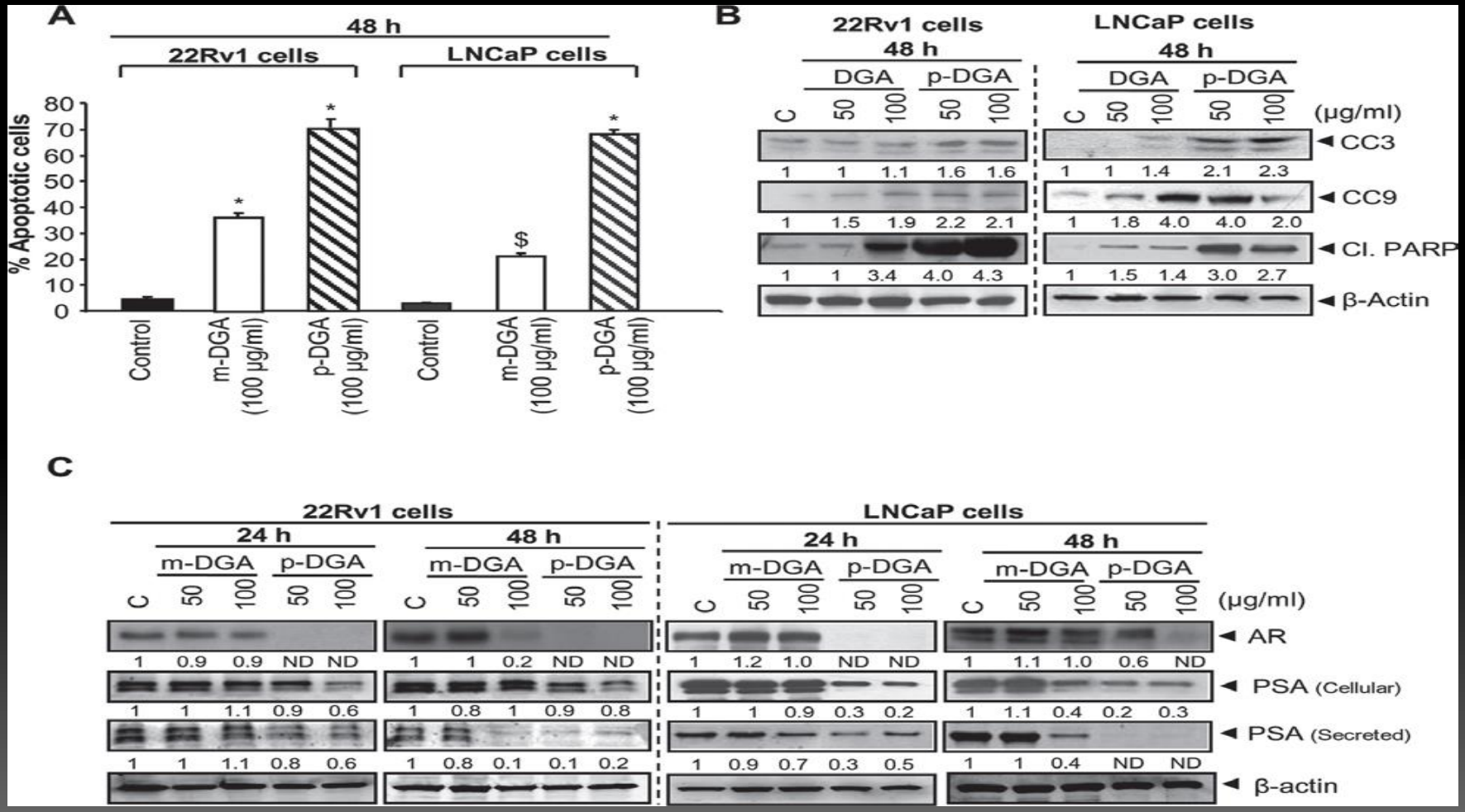
S. Shrotriya et al., Carcinogenesis, 2012, 33 (8), 1572-1580



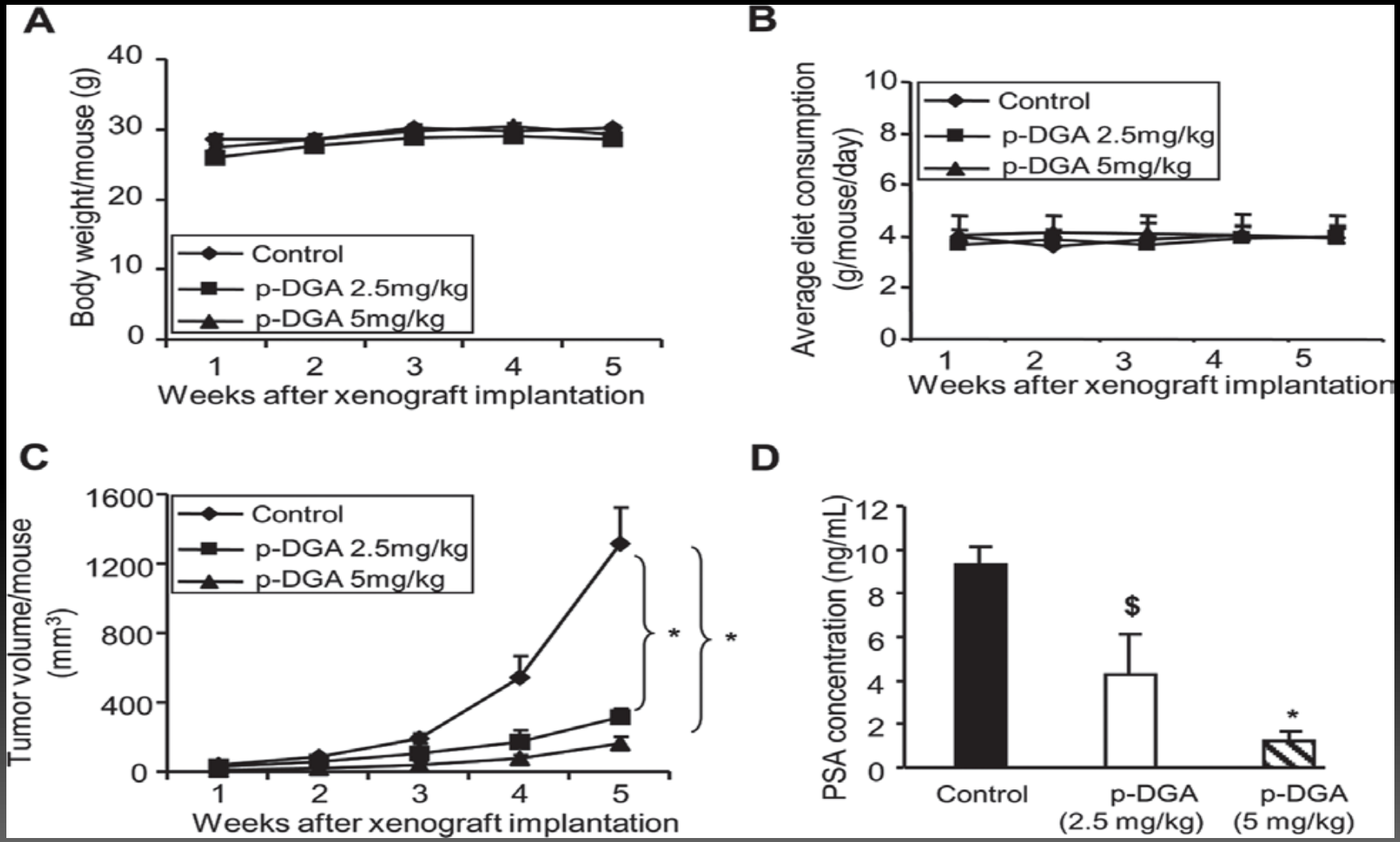
Molecular studies suggested that p-DGA (Zebra columns) and m-DGA (White columns) caused G1 arrest in PCA cells through modulating the expression of cell cycle regulators, especially an increase in Cyclin-dependent kinase inhibitors (CDKIs) (p21 and p27). Thus, p-DGA (Zebra columns) and m-DGA (White columns) induce cell cycle arrest by modulating cell cycle regulatory molecules in human PCA cells. Human PCA 22Rv1 and LNCaP cells were treated with vehicle or m-DGA or p-DGA (50 and 100 µg/mL) for 24 and 48 h. At the end of each time point, cells were collected and (A) Stained using saponin/PI and analyzed for cell cycle distribution by flow cytometry; (B) Whole cell lysates were prepared and western blotting was performed for desired cell cycle regulatory proteins. Membranes were re-probed with β-actin to check equal protein loading. The data are presented as mean (n=3) ± SEM and represents three independent experiments. *, P<0.001; $, P<0.05. The densitometry data presented below the bands are "fold change" as compared with control after normalization with respective loading control (β-actin). ND: Not detectible.



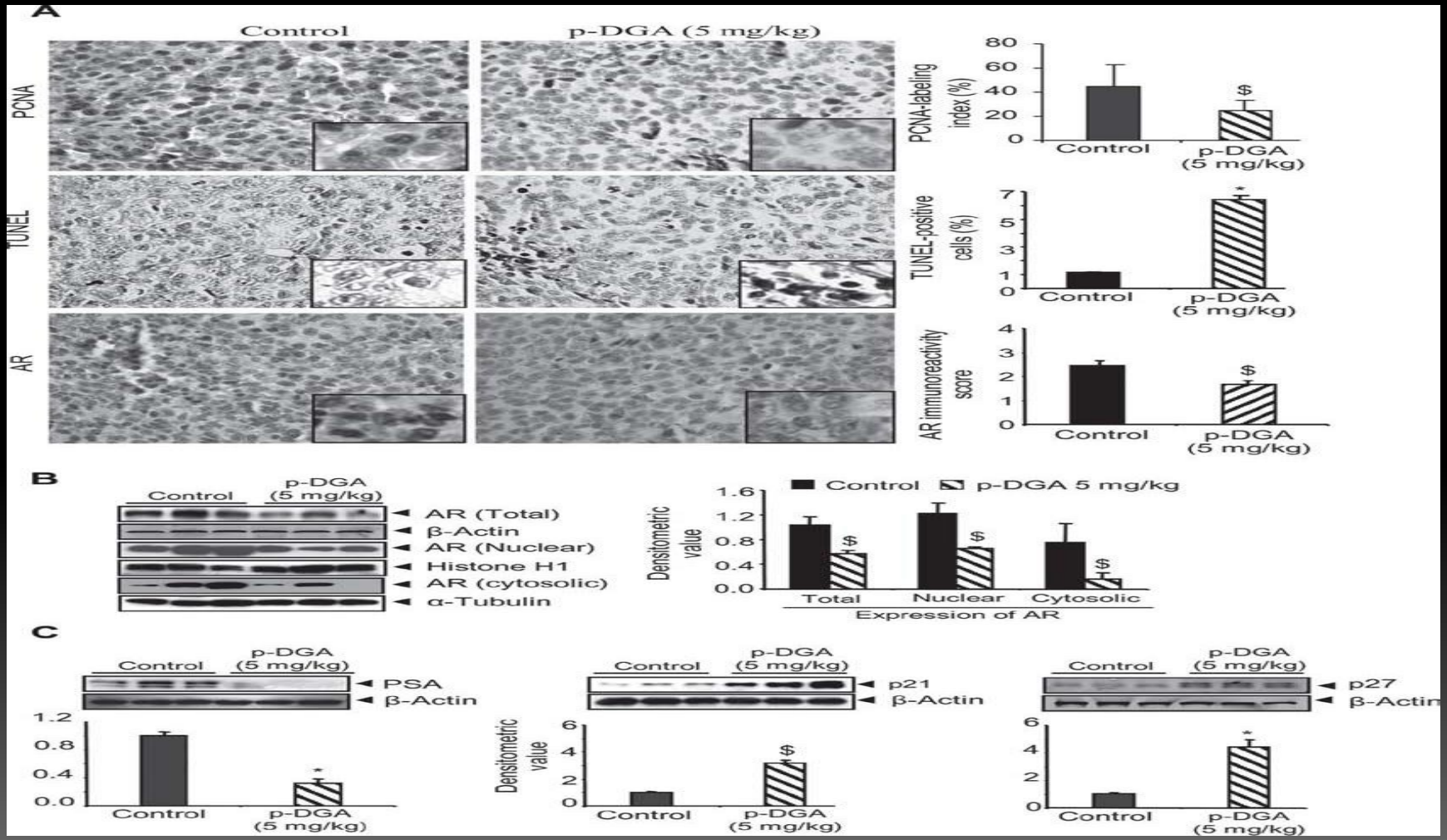
Effect of p-DGA and m-DGA on apoptosis and AR in human PCA cells. Thus, p-DGA (Zebra columns) and m-DGA (White columns) induced apoptotic death in PCA cells by activating caspases and also strongly decreased Androgen Receptor (AR) and Prostate-Specific Antigen (PSA) expression. Human PCA 22Rv1 and LNCaP cells were treated with vehicle or p-DGA or m-DGA (50 and 100 µg/mL) for 24 and 48 h. (A) After 48h of treatment, both adherent and non-adherent cells were collected, stained with annexin V/PI and analyzed by flow cytometry for the apoptotic cell population. The data are presented as mean (n=3) ± SEM and represents two independent experiments. *, P<0.001; $, P<0.05. (B) Whole cell lysate were prepared after treating 22Rv1 and LNCaP cells with m-DGA or p-DGA for 48 h and used to analyze the protein expression of cleaved caspase 3 (CC3), cleaved caspase 9 (CC9), and cleaved PARP (Cl. PARP) by western blotting. (C) Western blotting was performed for AR and PSA; and membranes were re-probed with β-actin to check equal protein loading. For the secreted PSA expression, media was collected and analyzed for PSA expression by immunoblotting. In each case, the media loading volume was normalized with the respective protein value of the cell lysate. The densitometry data presented below the bands are "fold change" as compared to control after normalization with respective loading control (β-actin). ND: Not detectible.



Effect of p-DGA oral administration on the growth of human PCA 22Rv1 tumors and secreted PSA (White and Zebra columns) in athymic nude mice. 22Rv1 cells at the density of 1×10^6 were injected subcutaneously on the right flank of each male athymic nude mouse; and p-DGA (2,5 mg//kg or 5,0 mg//kg body weight) was administered through oral gavage route 5 days/week for 5 weeks. (A) The body weight of the animals was monitored throughout the experiment duration and presented as body weight//mouse in grams (g). (B) The diet consumption of the animals was also monitored throughout the experiment duration and presented as average diet consumption//mouse/day in grams (g). (C) Tumor volume was measured and presented as tumor volume/mouse (mm^3). (D) At the end of the study, blood was collected from mice, plasma was isolated and PSA level was determined by ELISA. Data are presented as mean±SEM, where n=12 to 15 animals in each group for the data in panels A–C; and 4 animal samples for each group for the data shown in panel D. *, P<0.001; $, P<0.05.



In vivo effect of p-DGA feeding on the proliferation and apoptosis markers as well as AR, PSA and CDKIs expression in 22Rv1 tumors. (A) IHC was performed in 22Rv1 xenograft tissues and immunoreactivity for PCNA, TUNEL and AR was quantified. Representative photographs are presented at 400 X; insets represent further magnification of a part of the photographs. (B–C) Total cell lysates or nuclear and cytoplasmic fraction lysates were prepared from 22Rv1 xenograft tissues and analyzed for AR, PSA, p21 and p27 expression by western blotting. In each case, three random samples were analyzed from control and p-DGA treatment group (5 mg/kg body weight). Membranes were reprobed with β-actin (total cell lysates), histone H1 (for nuclear fractions) or α-tubulin (for cytosolic fractions) to check protein loading. The densitometric values were normalized with respective loading control values (β-actin, histone H1 or α-tubulin) and presented as mean±SEM.



Results of Anti-cancer Efficacy of p-DGA and m-DGA

Thus, a novel phytochemical poly[3-(3,4-dihydroxyphenyl)glyceric acid] (p-DGA) and its synthetic monomer 3-(3,4-dihydroxyphenyl)glyceric acid (m-DGA) suppressed the growth and induced death in prostate cancer (PCA) cells, LNCaP and 22Rv1, with comparatively lesser cytotoxicity towards non-neoplastic human prostate epithelial PWR-1E cells. Molecular studies suggested that both p-DGA m-DGA caused G1 arrest in PCA cells through modulating the expression of cell cycle regulators, especially an increase in Cyclin-dependent kinase inhibitors (CDKIs) (p21 and p27). In addition, p-DGA and m-DGA induced apoptotic death in PCA cells by activating caspases, and also strongly decreased Androgen Receptor (AR) and Prostate-Specific Antigen (PSA) expression. However, our results clearly showed that anticancer efficacy of p-DGA is more effective compared to its synthetic monomer (m-DGA). Consistent with *in vitro* results, our *in vivo* study showed that p-DGA feeding strongly inhibited 22Rv1 tumors growth by 76 and 88% at 2.5 and 5 mg/kg body weight doses, respectively, without any toxicity, together with a strong decrease in PSA level in plasma; and a decrease in AR, and PSA expression but increase in p21/p27 expression and apoptosis in tumor tissues from p-DGA-fed mice. Overall, present study identifies p-DGA as a potent agent against PCA without any toxicity, and supports its clinical application.

DISCUSSION

Currently, we lack the understanding about p-DGA biotransformation; however it is clear that a molecule of such a size and mass as p-DGA could not be passively absorbed from the gastrointestinal tract or interact directly with cell membrane receptors. Therefore, we cannot exclude that the observed biological effects are possibly caused by fragments of the p-DGA with much smaller size/mass. However, detailed pharmacokinetics studies are required in future to understand p-DGA absorption, distribution, metabolism, excretion and the liberation (if any) of fragments (or oligomers). The results from the present study also showed that p-DGA is extremely potent *in vivo* compared to its efficacy in cell culture studies. This could be due to its strong effect on tumor microenvironment (which is absent in cell culture studies) components such as endothelial cells, fibroblasts and so on. Therefore, we need to assess p-DGA effects on tumor microenvironment. Further, *in vitro* cells were exposed only once to p-DGA, whereas *in vivo* mice were orally administered p-DGA (5 days/week) for 5 weeks. Therefore comparatively stronger effect *in vivo* could also be due to the repetitive dosing over a period of time. Together, more studies in future would identify the mechanism(s) and targets for strong efficacy of p-DGA *in vivo.*

IN SUMMARY

Thus, our studies for the first time revealed that p-DGA inhibits the growth of androgen-dependent and androgen-independent PCA cells both *in vitro* and *in vivo*. Results also revealed the broad spectrum effects of p-DGA on AR and PSA levels, cell cycle, and apoptosis revealing some of the plausible underlying mechanisms. Nevertheless, convincing proof for the notion that p-DGA is a promising new tool in PCA management requires a potency comparison with other naturally occurring phenols exemplified by fisetin/quercetin and AR signaling-modulating drugs such as finasteride/dutasteride. In conclusion, present study is significant as we identified a natural nontoxic compound with efficacy against PCA that supports its further pre-clinical and clinical testing as well as its translational applicability in near future.

Conclusion

- **The first representative of a new class of natural polyethers - regular caffeic acid-derived polymer, namely POLY[3-(3,4-DIHYDROXYPHENYL)-GLYCERIC ACID] (p-DGA) or POLY[OXY-1-CARBOXY-2-(3,4-DIHYDROXYPHENYL)ETHYLENE] - has been isolated from comfrey species *Symphytum asperum*, *S. Caucasicum*, *S.officinale* and Bugloss (*Anchusa italica*).**

- **Most of the carboxylic groups (70%) of *Anchusa* polyether unlike the polymer of *S.asperum*, *S.caucasicum* and *S.officinale* are methylated.**

- **The racemic and enantioselective synthesis of a novel glyceric acid derivative, namely, 2,3-dihydroxy-3-(3,4-dihydroxyphenyl)-propionic acid – the monomer of p-DGA – as well as its anticancer efficacy against PCA is described.**

- **The caffeic acid-derived polymer has wide spectrum of biological activity: anticomplementary, antioxidant, antiinflammatory properties, burn and wound healing effect.**

- **Pre-clinical investigation revealed the strong efficacy of p-DGA against prostate cancer cells and identifies this polymer as a potent agent against PCA without any toxicity, and supports its clinical application suggesting high potential in prostate cancer patients.**

Acknowledgements

I would like to express my gratitude to my coauthors :

- **Prof. E. Kemertelidze, Drs. M.Merlani, L.Amiranashvili, L.Gogilashvili, K.Mulkijanyan (Tbilisi State Medical University Institute of Pharmacochemistry, Tbilisi, Georgia);**
- **Profs. A.I.Usov, A.S.Shashkov (Zelinsky Institute of Organic Chemistry, Moscow, Russia);**
- **Profs. R.P.Labadie, A.J.J. van den Berg, C.J.Beukelman, Drs B.H.Kroes, E. van den Worm (Utrecht University, Utrecht, The Netherlands);**
- **Prof. K. Papadopoulos (NCSR 'Demokritos', Institute of Physical Chemistry, Athens, Greece);**
- **Prof. R.Agarwal, Drs. C.Agarwal G.Deep, S.Shrotriya, K.Ramasamy, K.Raina (Colorado University, Denver, USA);**
- **Prof. B.Chankvetadze (Institute of Physical and Analytical Chemistry, Javakhishvili Tbilisi State University, Georgia);**
- Dr. **A.Salgado (Department of Medicinal Chemistry, Centro Nacional de Investigaciones Oncológicas (CNIO), Madrid, Spain)**

Photos

- H. Kreiss http://www.henriettesherbal.com
- J. Crellin http://www.floralimages.co.uk
- K. Mulkijanyan https://picasaweb.google.com/104458227325991028 72/Plants

THANK YOU FOR

YOUR PATIENCE

AND ATTENTION

Laboratory of Plant Piopolymers





Georgia, situated at the dividing line of Asia and Europe, bordered by the Russian Federation (in the North), Turkey (in the South), Armenia (in the South), Azerbaijan (in the East) and the Black Sea (in the West). Area: 69,700 sq km; Population: 4,677,401 (July 2005 est.); Capital: Tbilisi. The ancient name of Georgia is Iberia. Is it mere, singular coincidence or is there historical relationship between Peninsula Iberia and Caucasian Iberia?

Georgian alphabet

The Georgian language belongs to non of the language groups and has a very rich word derivation system. The Georgian alphabet is one out of 14 alphabets known in the world. The Georgian writing is very old and it was invented by the Georgian priests in 412 BC and reformed by the king Parnavaz in the 284 BC. The Georgian alphabet consists of 33 letters:

ა	ani	[a]
ბ	bani	[b]
გ	gani	[g]
დ	doni	[d]
ე	eni	[e]
ვ	vini	[v]
ზ	zeni	[z]
თ	tani	[t]
ი	ini	[i]
კ	k'ani	[k?]
ლ	lazi	[l]
მ	mani	[m]
ნ	nari	[n]
ო	oni	[o]
პ	p'ari	[p?]
ჟ	zhani	[ž]
რ	rae	[r]
ს	sani	[s]
ტ	t'ani	[t?]
უ	uni	[u]
ფ	pari	[p]
ქ	kani	[k]
ღ	ghani	[ɣ]
ყ	q'ari	[q?]
შ	shini	[š]
ჩ	chini	[č]
ც	tsani	[ts]
ძ	dzili	[dz]
წ	ts'ili	[ts?]
ჭ	ch'ari	[č?]
ხ	xani	[x]
ჯ	jani	[j]
ჰ	hae	[h]



The Living Pillar Cathedral



Saint Trinity Cathedral in Tbilisi



Catholicos-Patriarch of All Georgia ILYA II







Saint Trinity Church
















Courtesy Photo







Saint Trinity Church









Saint Trinity Church

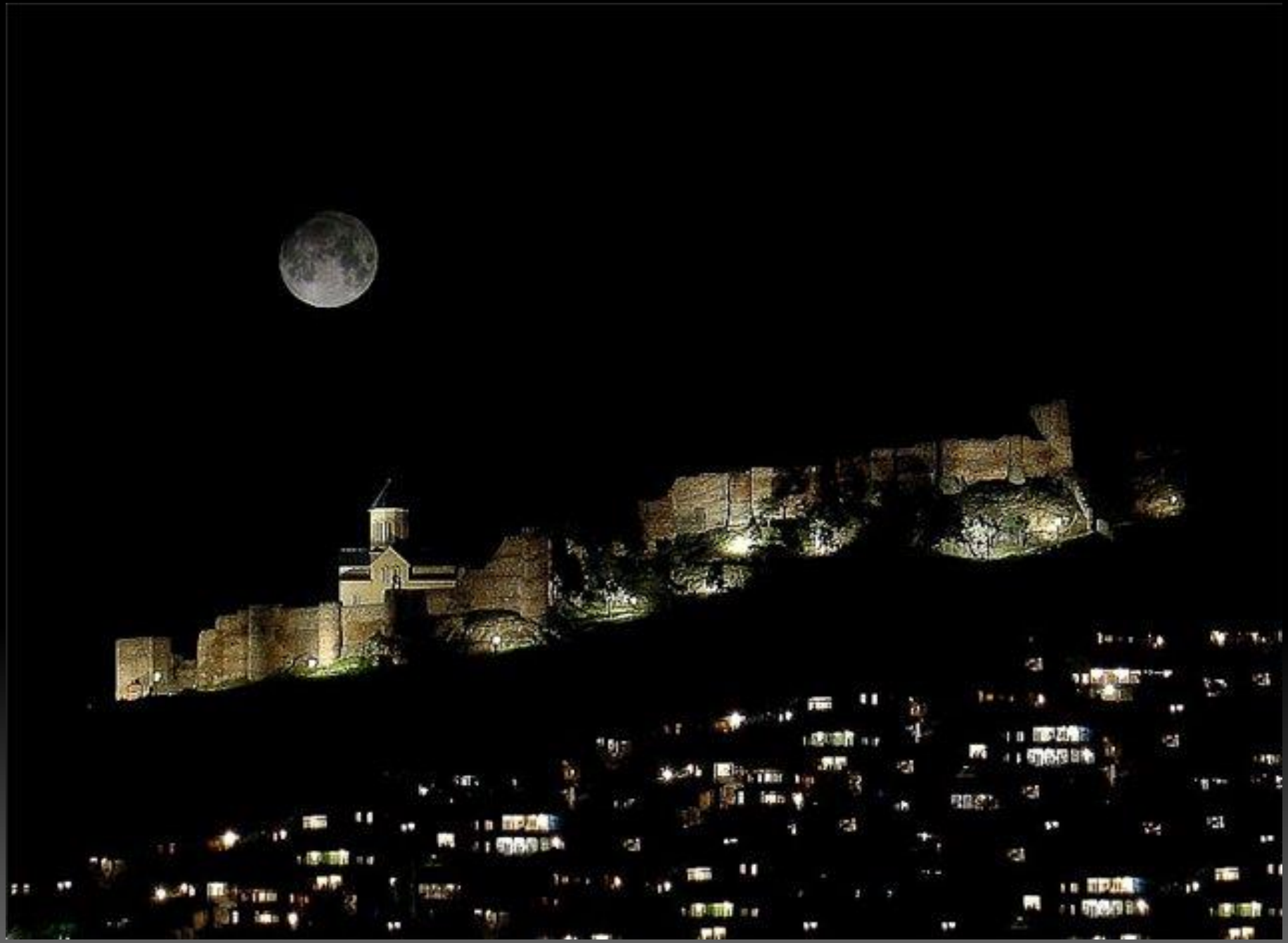





HOTEL








www.paata.ge



Georgian self educated artist (primitivist painter) NIKO PIROSMANI
"Fisherman in a Red Shirt"

